AWARD NUMBER: W81XWH-15-1-0039

TITLE: Targeting Tryptophan Catabolism: A Novel Method to Block Triple-Negative Breast Cancer Metastasis

PRINCIPAL INVESTIGATOR: Jennifer Richer

CONTRACTING ORGANIZATION: University of Colorado
Aurora, CO 80045

REPORT DATE: April 2018

TYPE OF REPORT: Annual

PREPARED FOR: U.S. Army Medical Research and Materiel Command
Fort Detrick, Maryland 21702-5012

REPORT DOCUMENTATION PAGE

Form Approved
OMB No. 0704-0188

1. REPORT DATE	2. REPORT TYPE	3. DATES COVERED
April 2018	Annual	1Apr2017 - 31Mar2018

4. TITLE AND SUBTITLE

Targeting Tryptophan Catabolism: A Novel Method to Block Triple-Negative Breast Cancer Metastasis

5a. CONTRACT NUMBER

5b. GRANT NUMBER
W81XWH-15-1-0039

5c. PROGRAM ELEMENT NUMBER

6. AUTHOR(S)

Jennifer Richer, Ph.D

E-Mail: Jennifer.richer@ucdenver.edu

5d. PROJECT NUMBER

5e. TASK NUMBER

5f. WORK UNIT NUMBER

7. PERFORMING ORGANIZATION NAME(S) AND ADDRESS(ES)

University of Colorado
Anschutz Medical Campus
12800 E. 19th Ave
Aurora, CO 90010

8. PERFORMING ORGANIZATION REPORT NUMBER

9. SPONSORING / MONITORING AGENCY NAME(S) AND ADDRESS(ES)

U.S. Army Medical Research and Materiel Command
Fort Detrick, Maryland 21702-5012

10. SPONSOR/MONITOR'S ACRONYM(S)

11. SPONSOR/MONITOR'S REPORT NUMBER(S)

12. DISTRIBUTION / AVAILABILITY STATEMENT

Approved for Public Release; Distribution Unlimited

13. SUPPLEMENTARY NOTES

14. ABSTRACT

Triple negative breast cancer (TNBC) cells upregulate the kynurenine pathway (KP) in forced suspension culture. The rate limiting enzyme in this pathway, TDO2 is responsible for tryptophan catabolism and production of the metabolite kynurenine (Kyn). Kyn was recently identified as an endogenous ligand for AhR, a transcription factor that was also upregulated in suspension. Kyn activation of AhR promotes motility of glioma cells. AhR is also in many immune cell types and its activation decreases T-cell activity leading to tumor immune escape. The goal of our proposal is to determine if we can target this pathway that may facilitate TNBC metastasis by enabling tumor cell invasiveness, anchorage independence and immune escape. Our hypothesis is that upregulation of kynerinine by TNBC facilitates survival in transit to metastatic sites and immune suppression and thereby mediates the highly metastatic nature of this subtype.

15. SUBJECT TERMS

None listed

16. SECURITY CLASSIFICATION OF:			17. LIMITATION OF ABSTRACT	18. NUMBER OF PAGES	19a. NAME OF RESPONSIBLE PERSON
a. REPORT	b. ABSTRACT	c. THIS PAGE			USAMRMC
Unclassified	Unclassified	Unclassified	Unclassified	66	19b. TELEPHONE NUMBER *(include area code)*

Table of Contents

Page

1. **INTRODUCTION:** Triple negative breast cancer (TNBC) cells strongly upregulate two related pathways, the kynurenine pathway (KP) in forced suspension culture. The KP is the principal route of tryptophan catabolism. Interestingly, the intermediate tryptophan metabolite kynurenine (Kyn) was recently identified as an endogenous ligand for AhR, a transcription factor that was also upregulated in suspension. Kyn activation of AhR promotes motility of glioma cells, and increased AhR expression and activity was found to be a characteristic of human and mouse mammary tumors. AhR is also in many immune cell types and its activation decreases T-cell activity leading to tumor immune escape. Since the rate limiting enzyme TDO2 increases in TNBC, the goal of our proposal is to determine if we can target this pathway that helps TNBC metastasize. Our hypothesis is that the ability to upregulate kynurenine pathway (KP) facilitates TNBC survival in suspension and mediates the highly metastatic nature of this subtype, and further, since AhR is expressed in both TNBC cells and immune cells such as effector T cells, Kyn binding to AhR can potentially elicit both autocrine effects on tumor cells themselves as well as paracrine immune-suppressive effects. To test our hypothesis we have designed the following **specific aims**: **Aim 1**. Determine if inhibition of TDO affects TNBC cell invasion, and growth on soft agar in an AhR dependent manner. **Aim 2.** Test whether inhibition of TDO-mediated kynurenine production affects the ability of TNBC to survive in the bloodstream or metastasize *in vivo* from the orthotopic site. **Aim 3**. Since immune cells such as effector T cells express AhR, we will investigate the paracrine immune-modulatory effect of Kyn secreted from TNBC. **Impact:** TDO and AhR can be targeted by small molecules, which are non-toxic in mice and there is interest in development of TDO2 and AhR inhibitors for a number of disease indications. Therefore, this represents an attractive new opportunity for targeted therapy for TNBC patients, which may revolutionize the treatment of this aggressive subtype. Following the proof of principal pre-clinical studies in this proposal, our discovery could rapidly lead to clinical trials offering new anti-metastatic treatment options for breast cancer patients.
2. **KEYWORDS:** Triple negative breast cancer (TNBC), kynurenine, tryptophan metabolism, anoikis resistance, metastasis
3. **ACCOMPLISHMENTS: What were the major goals of the project?** Our overall goals were to test the hypotheses that the ability to upregulate kynurenine via the enzyme TDO2 supports the highly metastatic nature of TNBC by two mechanisms since the receptor for kynurenine (KYN), AhR, is expressed in both TNBC cells and effector T cells, such that Kyn binding to AhR elicits both autocrine effects helping the tumor cells survive in transit as well as paracrine immune-suppressive effects. **The major goals as stated in the approved SOW are below along with completion status.**

Aim 1: Determine if inhibition of TDO2 affects TNBC cell migration, invasion, and anchorage independent growth and if these effects are mediated by kynurenine activation of AhR. (Months 1-12)

Task1. Confirm that production of Kynurenine increases in TNBC cells in suspension and that this is mediated by TDO2. Compare 3 TNBC lines (BT549, SUM-159 MDA-231) to 3 luminal lines (MCF7, ZR-75.1, T47D). **(Months 1-2) Complete and summarized in first year progress report and our first publication associated with this grant (D'Amato NC and Rogers T Cancer Research et al 2015) in the figures mentioned here.** To confirm our gene array data, we performed qRT-PCR for *TDO2* and *KYNU* in multiple breast cancer cell lines, including both luminal (ER+; MCF7 and T47D) and TNBC (ER-; MDA-231, BT549, and SUM159) lines, after 24hrs in suspension (Figure 1B and C). In all three TNBC lines tested, *TDO2* and *KYNU* were significantly increased in suspension compared to attached culture. In the two ER+ breast cancer cell lines tested, expression of these genes trended slightly higher in suspension but this change was not significant. Western blot analysis of whole cell extracts also demonstrated an increase in TDO2 and KYNU protein in TNBC cell lines (MDA-231, BT549, and SUM159) grown in suspension for 24hrs (Figure 1D and Supplemental Figure 3A). The increase in TDO2 protein was confirmed by IHC in BT549 cells grown in suspension for 48hrs compared to cells grown in the attached condition (Figure 1E). Global metabolomic profiling of intracellular and secreted metabolites from BT549 cells grown in standard attached conditions or in forced suspension for 24 hours was also performed. Two intermediate products of the kynurenine pathway, Kyn and formylkynurenine, were the intracellular metabolites with the highest fold-change increase in suspension. Among secreted metabolites, kynurenine had the third-highest fold-change increase (Supplemental Figure 2). Together with the gene expression data, this demonstrates that the kynurenine pathway is strongly upregulated

in TNBC cells upon loss of attachment. Using HPLC to verify the metabolomic profiling data, we found that secreted Kyn levels were more than two-fold higher in conditioned media from BT549 cells in forced suspension for 48hrs than in media from the same number of cells in the attached condition (Figure 1F). Furthermore, addition of the TDO2-specific inhibitor 680C91 to cells in suspension completely prevented the increase in secreted Kyn, demonstrating that increased secretion of Kyn in TNBC cells in suspension is dependent on TDO2 activity (Figure 1F).

Task 2. Determine if TDO2 or AhR knockdown or inhibition decreases migration **(Months 1-4) 100% completed and summarized in first year progress report and (D'Amato NC and Rogers T Cancer Research et al 2015) in figures specified and in the new submitted manuscript Rogers et al (first paper in appendix).** Pharmacological inhibition of TDO2 and AhR each significantly reduced migration of MDA-MB-231 and BT549 cells in a scratch wound assay, and again the combination was more effective than either inhibitor alone (Figure 4B). Knockdown of either TDO2 or AhR recapitulated this effect, significantly diminishing migration in the scratch wound assay in both BT549 and MDA-231 cells (Figure 4C and 4D). TDO2 overexpression vector transduced into luminal (ER+), immortalized normal mammary epithelial cells renders these cells more anchorage independent (increased growth on soft agar and they produced increased levels of kynurenine (Figure 2F and G in first submitted manuscript in appendix).

Task 3. Determine if TDO2 or AhR knockdown or inhibition decreases invasion **(Months 5-8) 100% completed and summarized below and (D'Amato NC and Rogers T Cancer Research et al 2015).** To test whether the increased TDO2 and AhR expression observed in cells grown in suspension affects invasive capacity, SUM159PT cells were grown for 48hrs either in the attached condition, or in forced suspension culture with or without addition of 10μM of the TDO2 inhibitor 680C91 or the AhR inhibitor CH-223191. After 24hrs, 25,000 viable cells were plated in a Matrigel-coated trans-well invasion chamber with continuous treatment. Cells grown in suspension for 24hrs were significantly more invasive than control cells grown in the attached condition (Figure 4E). The addition of the TDO2 inhibitor 680C91 during suspension culture greatly decreased the invasive capacity of viable cells. While the cells treated with the AhR inhibitor showed decreased invasion, this effect was not statistically significant (Figure 4E). We have yet to determine if overexpression of TDO2 increases cell invasion in vitro, but we have acquired a TDO2 overexpression vector that can be stably transduced into breast cancer cell lines (TNBC, luminal (ER+), immortalized normal mammary epithelial cells like the MCF-10A) and selected using puromycin.

Task 4. Test if inhibition or knockdown of TDO2 or AhR decrease anchorage-independent growth of TNBC cells in vitro **(Months 9-12) Completed and summarized in first year progress report and (D'Amato NC and Rogers T Cancer Research et al 2015).** Since TDO2 and AhR were upregulated by TNBC cells in suspension, we next tested their functional importance by assessing whether pharmacological inhibition or genetic knockdown could reduce anchorage-independent growth in soft agar or increase sensitivity of TNBC cells to anoikis in forced suspension culture. BT549 and SUM159PT cells were pre-treated in the attached condition with vehicle, the TDO2 inhibitor 680C91, or the AhR antagonist CH-223191 for 24hrs. Then an equal number of cells were plated in soft agar in the continued presence of treatment. Both 680C91 and CH-223191 significantly decreased anchorage-independent growth of BT549 and SUM159PT cells in soft agar (Figure 3A). To test the effect of Kyn on anoikis resistance, we treated cells in forced suspension culture for 48hrs with Kyn, and found that this significantly decreased apoptosis as measured by cleaved caspase activity compared to vehicle control treatment (Figure 3B). We then performed knockdown of TDO2 and AhR using two shRNA constructs each, and decreased protein expression was confirmed by western blot (Figure 3C). Knockdown of either TDO2 or AhR also significantly decreased growth of BT549 cells in soft agar (Figure 3D). Knockdown of either TDO2 or AhR also significantly increased apoptosis in BT549 and MDA-MB-231 cells grown in suspension for 48hrs (Figure 3E), demonstrating that TDO2 and AhR promote survival in anchorage-independent conditions. We have yet to determine if overexpression of TDO2 increases anchorage independent in vitro, but we have acquired a TDO2 overexpression vector that can be stably transduced into breast cancer cell lines (TNBC, luminal (ER+), immortalized normal mammary epithelial cells like the MCF-10A) and selected using puromycin.

Aim 2: Test whether inhibition of TDO2 and AhR affects the ability of TNBC to survive in the bloodstream following tail vein injection or to metastasize in vivo from the orthotopic site.

Task 1. Determine if TDO2 activity is critical for short term survival of TNBC cells in the vasculature (testing anoikis resistance in vivo) **(Months 13-16)** Completed and shown in Figure 6 of **(D'Amato NC and Rogers T Cancer Research et al 2015).** To test the potential contribution of TDO2 activity to the metastatic capacity of TNBC cells in vivo, we grew luciferase-expressing MDA-MB-231 cells in forced suspension conditions for 48hrs in the presence of either vehicle control or the TDO2 inhibitor 680C91. 250,000 viable cells, as determined by trypan blue staining, were then injected into the tail vein of NOD/SCID mice and luminescence was monitored over time. Seven days after injection, mice that received vehicle-treated cells had significantly higher luminescence, and this significant difference was maintained throughout (Figure 6A-B). At the conclusion of the experiment at Day 28 post-injection, lung luminescence was measured ex-vivo, and lungs from mice that received vehicle-treated cells had significantly higher luminescence compared to mice that received cells treated with the TDO2 inhibitor (Figure 6C). A significant decrease in the number of metastatic nodules in the lungs from mice receiving cells treated with 680C91 was also observed by H&E (Figure 6D). Together, these data demonstrate that TDO2 inhibition decreases the ability of TNBC cells to successfully metastasize following tail vein injection in vivo. As previously mentioned in our SOW, we planned on treating immune competent mice next systemically with 680C91 in their drinking water and then observing if metastasis was affected. The TDO2 inhibitor 680C91 has been previously shown to have poor stability *in vivo*. To circumvent this issue, we acquired a 2nd generation TDO2 inhibitor (LM10) from the Ludwig Institute for Cancer Research in Belgium through a materials transfer agreement (MTA), but we also acquired one from Curadev and are testing them both side by side in vitro to determine which to go with in vivo.

Task. 2. Determine if pharmacological inhibition of TDO2 decreases metastasis following tail vein injection **(Months 17-20) Completed** published in Figure 6 of **(D'Amato NC et al Cancer Research et al 2015).**

Task 3. Determine if treatment with a small molecule inhibitor of TDO2 decreases metastasis of TNBC cells from an orthotopic xenograft model (**Months 21-24**). **Not yet complete**. We are still determining whether the LM10 is the best TDO2 inhibitor inhibitor to use. It supposedly is more stable in vivo but does not seem to work for us in vitro well. We also want to knock down expression of TDO2 for comparison with TDO2 pharmacologic inhibitor to show that the effects are on target. New inhibitors that will target both IDO and TDO2 are in the pipeline and we want to test them. This was a big topic of discussion at the AACR meeting this year.

Aim 3: Identify the role of kyn paracrine action in tumor-induced immune modulation via AhR-expressing effector T cells. (Months 1-36) (100% complete). We have submitted these results to Mol Can Research two weeks ago and the paper is attached here as paper 2 in the appendix.

Task 1. Determine whether conditioned media from TNBC in suspension with or without TDO inhibition alters the number and function of effector T cells via the Kyn-AhR pathway (Months 1-15) (Complete)
We have determined that TDO2 is upregulated under anchorage independent conditions and by inflammatory signals (see figures 2 and 3) and as reported above, that it facilitates metastasis. The first paper in the appendix by Rogers et al also shows why TDO2 (normally expressed in the liver and placenta) can be expressed in TNBC, but not ER+ breast cancer.The second paper in the appendix from Greene LI et al in appendix shows results for all of the following subtasks. We first tested the effects of purified kynurenine on primary human T cells isolated from healthy donors and these results are shown in Figure 1.

Figure 1: Increased kynurenine leads to primary human CD8 T cell death, which is reversed by an AhR antagonist. (A) *Representative example of gating strategy for flow cytometric analysis: CD8 T cells were gated based on double positivity for CD8 (PE-Cy7) and CD3 (PerCP-Cy5.5). Cell death was determined by positive staining for the fixable viability stain BV421. Proliferation was measured by CFSE dilution.* ***(B)*** *Cells were activated with CD3 and CD28 antibodies for 5 days in the indicated concentration of kynurenine and CD8 T cell death was determined. Each dot represents cells from one human donor. N=9 donors, mean with standard deviation, one-way ANOVA.* ***(C)*** *Cells were treated with kynurenine as described in (B) and assayed for CD8 T cell proliferation. N=9 donors, one-way ANOVA.* ***(D)*** *Representative images (10x magnification) of CD8 T cells on activation Day 5 that were treated with indicated concentrations of kynurenine and either 10 µM of the AhR antagonist CH-223191 (AhRa) or DMSO.* ***(E)*** *CD8 T cells were activated, treated with 10 µM AhRa or vehicle control (DMSO), and assayed for cell death. N=6, mean with standard deviation, paired t-tests.*

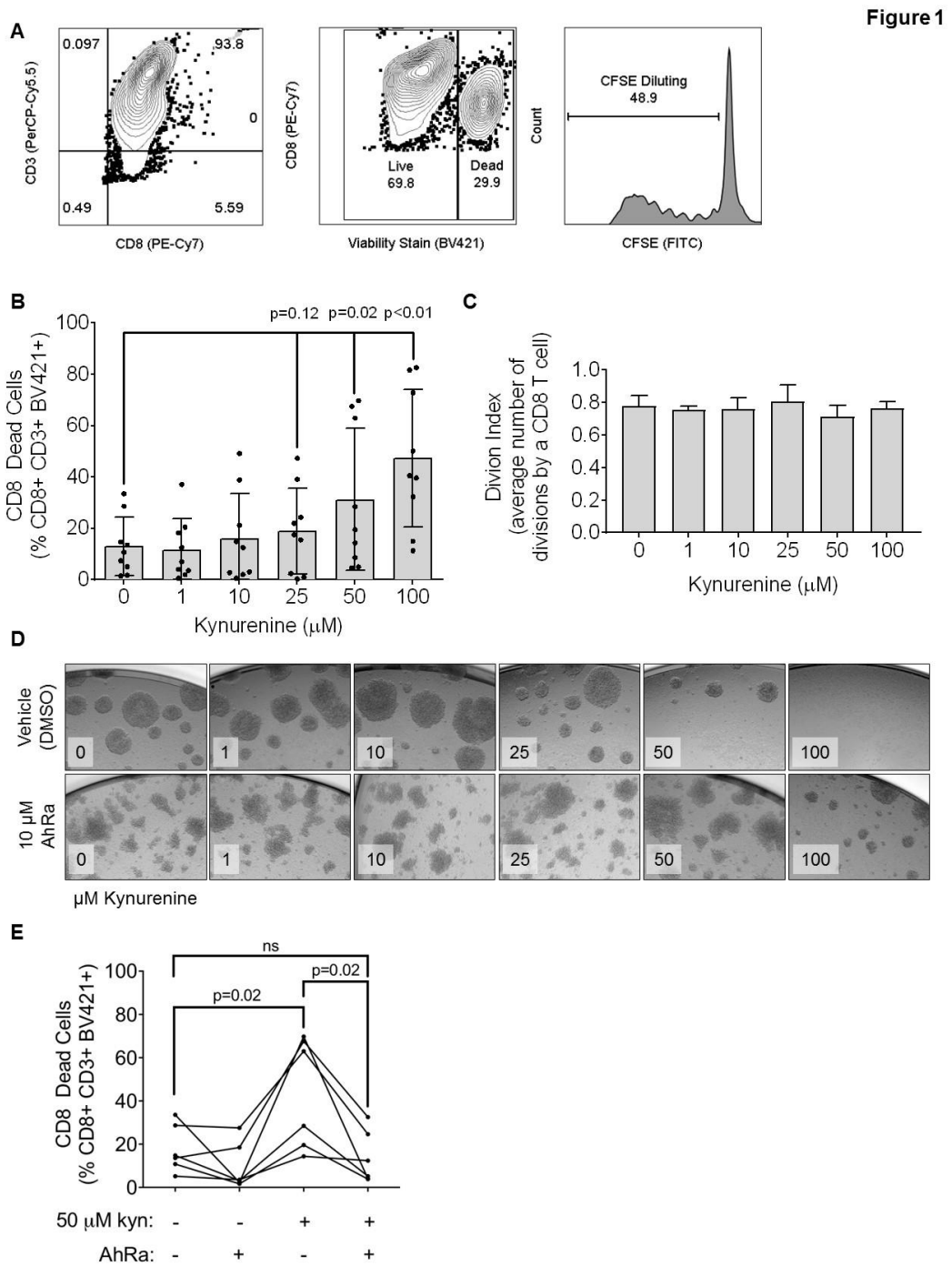

Figure 2 in the 2nd paper in the appendix, shown below, contains results for all of Task 1. We found that conditioned media (particularly from the TNBC cells grown in anchorage independent conditions increases CD8 T-cell viability. Our data also suggest that TDO2 inhibition more so that AhR inhibition contributes to lessening the effect of suspended conditioned media on the CD8 T-cells. The impact of conditioned media on T-regs is still being investigated, but we were able to detect an increase in CD4+,CD25+, Foxp3+ cells in the presence of purified kynurenine.

Figure 2 (in paper) legend: The effect of conditioned media from suspended TNBC cells on primary human CD8 T cells is similar to that of purified kynurenine, and is reversed by TDO2 inhibitor 680C91. ***(A)*** *Conditioned media was collected from BT549 TNBC cells grown in attached (ATT) or suspended (SUS) culture conditions for either 24 or 48 hours as indicated. CD8 T cells were isolated from the blood of normal donors and activated for 5 days with CD3 and CD28 antibodies in the conditioned media. Each line represents the response of CD8 T cells from one donor. Cell death was measured as described in Figures 1A and B. N=9, paired t-tests.* ***(B)*** *Representative flow cytometric analysis of CD8 T cells for IFNγ production is shown.* ***(C)*** *IFNγ production by CD8 T cells cultured in conditioned media for 48 hours. N=7, paired t-tests.* ***(D)*** *CD8 T cells were activated in conditioned media and either 0.1 μM 680C91 (to inhibit TDO activity) or vehicle control (DMSO). Each line represents the response of CD8 T cells from one human volunteer donor. N=5, paired t-tests.* ***(E)*** *CD8 T cells were activated in conditioned media and treated with either 10 μM CH-223191 (to inhibit AhR activation) or vehicle control (DMSO). N=5, paired t-tests.*

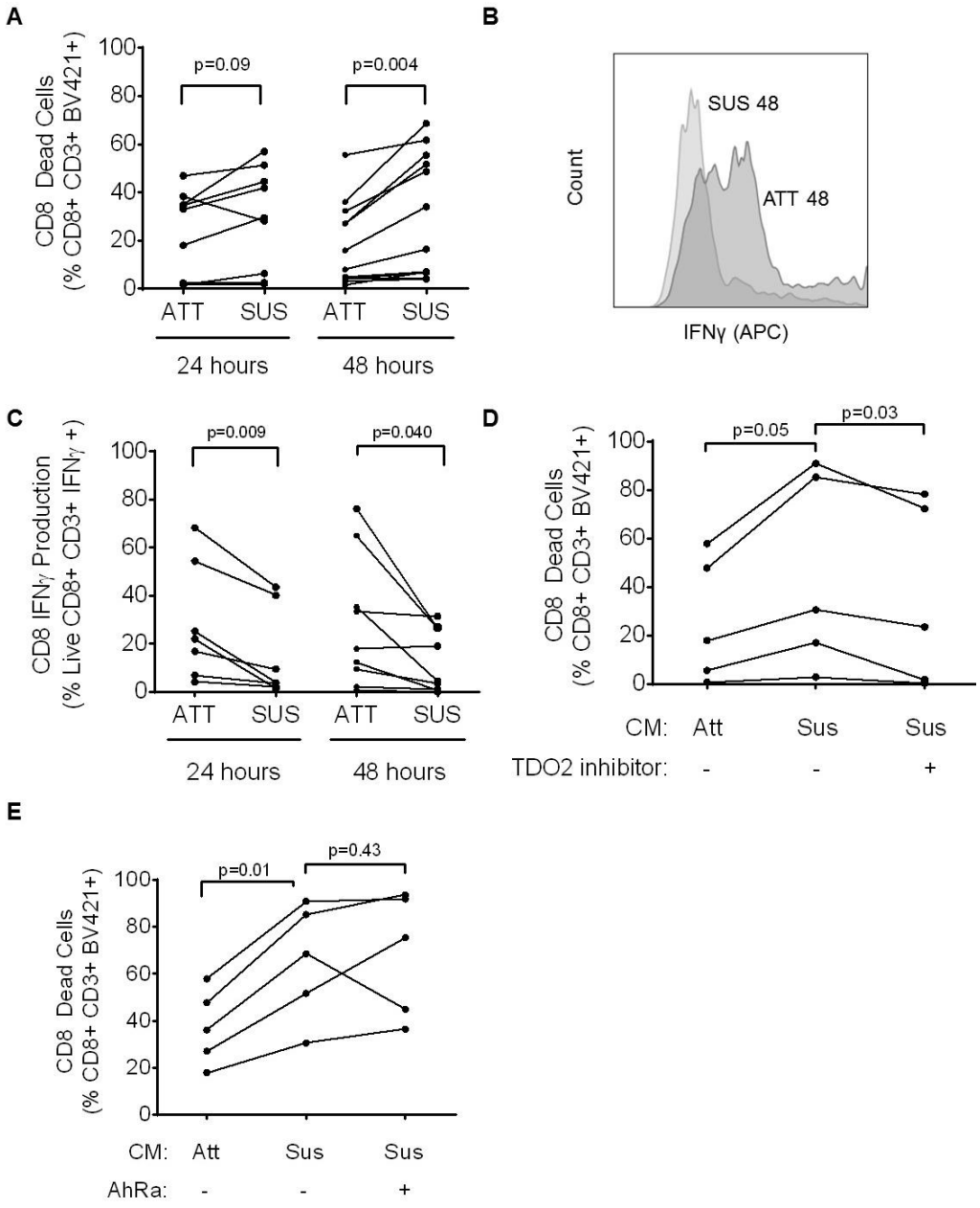

a. Isolate CD8+ and CD4+ T cells from normal donors and breast cancer patients. CD8+ and CD4+ T-cells were isolated from the blood of healthy donors under the IRB-approved protocol using positive selection kits (Dynabeads, Invitrogen) to get a pure population of CD3+ CD8+ T-cells from the blood of a healthy volunteer donors.

b. Activate T cells by coculture with αCD3 and αCD28 in the presence of conditioned media of TNBC cells (SUM-159 and BT549) grown in either attached condition, suspended, or suspended + 680C91. T-cells were successfully activated over the course of 5 days using soluble anti-CD28 (1 ug/ml) and plate-bound anti-CD3 (0.5 ug/ml). The concentration of anti-CD3 and the number of T-cells plated were optimized to ensure good activation without over-stimulating the T-cells.

c. Analyze T cell subsets by flow cytometry, and test proliferative capacity by CFSE, T cell viability using a fixable viability stain, and the generation of Treg cells (CD4+,FoxP3+,CD25+). After the 5-day activation in conditioned media from TNBC cells that were grown in attached, suspended, or suspended + 680C91 conditions, T-cells were analyzed using flow cytometry. The proliferative capacity of the T-cells was

measure by CFSE dilution (% diluted), and T-cell death was measured by incorporation of a fixable viability dye (eBioscience). The results of these experiments were shown in the last progress report.

d. Test for functional Treg induction by coculture of stimulated CD8+ T cells from normal donors with CD4+ FoxP3+CD25+ Treg cells generated in the presence of conditioned media from TNBC cells grown in either attached condition, suspended, or suspended + 680C91. The T-reg functionality assays are being optimized with the help of Dr. Jill Slansky's laboratory.

Task 2. Analyze the cytokine production of T cells stimulated with and without the TNBC-conditioned media and determine if similar cytokines are present in women with metastatic TNBC, including the AhR expression in their T cells in comparison to healthy donors **(Months 5-15). (50% complete).**

a. Isolate CD8+ and CD4+ T cells from normal donors and breast cancer patients. Completed. See Figure 2 in paper 2 in appendix**.** Activate T cells by coculture with αCD3 and αCD28 in the presence of conditioned media of TNBC cells grown in either attached condition, suspended, or suspended + 680C91.

b. Analyze cytokines produced by T cells using Proinflammatory Panel 1 multiplex detection kit (MesoScale Discovery) and by using intracellular stains for interferon-gamma and granzyme-B followed by flow cytometry. We are still optimizing the Mesoscale multiplex detection kit, but we have used intracellular stains for interferon-gamma and granzyme B and analyzed these stains using flow cytometry. We found that conditioned media from suspended TNBC cells (BT549) does reduce interferon gamma production by CD8 T-cells. T (Figure 2 in paper and above).

c. Perform western blotting and qRT-PCR to assess levels of AhR and AhR target genes such as CYP1A1 and CYP1B1 in T cells culture in different conditioned medias. These experiment are in progress.

d. Perform western blotting using nuclear/cytosolic fractionation to assess changes in nuclear localization of AhR in T cells cultured in different conditioned medias**.** These experiments are in progress.

Task 3. Determine if metastatic potential of a syngeneic mouse breast cancer model can be altered by TDO inhibition and whether there is alteration of the tumor immune microenvironment with decreased infiltration and/or function of the tumor-infiltrating lymphocytes (**Months 15-36**). Received institutional IACUC approval as well as DOD approval. These experiments will be done this year.

e. $7x10^3$ GFP-luciferase expressing 66CL4 murine breast cancer cells will be injected into the mammary fat pad of six to eight-week-old female BALB/c mice. Cells will be pretreated with 680C91 or vehicle control for 24hrs. Mice will receive either 160mg/kg/day 680C91 or LM10 or vehicle in drinking water (10 mice per group – 4 groups)

f. Monitor luciferase expression via IVIS imaging twice per week

g. At day 25 post-injection remove tumor, spleen, and lymph nodes

h. Tumors will be stained by IHC to assess immune cell infiltration, cytokine expression, and TDO2 and IDO expression. Multiple immune cell types will be assessed

i. CD4+ and CD8+ T cells from tumor tissue, spleen, and lymph nodes will be dissociated and identified, then stained for markers of activation, generation of Tregs, or exhaustion by flow cytometry

We have waited on the experiments above to identify the best TDO2 inhibitor for the in vivo experiment, particularly. The drugs in clinical trials currently target IDO and not TDO2. Both of these enzymes evolved to catabolize tryptophan to the same metabolites including kynurenine, but all of our data and the publically available data shown blow, indicate that TDO2 is more relevant in breast cancer. We applied for and received a no cost extension to conduct these experiments (documentation in appendix after manuscripts).

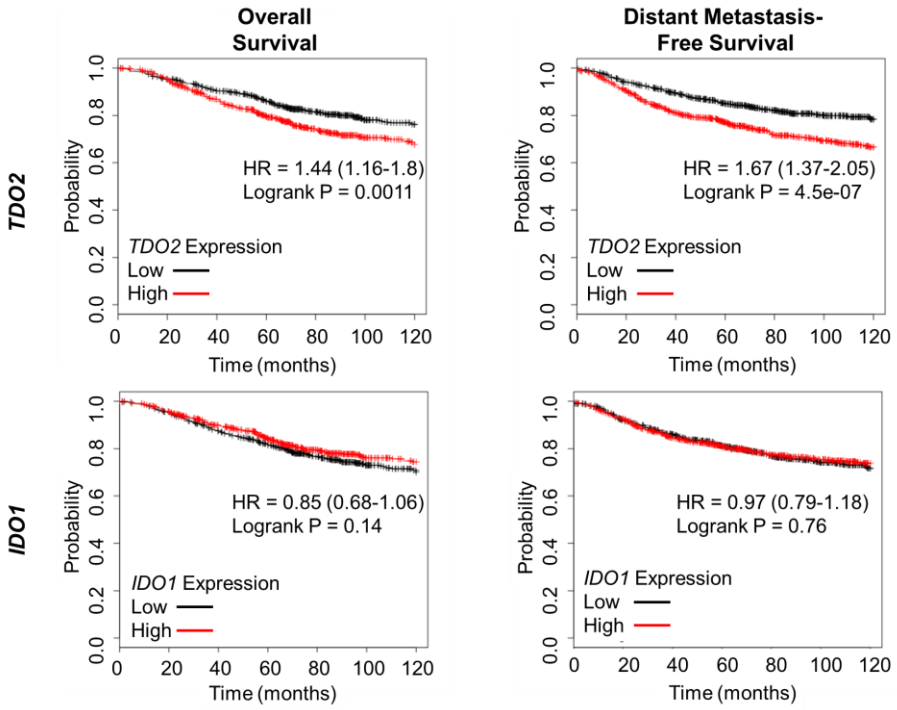

Figure 3: TDO2 expression correlates with breast cancer outcomes, while expression of the more commonly studied IDO1 does not. (A) *Patients were split into TDO2-high (red, n=699) or TDO2–low (black, n=703) groups based on median TDO2 gene expression. Overall survival (left) and distant metastasis-free survival (right) was plotted using KmPlot.com.* ***(B)*** *Patients were split into IDO1-high (red, n=701) or IDO1–low (black, n=701) groups based on median gene expression, and overall survival and distant-metastasis free survival was plotted. N=1402, hazard ratios are given with 95% confidence intervals, logrank test.*

Task 4. Determine whether kynurenine effects the cytotoxic function of CD8+ T-cells *in vivo* using an *in vivo* cytotoxicity assay (**Months 27-30**) will be completed this year.

j. Treat 66CL4 cells with 680C91 or LM10 or vehicle and Mitomycin C. Stain these cells and non-specific syngeneic (BALB/c background) spleen cells with different concentrations of carbofluorescein succinimidyl ester (CFSE): 66CL4 cells will be labeled with 10 uM CFSE, and splenocytes will be labeled with 1 uM CFSE

k. Inject 2.5 million cells of each target intravenously into female BALB/C mice (10 mice per group – 2 groups)

l. 24 hours later, isolate spleen and draining lymph nodes and isolate lymphocytes. Quantify relative numbers of cells using flow cytometry to determine the number of cells in the two peaks of CFSE staining (%CFSE-low cells)/(%CFSE-high cells).

What opportunities for training and professional development has the project provided? Two graduate students, Thomas Rogers and Lisa Greene are the graduate students that have worked on this project. **Thomas Rogers, Cancer Biology Doctoral Candidate 5th yr,** had obtained a F31 NRSA as reported in the last progress report, but the NCI had a new mechanism, the F99/K00 Predoctoral to Postdoctoral Fellow Transition Award (F99/K00) and Thomas was the student selected from a competitive pool at our institution to submit an application for this new mechanism and he was awarded this grant: NCI 1F99CA212230-01 (NCI Predoctoral to Postdoctoral Fellow Transition Award) Title: Targeting a Kynurenine-Driven Autocrine Loop to Block Triple-negative Breast Cancer Metastasis Dates: 09/19/2016-8/31/2018 As a result of obtaining this award, which funds his postdoctoral work after he obtains his doctorate degree focusing for his work with me, Thomas Rogers interviewed the following prestigious places for a postdoctoral position: Dr. Costas Lyssiotis- University of Michigan, Dr. Jason Locasale- Duke University, Dr. Dan Nomura- University of California-Berkeley and Dr. Ralph DeBerardinis- UT Southwestern. Thomas decided to go with Dr. Ralph DeBerardinis, who is very well regarded in the field of tumor metabolism. Thomas defended his dissertation at the end of June 2017 and moved to Dallas to start his postdoctoral fellowship last fall.

Lisa Greene, Cancer Biology Doctoral Candidate 4th yr, also obtained a F31 NRSA (Ruth L. Kirschstein National Research Service Award), "Targeting TDO2 as a mediator of T-cell function in triple-negative breast cancer." NIH NCI 1F31CA203486. 2016-2019. Dates: 03/07/2016-3/07/2019. She just defended her dissertation on this topic and has decided to go to medical school. After being accepted at 5 different schools she has decided to attend Northwestern University Feinberg School of Medicine in the fall of 2018.

How were the results disseminated to communities of interest?

In June 2016 Dr. Richer gave a lecture at the Lankenau Institute for Medical Research, Philadelphia, PA guest of LIMR Director George Prendergast, Ph.D. who works on IDO in cancer, entitled "Kynurenine Pathway and TDO2 in Triple Negative Breast Cancer."

Dr. Richer also gave a talk on this topic at the Endocrine Society: March 2018 for an invited Symposium presentation: Steroid Receptors and Inflammation titled "Triple-Negative Breast Cancer Highjacks a Developmental Program of Immune Suppression."

What do you plan to do during the next reporting period to accomplish the goals? This coming year we will complete Aim 3 Tasks 2-4. Determine if treatment with a small molecule inhibitor of TDO2 decreases metastasis of TNBC cells from an orthotopic xenograft model. We will also be conducting Task Aim 3 to Determine if metastatic potential of a syngeneic mouse breast cancer model can be altered by TDO inhibition and whether there is alteration of the tumor immune microenvironment with decreased infiltration and/or function of the tumor-infiltrating lymphocytes

4. **IMPACT:**
    - **What was the impact on the development of the principal discipline(s) of the project?** "

      This research strongly suggests that TDO2 is likely the primary enzyme that catabolizes tryptophan that should be targeted in breast cancer and that by targeting this enzyme we may be able to reduce breast cancer metastasis by decreasing the tumor cell's ability of the cells to survive in suspension, but also reverse their ability to suppress the immune system.

    - **What was the impact on other disciplines?** Nothing to Report.
    - **What was the impact on technology transfer?**
        - This project is likely to make an on commercial technology because it shows evidence that TDO2 is likely the primary enzyme that catabolizes tryptophan that should be targeted in breast cancer. The current drugs that are in clinical trials target IDO, not TDO2.
    - **What was the impact on society beyond science and technology?** Gave two trainees great opportunities to present their work and further their career development.

5. **CHANGES/PROBLEMS:** *e:*
    - **Changes in approach and reasons for change** *comparing TDO2 inhibitors to direct knockdown of TDO2.*
    - **Actual or anticipated problems or delays and actions** *None*
    - **Changes that had a significant impact on expenditures** *None*
    - **Significant changes in use or care of human subjects, vertebrate animals, biohazards, and/or select agents**
        - *Also specify the applicable Institutional Review Board/Institutional Animal Care and Use Committee approval dates. Approval of IACUC protocol was awarded*
    - **Significant changes in use or care of human subjects.** None

- **Significant changes in use or care of vertebrate animals.** None
- **Significant changes in use of biohazards and/or select agents.** None

6. **PRODUCTS:**
   - **Publications, conference papers, and presentations.**. The manuscript listed below was a result of this project and two submitted manuscripts are attached in the appendix and the presentations are listed above

Journal publications:
D'Amato NC, **Rogers TJ***, Gordon MA, Greene LI, Cochrane DR, Spoelstra NS, Nemkov TG, D'Alessandro A, Hansen KC, Richer JK. A TDO2-AhR Signaling Axis Facilitates Anoikis Resistance and Metastasis in Triple-Negative Breast Cancer. Cancer Res. 2015 Nov 1;75(21):4651-64. PubMed PMID: 26363006; PubMed Central PMCID: PMC4631670. DOD support was acknowledged.

Manuscripts submitted:

Greene LI, Bruno TC, Christenson JL, Borges VF, Slansky JE, and **JK Riche**r. A role for tryptophan 2,3-dioxygenase in CD8 T cell suppression and evidence of tryptophan catabolism in breast cancer patient plasma. Submitted 2018.

An immune-suppressive program reminiscent of fetal trophoblasts enabled by loss of microRNA-200c in triple negative breast cancer. Rogers TJ, Greene LI, Christenson JL, O'Neill K, Williams MM, Gordon MA, Nemkov T, D'Alessandro A, Degala G, Shin J, Tan AC, Torkko K, Lambert J and **JK Richer**. Submitted 2018.

Website(s) or other Internet site(s)
None at this time.

Technologies or techniques
None at this time.

Inventions, patent applications, and/or licenses
None at this time.

Other Products
Identify any other reportable outcomes that were developed under this project. Examples include:

- biospecimen collections: FFPE blocks of lungs with metastases of MDA-MB-231 xenografts of tumors pretreated with or without TDO2 inhibitor
- research material: knowledge of PDX that express TDO2 or AhR.

7. **PARTICIPANTS & OTHER COLLABORATING ORGANIZATIONS**
   - **What individuals have worked on the project?** WE had technical support from Michelle Borakove in the laboratory of our collaborating oncologist, Dr. Virginia Borges as well as animal technician Beatrice Babbs in the Richer lab, Greg Degala for western blots and tissue culture and Nicole Spolestra for tissue culture and IHC. Angelo Allesandro who directs the metabolomics lab was on the grant for all measurements of tryptophan and kynurenine in the media from TNBC.
   - **Has there been a change in the active other support of the PD/PI(s) or senior/key personnel since the last reporting period?**
     - No

- **What other organizations were involved as partners?**
  - *No*

8. **SPECIAL REPORTING REQUIREMENTS** N/A

9. **APPENDIX**

Two submitted manuscripts and the no cost extension are presented in the appendix.

Modulation of Epithelial to Mesenchymal Transition by miR-200c Alters Tryptophan Catabolism and a Program of Immune Suppression in Triple Negative Breast Cancer

Thomas J. Rogers[1], Jessica L. Christenson[1], Lisa I. Greene[1], Kathleen I. O'Neill[1], Michelle M. Williams[1], Michael A. Gordon[1], Travis Nemkov[2], Angelo D'Alessandro[2], Greg D. Degala[1], Jimin Shin[3], Aik-Choon Tan[3], Diana M. Cittelly[1], James R. Lambert[1] and Jennifer K. Richer[1]

[1]Department of Pathology, University of Colorado Anschutz Medical Campus; [2]Department of Biochemistry and Medical Genetics, University of Colorado Anschutz Medical Campus; [3]Department of Medical Oncology, University of Colorado Anschutz Medical Campus, Aurora, CO USA

RUNNING TITLE
miR-200c Targets TDO2 in Triple-Negative Breast Cancer

KEYWORDS
Tryptophan-2,3-dioxygenase, TDO2, microRNA-200, triple-negative breast cancer, anti-tumor immunity

FINANCIAL SUPPORT
DOD BCRP Breakthrough Level 2 award W81XWH-15-1-0039 to JKR; CU Cancer Center's Women's Event/The Salah Foundation to JKR; F99 CA212230-01 NCI Pre to Postdoctoral Fellow Transition Award to TJR; NRSA T32 CA190216-01A1 to JLC; NRSA F31 CA203486-01A1 to LIG.

CORRESPONDING AUTHOR
Jennifer K. Richer, Ph.D.
Department of Pathology
University of Colorado, Anschutz Medical Campus
12800 E 19th Ave
Aurora, CO 80045, USA
Phone: (303) 724-3735
Fax: (303) 724-3712
Email: jennifer.richer@ucdenver.edu

CONFLICTS OF INTEREST
The authors declare no competing interests.

WORD COUNT:

FIGURES: 9 (5 supplemental)

TABLES: 2 (2 Supplemental)

Abstract (196/250)

Tryptophan-2,3-dioxygenase (TDO2), a rate-limiting enzyme of tryptophan catabolism, is induced in triple negative breast cancer (TNBC) cells by inflammatory signals and anchorage independent conditions. The tryptophan catabolite kynurenine activates the aryl hydrocarbon receptor and promotes anchorage independent survival, invasiveness and lung colonization in a TNBC preclinical model. Here we sought to identify mechanism(s) that permit TNBC to express TDO2 and other genes/proteins not expressed by estrogen receptor alpha positive (ER+) breast cancer cells. The microRNA-200c, is extremely low in TNBC compared to ER+ lines and targets and represses genes involved in epithelial to mesenchymal transition (EMT). In addition to reversing a large majority of a pan-EMT signature, restoration of miR-200c significantly reduced TDO2, consequent kynurenine production, and multiple other immune-suppressive factors including TDO2, PD-L1/2, HMOX-1, and GDF-15. Thus, manipulation of miR-200c divulged a mechanism whereby TNBC hijack a gene expression program reminiscent of that used by trophoblasts to achieve fetal tolerance. TNBC can thereby utilize multiple methods beyond the proximity-dependent action of PD-L1 to evade immune attack. Knowledge of the transcriptional and post-transcriptional regulation of tumor derived immune-suppressive factors may facilitate development of novel therapeutic strategies that complement current immunotherapy to reduce mortality for TNBC patients.

Implication: Loss of miR-200c permits TNBC to hijack a program of immune-suppressive factors.

Introduction

Triple-negative breast cancer (TNBC), which lacks expression of estrogen receptor (ER), progesterone receptor (PR), and amplification of the growth factor receptor HER2, accounts for between 10-20% of all breast cancers diagnosed. Currently there are no FDA approved targeted therapies for this aggressive breast cancer subtype. TNBC recurs more often and more rapidly than other subtypes, with peak risk of recurrence following surgery at 1-3 years [1]. If metastatic at time of initial diagnosis, TNBC has a ~~poor prognosis, with~~ median survival of 13 months [2, 3]. This poor prognosis is thought, at least in part, to be due to . ~~It is thought t~~that the ~~poor prognosis of TNBC is~~ at ~~least in part due to~~ high metastatic potential, facilitated by an oncogenic epithelial to mesenchymal transition (EMT) that enhances invasiveness and anchorage independence. Indeed partial EMT or mixed populations facilitate metastasis in preclinical models [4] and circulating breast tumor cells enriched for EMT markers increase with patient relapse [5].

ER positive breast cancer cell lines, which maintain epithelial markers, undergo significant programmed cell death under anchorage independent conditions (termed “anoikis” [6]), while TNBC ~~cell~~ lines are relatively resistant to anoikis due to altered protein expression [7, 8] and multiple metabolic changes [9], including increased tryptophan catabolism via the enzyme tryptophan-2,3-dioxygenase (TDO2) [10]. The enzymes indoleamine 2,3-dioxygenase 1 (IDO1), IDO2, or TDO2 can mediate the rate limiting step of tryptophan catabolism. Under anchorage independent conditions, human TNBC ~~cell~~ lines increase intracellular and secreted levels of the tryptophan catabolite kynurenine (Kyn), via increased TDO2 levels and activity, while ER+ breast cancer lines are unable to upregulate TDO2, and *TDO2* mRNA is higher in tumors from patients with ER- disease as compared to ER+ [10].

Increasing evidence supports a tumor promotional role of tryptophan catabolism in many solid tumor types, including breast cancer. Tryptophan catabolism produces Kyn metabolites and also facilitates *de novo* synthesis of NAD^+. Kyn functions in an autocrine fashion by binding to

the aryl hydrocarbon receptor (AhR) in tumor cells leading to enhanced survival [10-12] and in a paracrine fashion, by binding to AhR in CD8+ T-cells, to suppress anti-tumor activity [11, 13, 14], or by expanding the regulatory T-cell population to exhaust the anti-tumor response [13].

The microRNA-200 (miR-200) family is highly expressed in normal epithelial cells and in well-differentiated ER+ breast cancer as compared to TNBC [15, 16]. K~~These miRNA are k~~nown as "guardians of the epithelial phenotype" members of this miRNA family ~~because they~~ are potent suppressors of EMT via direct targeting of Zinc Finger E-Box Binding Homeobox 1 and 2 (ZEB1/2) and other transcriptional repressors of E-cadherin [17, 18]. In fact miR-200 family members directly target numerous mesenchymal, neuronal and embryonic stem cell genes, such that their loss in TNBC allows aberrant expression of "non-epithelial" proteins that facilitate multiple steps in the metastatic cascade [19, 20]. R~~Interestingly, r~~estoration of miR-200c in a genetically engineered mouse model of claudin-low TNBC dramatically decreased metastasis [21], though a role for the immune system was not examined in that study. Recently, EMT was shown to affect immune function and metastasis in a mouse mammary carcinoma syngeneic model [22].

Here we report that restoration of miR-200c to TNBC not only reversed a pan-EMT gene signature, but also significantly decreased TDO2 ~~expression and both~~ and consequent production of intracellular and secreted Kyn. Indeed, restoration of miR-200c reversed a program of immunosuppressive factors, many of which are typically made by placental trophoblasts to achieve fetal tolerance during pregnancy.

Materials and Methods

Cell Lines

All cell lines were authenticated by Short Tandem Repeat DNA Profiling (Promega; Fitchburg, WI) at the University of Colorado Cancer Center (UCCC) Tissue Culture Core, and tested for mycoplasma every three months. Only cells under five passages were used in this study. Hs578T and SUM159PT cells were purchased from the UCCC Tissue Culture Core and the rest directly from ATCC. SUM159PT (SUM159) cells were grown in Ham's F-12 with 5% fetal bovine serum (FBS), penicillin/streptomycin (P/S), hydrocortisone, insulin, HEPES and L-glutamine supplementation. BT549 were cultured in RPMI Medium 1640 with 10% FBS, P/S and insulin. MDA-MB-453 (MDA-453), were grown in DMEM Medium with 10% FBS and P/S.MDA-MB-231 (MDA-231) were grown in MEM with 5% FBS, HEPES, L-glutamine, nonessential amino acids, and insulin. MCF7 cells were obtained from Dr. Kate Horwitz at the University of Colorado Anschutz Medical Campus and were grown in DMEM with 10% FBS and L-glutamine.

Reagents

Interlukin-1 beta (IL-1β) and tumor necrosis factor alpha (TNF-α) were purchased from Affymetrix eBioscience and used at a final concentration of 10ng/µl. Negative, scrambled control (SCR) or miR-200c mimics were purchased from Ambion and used at a final concentration of 50nM. miRNA mimic and luciferase reporter transfections were performed using either RNAi Max or Lipofectamine 3000 purchased from Thermo Fisher Scientific and experiments were conducted following the supplied protocols. The TDO2 overexpression plasmid (TDO2-OE) and its corresponding empty vector (EV) control were obtained from Sino Biological, catalog # HG13215-UT and CV011.

I~~Generation of I~~nducible system for miR-200c expression

BT549 cells were transduced with the doxycycline (DOX) inducible lentiviral vector pTripZ (Dharmacon) encoding the precursor sequence for miR-200c (pTripZ-200c). Control cells were

transduced with pTripZ empty vector (pTripZ-EV, pooled population). Stable expression was selected using 1 µg/mL puromycin, and multiple pTripZ-200c clones were tested to identify which had low/absent background expression of miR-200c and at least 500-fold expression of miR-200c in the presence of 1 µg/mL doxycycline (DOX) inducer.

Sample Preparation/UHPLC-MS analysis of cell lines

Cells were counted, pelleted at 1500xG at 4ºC, and stored at -80°C until analysis. Prior to LC-MS analysis, samples were placed on ice and re-suspended with methanol:acetonitrile:water (5:3:2, v:v) at a concentration of 2 million cells per ml. Media samples were extracted with the same solution at a dilution of 1:25 (v/v). Suspensions were vortexed continuously for 30 min at 4°C. Insoluble material was removed by centrifugation at 10,000 g for 10 min at 4°C and supernatants were isolated for metabolomics analysis by UHPLC-MS. Briefly, the analytical platform employs a Vanquish UHPLC system (Thermo Fisher Scientific, San Jose, CA, USA) coupled online to a Q Exactive mass spectrometer (Thermo Fisher Scientific, San Jose, CA, USA). Samples were resolved over a Kinetex C18 column, 2.1 x 150 mm, 1.7 µm particle size (Phenomenex, Torrance, CA, USA) equipped with a guard column (SecurityGuard™ Ultracartridge – UHPLC C18 for 2.1 mm ID Columns – AJO-8782 – Phenomenex, Torrance, CA, USA) using an aqueous phase (A) of water and 0.1% formic acid and a mobile phase (B) of acetonitrile and 0.1% formic acid. Samples were eluted from the column using either an isocratic elution of 5% B flowed at 250 µl/min and 25ºC or a gradient from 5% to 95% B over 1 minute, followed by an isocratic hold at 95% B for 2 minutes, flowed at 400 µl/min and 30ºC. The Q Exactive mass spectrometer (Thermo Fisher Scientific, San Jose, CA, USA) was operated independently in positive or negative ion mode, scanning in Full MS mode (2 µscans) from 60 to 900 m/z at 70,000 resolution, with 4 kV spray voltage, 15 shealth gas, 5 auxiliary gas. Calibration was performed prior to analysis using the Pierce™ Positive and Negative Ion Calibration Solutions (Thermo Fisher Scientific). Acquired data was then converted from .raw to .mzXML file format using Mass Matrix (Cleveland, OH, USA). Metabolite assignments, isotopologue distributions, and correction for expected natural abundances of deuterium, ^{13}C, and ^{15}N isotopes were performed using MAVEN (Princeton, NJ, USA). Graphs, heat maps and statistical analyses (either T-Test or ANOVA), metabolic pathway analysis, PLS-DA and hierarchical clustering was performed using the MetaboAnalyst 3.0 package (www.metaboanalyst.com). Hierarchical clustering analysis (HCA) was also performed through the software GENE-E (Broad Institute, Cambridge, MA, USA). XY graphs were plotted through GraphPad Prism 5.0 (GraphPad Software Inc., La Jolla, CA, USA).

Quantitative RT-PCR

Total RNA was isolated using TRIZOL RNA Isolation (QIAGEN) according to the manufacturer's instructions. cDNA was synthesized with the qScript cDNA SuperMix (QuantaBio). qRT-PCR was performed in an ABI 7600 FAST thermal cycler. SYBR Green quantitative gene expression analysis was performed using ABsolute Blue qRT-PCR SYBR Green Low ROX Mix (ThermoScientific) and the following primers: *TDO2* forward 5'- CGGTGGTTCCTCAGGCTATC-3' and reverse 5'- CTTCGGTATCCAGTGTCGGG-3'; *IL6* forward 5'-AAGCCAGAGCTGTGCAGATGA-3' and reverse 5'- AACAACAATCTGAGGTGCCCA; *HMOX-1* forward 5'-CAGGCAGAGAATGCTGAGTTC-3' and reverse; *GDF-15* forward 5'-CTCAGGACGCTGAATGGCTCT-3' and reverse 5'-GGGTCTTGCAAGGCTGAGCTG-3'; *PD-L1* forward 5'-TATGGTGGTGCCGACTACAA-3' and reverse 5'-TGGCTCCCAGAATTACCAAG-3'; *ZEB1* forward 5'-TCCATGCTTAAGAGCGCTAGCT-3' and reverse 5'-ACCGTAGTTGAGTAGGTGTATGCCA-3'; *GAPDH* forward 5'-GTCAGTGGTGGACCTGACCT-3' and reverse 5'-AGGGGTCTACATGGCAACTG-3'; *β-actin*: FP-CTGTCCACCTTCCAGCAGATG RP-CGCAACTAAGTCATAGTCCGC. Taqman quantitative gene expression analysis for *miR-200c* and *U6* was performed with primer-specific reverse

transcriptase using the following TaqMan MicroRNA Assays (Applied Biosystems/ThermoFisher): *miR-200c* assay ID #002300; *U6* assay ID #001973. All experiments were performed in biological triplicate.

Immunoblotting

Whole-cell protein extracts (50 µg) were denatured, separated on SDS-PAGE gels, and transferred to polyvinylidene fluoride membranes. After blocking in 5% BSA in Tris-buffered saline–Tween, membranes were probed overnight at 4°C. The following antibodies were used in this study: TDO2 (Sigma, #HPA039611, 1:1000), HMOX-1 (Cell Signaling, #5061, 1:1000), ZEB1 (Sigma, #HPA027524, 1:2000), α-tubulin (Sigma, #T5168, 1:10,000), and β-Actin (Cell Signaling, #3700, 1:4000). Polyclonal antisera directed against GDF-15 was generated using the C-terminus peptide KTDTGVSLQTYDDLLA (Zymed, San Francisco, CA). Affinity purified GDF-15 antibody was prepared using the SulfoLink coupling resin according to the manufacturer's instructions (ThermoFisher, Waltham, MA). Following secondary antibody incubation, results were detected using Western Lighting Chemiluminescence Reagent Plus (Perkin Elmer; Waltham, MA). Densitometry quantifications were performed using ImageJ. First, all bands were normalized to their respective α-Tubulin or β-Actin loading control. The values shown in figures are reported as a fold change compared to either untreated cells or cells ~~that were~~ transiently transfected with scrambled mimic (SCR) or DOX.

Flow Cytometry

Single-cell suspensions of BT549 cells were prepared and stained using the anti PD-L1 (Clone MIH1, eBioscience) following manufacturer's instructions, then fixed in 1% paraformaldehyde and stored at 4º C until analysis. Flow cytometry was conducted using the BD LSRFortessa cell analyzer (BD Biosciences) and data were analyzed using FlowJo software (Tree Star, Inc.).

Gene expression array analysis

BT549-pTripZ-200c cells, plated in triplicate, were cultured in DOX for 48 hours. RNA was isolated using the RNeasy PLUS kit (Qiagen; Germantown, MD) and quality was measured on an Agilent 2100 Analyzer (Agilent Technologies; Santa Clara, CA), RIN (RNA integrity number) ranged from 9.6-10.0. Gene expression was measured using the Affymetrix Human Transcriptome 2.0 array hybridization performed by the University of Colorado Cancer Center Genomics and Microarray core facility. The data were deposited in the Gene Expression Omnibus (GEO) database as GSE108271. Data was analyzed by one-way ANOVA performed at the gene and probe (exon) levels using Partek Genomics Suite software (Partek; St. Louis, Missouri). Microarray data were normalized using Robust Multiarray Average method using Affymetrix Power Tools. Multiple probe sets for the same gene were collapsed using average expression. Genes with adjusted p-values using t-test and after multiple corrections (adj $P<0.1$) and fold change > 1.2 were selected as differentially expressed between the two groups. Gene Set Enrichment Analysis was performed using GSEA software and KEGG gene sets. Gene sets with $P< 0.05$ (after 1000 gene set permutations) were deemed to be enriched in each group.

Pan-carcinoma EMT signature analysis

To determine the EMT states of the untreated and DOX-treated BT549 cells, we compared our gene array results to the published pan-carcinoma EMT signatures from Mak et al [23]. The "pan-carcinoma EMT signature" genes were extracted from the normalized gene expression data of the untreated and DOX-treated BT549 cells. Unsupervised clustering was performed using CLUSTER 3.0 with Spearman correlation with average linkage. Cluster was visualized using Java TreeView.

Cloning of TDO2 3'UTR and Site-Directed Mutagenesis

The 3'UTR of TDO2 was amplified from the BAC plasmid RP11-401G24. Primers were designed to amplify the 3'UTR of TDO2 and to additionally add restriction enzyme cut sites for Sac1 (5' end) and Xho1 (3'end): XhoI-TDO2: AGACCG**CTCGAG**AATCGTCTGCAAAATCTATG SalI-TDO2: GAACGC**GTCGAC**TACAGGGAGAAAGATTAATAC. Once amplified, the insert was cloned into the pmiR-GLO vector (Promega) using the corresponding restriction enzyme cut sites. The pmiR-GLO vector containing the 3'UTR of TDO2 was confirmed by gel electrophoresis and its sequence confirmed by the DNA Sequencing Core at the University of Colorado (Aurora, CO).

Luciferase reporter activity

Reporter activation was determined using the Dual-Luciferase Reporter Assay System (Promega) according to the manufacturer's protocol. Briefly, cells were lysed for 15 minutes at room temperature using 1× passive lysis buffer. Lysed cells were collected and centrifuged at 14,000 rpm for 15 minutes at 4°C to eliminate cell debris. The supernatant was used immediately or diluted with 1× passive lysis buffer for determination of luciferase activity. For analysis, TDO2 3'UTR activity was normalized to the internal Renilla signal to control for differences in transfection efficiency.

Measurement of anchorage-independent growth

Soft-agar assays were performed in 0.5% bottom and 0.25% top-layer agar (Difco Agar Noble; BD Biosciences). Cells were fully embedded in the top-layer agar. Media was refreshed every 4 days.

Correlation Analysis of *LAT1* Expression and Breast Cancer Clinical Outcomes

To determine the correlation of *LAT1* and clinical outcomes in breast cancer patients, analysis was performed using the website KMplot.com (which integrates data from GEO, EGA, and TCGA databases). All subtypes were considered in this analysis of up to 1750 breast cancer patients.

Statistical analysis

Statistical analysis was performed using GraphPad Prism 5. Student t test, ANOVA with Tukey post-hoc test, and two-way ANOVA with Bonferroni multiple comparison test were used as noted. P values are denoted as follows: *, P< 0.05; **, P< 0.01; ***, P< 0.001; ****, P< 0.0001; ns, not significant.

Results

Restoration of miR-200c to TNBC cells leads to widespread reversal of not only an EMT signature, but also an immunosuppressive signature that includes *TDO2*

BT549 cells were engineered to express miR-200c in a doxycycline (DOX)-inducible manner using the TripZ system. BT549 cells were treated with or without DOX for 48 hours to induce miR-200c, RNA was collected, gene expression analysis performed, and unsupervised hierarchical clustering of the top 164 differentially expressed genes (P< 0.05, log-rank test) is shown in heatmap form in Figure 1A. qRT-PCR demonstrated that DOX induced a significant increase in miR-200c expression in BT549-Tripz-200c cells, but not in BT549-Tripz-EV cells, and that expression of the miR-200c target ZEB1 was significantly reduced at the mRNA and protein levels in DOX-treated BT549-Tripz-200c cells (Figure 1B) but not empty vector cells. Comparison of genes altered by induction of miR-200c in BT549-Tripz-200c cells to a recently

published ”pan-carcinoma EMT signature” [23] revealed that when miR-200c was increased in DOX-treated BT549 cells 60% (15/25) of the epithelial signature increased and 80% (41/51) of the mesenchymal signature decreased (Supplemental Figure S1A).

GSEA analysis revealed a previously unrecognized change in ~~that~~ a number of pathways involved in immune modulation ~~decreased in miR-200c-induced cells,~~ including allograft rejection, complement and coagulation pathways, cytokine/cytokine receptor signaling, and tryptophan metabolism~~-~~ in miR-200c-induced cells, (Figure 1C, Supplemental Figure 2, Supplemental Table S1). GSEA analysis of the genes involved in tryptophan metabolism revealed a number of Kyn pathway-specific genes suppressed by miR-200c including *TDO2*, *KMO*, and *KYNU* (Supplemental Table S1). Furthermore, we compared our array results from human TNBC cells with miR-200c restored to an immune-competent mouse model of triple-negative mammary carcinoma in which restoration of miR-200c decreased metastasis (GSE62230) [21] and found a significant number of overlapping genes, including *TDO2,* Heme oxygenase 1 (*HMOX-1*)*, CD274* Programmed death-ligand 1 *(PD-L1)*, and Inhibitor Of Nuclear Factor Kappa B Kinase Subunit Beta (*IKBKB*) (Supplemental Figure S1B). GSEA analysis also identified pathways upregulated following restoration of miR-200c including TCA cycle, oxidative phosphorylation and adherens junctions (Supplemental Table S2). The miR-200c-induced decrease in *TDO2*, ~~Programmed death-ligand 1 (~~*PD-L1/CD274*~~)~~, ~~Heme oxygenase 1 (~~*HMOX-1*~~)~~, and Growth Differentiation Factor 15 (*GDF-15*) was confirmed by qRT-PCR from RNA isolated from BT549 cells treated with DOX for 48 hours in an independent experiment from that used for the initial array data (Figure 1D; $P<0.05$)

TDO2 is a direct target of miR-200c, and restoration of miR-200c decreases TNBC kynurenine production

To further validate the decrease in TDO2 expression upon miR-200c restoration, four TNBC cell lines (BT549, Hs578T, MDA-453, and SUM159) were transiently transfected with either a miR-200c mimic or scrambled control (SCR) mimic for 48 hours. qRT-PCR revealed a decrease in *TDO2* mRNA in all four cell lines following miR-200c transfection (Figure 2A). Western blot analysis of whole-cell protein lysate showed a decrease in ZEB1 and a decrease in TDO2 following a 72 hour miR-200c transfection in three TNBC cell lines (Figure 2B). A predicted miR-200bc/429 binding site was identified using TargetScan in the *TDO2* 3’UTR (nucleotide position 5’-395-400-3’). To test whether miR-200c directly binds to and targets *TDO2,* the entire 3’UTR of *TDO2* was cloned downstream of luciferase in the pmiR-GLO reporter plasmid (Figure 2C). When this reporter was transfected into BT549 cells with miR-200c mimic or SCR, miR-200c significantly decreased luciferase activity compared to SCR. This effect was reversed upon mutation of the predicted binding site for miR-200c in the *TDO2* 3’UTR (Figure 2D). To test the impact of miR-200c and subsequent reduction in TDO2 protein on tryptophan catabolism in TNBC, UHPLC-MS was performed following miR-200c induction in the BT549 TripZ DOX-inducible system for 72 hours. Both intracellular and secreted Kyn levels were significantly reduced (Figure 2E). These effects were also observed following transient transfection with miR-200c in the Hs578T and MDA-453 TNBC cell lines (Figure 2E).

Exogenous expression of TDO2 in ER+ breast cancer cells increases anchorage independent growth

We previously reported that TDO2 mRNA and protein are very low or undetectable in ER+ breast cancer cells and these cells do not survive well under anchorage independent conditions compared to TNBC lines [10]. Therefore, to determine whether increased TDO2 would promote anchorage independent survival, ER+ MCF7 cells were transfected with either TDO2-

expression vector (TDO2 OE) lacking the 3'UTR or empty vector (EV) for 24 hours and plated in soft agar. After 11 days, colonies were stained and quantified to assess anchorage independent growth. MCF7-TDO2 OE demonstrated significantly enhanced growth on soft agar as compared to MCF7 EV cells (Figure 2F). Western blot of whole-cell lysate collected prior to growth on soft agar confirmed TDO2 overexpression in the MCF7-TDO2 OE cells as compared to MCF7-EV (Figure 2F). Further, to functionally confirm the activity of the exogenous TDO2, we confirmed that MCF7-TDO2 OE cells had increased intracellular and secreted Kyn levels compared to MCF7-EV cells by UHPLC-MS (Figure 2G).

Restoration of miR-200c decreases TDO2, PD-L1/2, HO-1, and GDF-15 even in the presence of inflammatory stimuli

TDO2 is significantly upregulated in TNBC cells in forced-suspension culture and this upregulation is mediated by increased NFκB activity [10]. Given these findings, we examined whether miR-200c would repress NFκB-mediated stimulation of TDO2 expression. BT549-200c inducible cells were treated with or without DOX in the presence or absence of the NFκB activating cytokines IL-1β and TNF-α for 48 hours. Following treatment with DOX, relative miR-200c levels significantly increased and were unaffected by NFκB activating cytokines (Supplemental Figure 3A). Both TDO2 mRNA and protein were significantly upregulated following cytokine treatment, but suppressed in the presence of DOX, indicating that miR-200c suppressed TDO2 even in the context of inflammatory stimuli (Figure 3A). As a positive control we examined Interleukin-6 (*IL-6*), a known NFκB target, and it significantly increased following treatment with IL-1β and TNF-α (Figure 3B). *IL-6* decreased with restoration of miR-200c in the array study (Figure 1A) and this was confirmed in an independent experiment (Figure 3B). Interestingly, the positive regulator of NFκB activity *IKBKB* was reduced by restoration of miR-200c (Figure 1A), which may contribute to decreased NFκB-mediated regulation of *TDO2*.

Microarray analysis revealed that in addition to reduced *TDO2*, miR-200c decreased multiple other genes encoding immunomodulatory proteins (Figures 1A, Supplemental Figure S2). *HMOX-1*, which encodes heme oxygenase 1 (HO-1), was reduced by restoration of miR-200c in the microarray analysis (fold change -2.13; P=9.40E-05). Following transient transfection of BT549, Hs578T, MDA-MB-453, and SUM159 TNBC lines with miR-200c mimic for 48 hours, qRT-PCR analysis confirmed significant reduction in *HMOX-1* (Supplemental Figure S3B). HO-1 protein was also decreased upon addition of miR-200c for 72 hours (Figure 3C). HMOX-1 has been shown to be upregulated by progesterone in the uterus [24] and while TNBC cell lines do not express progesterone receptors (PR), some, including MDA-453, express high levels of androgen receptor (AR) protein, which binds to an identical consensus response element as PR. While MDA-453 cells at baseline did not express detectable levels of HO-1 protein (Figure 3C), when treated with the AR ligand dihydrotestosterone (DHT) HO-1 was dramatically induced and miR-200c repressed the DHT-induced increase in HO-1, demonstrating novel transcriptional and post-transcriptional regulation of this protein by liganded AR and miR-200c (Figure 3D).

GDF-15, which encodes ~~encoding~~ an anti-inflammatory cytokine, was decreased at the mRNA level in BT549-200c cells following DOX induction of miR-200c in the initial array analysis (fold change = 0.59, adj. P=0.12). Analogous to the experiment in Figure 3A demonstrating that ~~described where we demonstrate~~ TDO2 was induced ~~induction~~ by inflammatory cytokines and suppressed~~ion~~ by miR-200c, we examined whether miR-200c would repress NFκB-mediated stimulation of GDF-15 expression. BT549-200c inducible cells were treated with or without DOX in the presence or absence of the NFκB activating cytokines IL-1β and TNF-α for 48 hours. Similar to TDO2, GDF-15 protein was ~~significantly~~ upregulated by 4.4 fold ~~-~~following cytokine

treatment, but suppressed in the presence of DOX, indicating that miR-200c suppressed GDF-15 even in the context of inflammatory stimuli (Figure 3E top). The same was true in MDA-MB-453 cells, in which the NFκB activating cytokines significantly upregulated GDF-15, but addition of miR-200c mimic suppressed GDF-15 protein expression at baseline and in the face of the cytokine treatment (Figure 3E bottom).GDF-15 is upregulated by androgens in prostate cancer cells [25]. To determine if GDF-15 is also ~~GDF-15 can be~~ regulated by androgens ~~AR~~ in breast cancer cells ~~as well~~, MDA-MB-453 ~~cells~~ were treated with DHT and immunoblot analysis for GDF-15 was performed. ~~An increase in~~ GDF-15 protein increased ~~was observed at 48 and 72 hours~~ following ~~48 or 72 hours of~~ DHT exposure ~~treatment~~ and both the baseline and DHT induced GDF-15 were ~~this effect was~~ inhibited ~~blocked~~ in the presence of ~~by restoration of~~ miR-200c mimic compared to scrambled control (SCR) (Figure 3F). ~~Furthermore, GDF-15 protein increased with NFκB activation cocktail and miR-200c restoration blocked this induction (Figure 3G).~~

PD-L1 was recently identified as a target of miR-200c in lung cancer and MCF7 breast cancer cells [26, 27]. Since *PD-L1* was significantly decreased at the mRNA level in BT549-200c cells following DOX induction in the initial array analysis (Figure 1A), we treated BT549-Tripz-200c cells with IFNγ to induce *PD-L1* expression, and found that miR-200c significantly reduced the IFNγ-mediated upregulation of *PD-L1*, as measured by qRT-PCR (Figure 4A). Restoration of miR-200c also significantly reduced IFNγ-induced *PD-L2* expression (Figure 4B). The reduction in PD-L1 protein following restoration of miR-200c was confirmed by flow cytometry (Figure 4C).

The model in Figure 4D illustrates how restoration of miR-200c-mediated decreases in TDO2-dependent tryptophan depletion and Kyn secretion along with decreased GDF-15 and HO-1 might affect T-cells in a non-contact dependent fashion in addition to reducing the contact-dependent immune suppressors, PD-L1 and 2.

Discussion

Here we report a novel mechanism of control of tumor tryptophan catabolism, involving post-transcriptional regulation by miR-200c. The miR-200 family is a critical determinant of the epithelial phenotype that directly targets transcriptional repressors of E-cadherin such as ZEB1 and ZEB2, Twist, and Snail that mediate normal EMT during development and aberrant EMT in carcinomas to facilitate metastasis [17, 18]. This family of miRNA targets many mesenchymal and neuronal genes involved in motility, invasiveness, anoikis resistance, chemoresistance and stem cell-like properties such as Tropomyosin-Related Kinase B (TrkB), Neurotrophin 3 (NTF3), Moesin, Tubulin Beta 3 Class III (TUBB3), and Suppressor Of Zeste 12 Protein Homolog (SUZ12) [19, 28]. MiR-200 family members are lost or repressed in TNBC, as well as other dedifferentiated aggressive carcinomas, by various methods including micro-deletions or silencing [29, 30]. Here we report that restoration of miR-200c to TNBC cells not only profoundly reverses the EMT signature, but also inhibits expression of a group of genes that encode immune suppressive factors.

Increasing evidence supports a role for tryptophan catabolism via the Kyn pathway in tumor progression. TDO2-mediated production of Kyn supports tumor cell anchorage independent growth and invasion [10-12] in an autocrine manner, but also suppresses T-cell mediated tumor rejection [11, 31] and expansion of regulatory T-cells [13]. Although the majority of studies of the Kyn pathway in cancer have focused on IDO1, our data and others suggest that TDO2 may be relevant in TNBC and other types of cancer [10-12]. In addition to demonstrating positive regulation of TDO2 by NFκB activation in TNBC [10], we observe ~~now report~~ post-transcriptional

control of *TDO2* by miR-200c, explaining why this enzyme is expressed in TNBC, but not ER+ cell lines, where miR-200c is high [32]. TDO2 mRNA and protein are decreased as a consequence of direct targeting of the TDO2 3'UTR by miR-200c, and Kyn production is reduced in the presence of miR-200c (Figure 2A-E). If exogenous TDO2 is expressed in ER+ cells it increases survival on soft agar and expression of Kyn (2F and G), Both baseline and NFκB stimulated TDO2 are reduced in the presence of miR-200c (Figure 3A and B). Interestingly, *IKBKB*, a positive regulator/activator of NFκB, was significantly downregulated following the restoration of miR-200c (Figure 1A), further adding a possible mechanism by which miR-200c affects NFκB activity and thereby influences both transcriptional and post-transcriptional regulation of TDO2.

Multiple clinical trials are underway with IDO inhibitors such as Indoximod (D-1-methyl-tryptophan (NewLink Genetics) and INCB024360 (Incyte) to block IDO activity in tumors and boost cytotoxic T-cell responses. However, these compounds do not inhibit TDO2 [33, 34]. Data presented here and in our previous report [10] suggest that new drugs that inhibit both IDO1 and TDO2 may be more effective in TNBC.

The reversal of multiple genes involved in immune-suppression is a previously unappreciated action of miR-200c. GSEA analysis of changes mediated by miR-200c showed a reduction in pathways such as allogenic rejection, graft-versus-host disease and many other pathways involved in immune-suppression and tolerance. Interestingly, extravillar cytotrophoblasts undergo EMT to facilitate infiltration into the maternal decidual stroma and make immune-suppressive substances to ensure embryo maintenance/fetal tolerance during pregnancy [35]. Shared gene expression profiles between TNBC and trophoblasts are thought to be due to adaptations to similar environmental conditions such has hypoxia, tissue invasion, protection against xenobiotics and avoidance of immune recognition [35]. Thus, although it was previously recognized that trophoblast mimicry might facilitate cancer progression, a mechanism for this "transdifferentiation" was not identified. Herein, restoration of miR-200c to TNBC cells suppressed the ability of TNBC to make these immune-suppressive factors, suggesting that this miRNA serves as the "brakes" by which this gene expression program is typically not expressed in normal epithelium or even ER+ breast cancer. illuminated that lack of this miRNA permits TNBC to highjack this program of immunosuppressive factors similar to those utilized to prevent rejection of the fetus, during early pregnancy.

Mellor and Munn described the role of tryptophan catabolism in the prevention of T-cell-driven complement activation and inflammation during pregnancy [36]. Inhibition of IDO or TDO2-mediated tryptophan catabolism in pregnant mice induces fetal loss, supporting its role in maternal fetal tolerance [36]. The immunosuppressive effects of both tryptophan depletion and increased tryptophan metabolites such as Kyn are well established [11, 13, 37]. TDO2 plays a significant role in endometrial decidualization, a hormonally regulated process critical for the maintenance of pregnancy, where it suppresses activation of decidual T-cells [38].

Tryptophan uptake is mediated by LAT1 (SLC7A5) and we find that breast cancer cells upregulate *LAT1* under anchorage independent conditions (Supplemental Figure S4A), where we first reported increased TDO2 levels and activity [10]. *LAT1* is higher in breast cancer compared to normal breast epithelium, in ER- tumors compared to ER+ and correlates with increased grade and poor overall survival in all breast cancer subtypes in the Curtis dataset (Supplemental Figure S4B-E). Furthermore, the KM Plotter tool (kmplot.com), which integrates data from GEO, EGA, and TCGA databases, indicated that high *LAT1* is associated with both shorter overall survival and metastasis-free survival (Supplemental Figure S4F-G). Similar to our pathway analysis of genes altered by restoration of miR-200c (Figure 1C), a recent study of

the metabolic properties of an immortalized, breast epithelial cell line and its EMT counterpart, found glycolysis and OXPHOS associated with the epithelial phenotype, while amino acid anaplerosis and fatty acid oxidation were drivers of the mesenchymal phenotype and interestingly, LAT1 was deemed “essential for mesenchymal cell survival” [39].

Our data support recent reports that *PD-L1 (CD274)* is directly targeted by miR-200c [26, 27], and we confirm this finding at the protein level by flow cytometry. In addition, we find that restoration of miR-200c also reduced *PD-L2* induction by INFγ (Figure 4A-C). Like PD-L1, PD-L2 (CD273) is expressed on both antigen-presenting cells and tumor cells and interacts with PD-1 on T-cells to inhibit anti-tumor function [40]. High tumor PD-L2 indicated a better clinical response in patients treated with pembrolizumab (Keytruda), suggesting that PD-1 blockade may function through inhibition of both ligands [41].

HO-1 is an anti-inflammatory, immunosuppressive, pro-angiogenic enzyme involved in suppression of CD8+ T-cells through expansion of T-regulatory cells necessary for fetal tolerance during pregnancy [42]. Here we show that restoration of miR-200c significantly decreased HMOX-1 mRNA and protein (Figure 3C). *HMOX-1* is overexpressed in a number of human cancer types including breast and predicts shorter overall survival in breast cancer [43]. In clear-cell renal cell carcinoma cells, miR-200c targeted *HMOX-1* [44]. Interestingly, reduced progesterone levels induced by gestational stress in mice led to lowered HMOX-1, fewer tolerogenic CD8+/CD122+ T-cells, increased cytotoxic CD8+ T-cells and intrauterine growth restriction [24]. While TNBC do not express PR, 20-50% express some AR protein and indeed the androgen DHT increased HO-1 protein in AR+ TNBC ~~(Figure~~) but this effect is blocked by miR-200c~~4F~~ (Figure 3D~~)~~.

GDF-15, also known as Placental TGF-Beta (PTGFB), is highly expressed in placenta and decidual stromal cells in the uterus [45]. In malignant gliomas, depletion of GDF-15 enhanced natural killer cell clearance of tumors [46]. In the normal prostate, GDF-15 is inversely correlated with inflammation [47]; however, circulating GDF-15 levels are often elevated in prostate cancer patients compared to men without cancer [25] and is upregulated by androgens in prostate cancer [48]. *GDF-15* was significantly decreased by restoration of miR-200c to TNBC and DHT increased GDF-15 protein in MDA-453 breast cancer cells that represent the luminal AR (LAR) subtype of TNBC (Figure 3F~~4G~~), as did NFκB stimulation, and both effects were blocked by miR-200c (Figure 3E~~4H~~and F).

Restoration of miR-200c decreased metastasis in an immune competent mouse model of claudin-low TNBC; however changes in the immune response were not examined [21]. Comparison of gene expression data from that study (GSE62230) to the human TNBC cells studied here revealed overlap in genes reduced upon induction of miR-200c, including *TDO2, HMOX-1, IKBKB and PD-L1* (Supplemental Figure S1B). While future studies are necessary to determine how to best reverse tumor-induced tolerance and re-activate the immune system in BC, the current study identifies multiple genes/proteins expressed by TNBC and repressed by restoration of miR-200c, that are reminiscent of those utilized by trophoblasts to achieve fetal tolerance, such as *TDO2*, *PD-L1/2, GDF-15* and *HMOX-1*. Interestingly, the miR-200c family regulates the epigenetic modifier PcG protein Enhancer of Zeste Homolog 2 (EZH2), which was recently shown to control the adaptive response to immunotherapies in melanoma [49]. While systemic delivery of miRNA for treatment of solid tumors is still problematic, our study provides insight into the transcriptional and post-transcriptional regulation of specific proteins utilized by TNBC to evade immune attack.

ACKNOWLEDGMENTS

The authors acknowledge the use of the University of Colorado Cancer Center/National Institute of Health National Cancer Institute Cancer Core Support Grant P30 CA046934, specifically the Tissue Biobanking and Processing Core and Tissue Culture Core. The authors also acknowledge the use of the DNA Sequencing Core at the University of Colorado-Anschutz Medical Campus.

Figure Legends

Figure 1. Restoration of miR-200c to TNBC represses an epithelial to mesenchymal program and pathways involved in immune suppression. BT549-TripZ-200c cells containing the pre-miR-200c sequence in the DOX inducible pTripZ vector were treated in triplicate with 1 µg/mL Doxycycline (DOX) or vehicle for 48 hours. **(A)** Heat map of differentially expressed genes (adjusted p-value < 0.10 and fold-change > 1.2) between untreated (DOX-) and induced (DOX+) BT549-TripZ-200c cells in triplicate. **(B)** In both BT549-TripZ-200c and BT549 cells with empty pTripZ vector (BT549-TripZ EV), *miR-200c* and *ZEB1* were measured by qRT-PCR and normalized to *U6 and 18S* respectively, and presented as fold change of DOX+ cells relative to untreated counterpart cells. ****P<0.0001, unpaired t-test. Insert shows corresponding western blot for ZEB1. **(C)** Gene Set Enrichment Analysis of pathways involved in immunosuppression enriched in DOX- and DOX+. **P<0.01, *P<0.05, unpaired t-test. **(D)** Select genes measured by qRT-PCR from RNA isolated from independent BT549-200c cells DOX- and DOX+ for 48 hours.

Figure 2. Restoration of miR-200c to TNBC decreases TDO2 and miR-200c directly targets *TDO2* through a binding site in the 3'UTR, resulting in a functional reduction in intracellular and secreted kynurenine. (A) Relative TDO2 mRNA levels were determined by qRT-PCR in multiple TNBC cell lines following transient transfection with either a negative control mimic or miR-200c mimic after 48 hours. ***P<0.001, **P<0.01, unpaired t-test. **(B)** Western blot for TDO2 and ZEB1 in multiple TNBC lines following transient transfection with either a negative control mimic or miR-200c mimic for 72 hours. **(C)** Schematic of the 3'UTR of TDO2 that was cloned into the pmiR-Glo luciferase vector. Predicted binding site of miR-200c is at position 395-400. Site-directed mutations indicated by the asterisks. **(D)** Luciferase activity of the WT and mutated TDO2 3'UTR following transient transfection of BT549 cells with either a negative control mimic or miR-200c mimic after 48 hours. ****P<0.0001, one-way ANOVA analysis. **(E)** Relative Kyn levels in BT549 cells expressing a stable transduced, DOX-inducible empty vector or miR-200c vector after 72 hours of DOX induction, as determined by UPLC-MS.

~~(F-G)~~ Relative Kyn levels were also measured in Hs578T and MDA-453 following transient transfection with either SCR mimic or miR-200c mimic 72 hours prior. **(F)** ~~(H)~~ MCF7 cells were transiently transfected with an expression vector for TDO2 cells (OE) or empty vector (EV) and TDO2 protein was detected by immunoblot 24 hours after transfection. MCF7 cells with TDO2 OE or EV control were grown in soft-agar and colony number was determined after 11 days. **(G!)** Intracellular and secreted Kyn was measured by UPLC-MS in MCF7-EV or MCF7-TDO2-OE cells after 72 hours.

Figure 3. Restoration of an epithelial phenotype abrogates immunomodulatory gene expression in TNBC cells. (A) Relative TDO2 and **(B)** IL6 mRNA levels in BT549-200c cells after 72 hours of no treatment, DOX alone, NFkB activation (TNF-α, IL-1β) alone, or the combination of DOX and NFkB activation. Relative TDO2 and IL6 levels were normalized to B-actin. ***P<0.001, **P<0.01 by unpaired t-test. **(C)** Western blot for TDO2 and ZEB1 in BT549-200c cells after 72 hours of no treatment, DOX alone, NFkB activation alone, or the combination of DOX and NFkB activation. α-Tubulin was used as a loading control. **(D)** Western blot for HMOX-1 in multiple TNBC lines following transient transfection with SCR mimic or miR-200c mimic for 72 hours. **(E)** Western blot for HMOX-1 in MDA-453 cells following transient transfection with either a scrambled, non-targeting mimic or miR-200c mimic treated with or with DHT for 48 hours. ~~**(F)** (GDF-15 in the various cell lines)- waiting on this – do we have RT-PCR too? If we don't we should show the HMOX RNA in supplemental.~~ (E) Western blot for GDF-15 in BT549-200c cells after 72 hours of no treatment, DOX alone, NFkB activation alone, or the combination of DOX and NFkB activation. α-Tubulin was used as a loading control. ~~(G)~~(F) Western blot for GDF-15 in MDA-453 cells following transient transfection with either a scrambled, non-targeting mimic or miR-200c mimic and then treated with or with DHT for 48 or 72 hours. ~~(H)~~(G) Western blot for GDF15 in MDA-453 cells following transient transfection with either a scrambled, non-targeting mimic or miR-200c mimic and then treated with or without NFkB activation cocktail (TNFα and IL-1β, 10 ng/μL each) for 48 hours. α-Tubulin was used as a loading control.

Figure 4. miR-200c regulates PD-L1 and 2 and other immunosuppressive factors in Triple-Negative Breast Cancer. BT549 cells expressing a stably transduced, DOX-inducible miR-200c vector were treated with DOX to induce expression of miR-200c, or vehicle control. **(A)** Relative PD-L1 mRNA levels were determined by qRT-PCR in 24 hours after DOX treatment began, cells were treated with interferon γ (IFNγ, 10 ng/mL) or vehicle. Cells were harvested 72 hours after the commencement of DOX treatment. ****P<0.0001, as determined by one-way ANOVA. **(B)** Relative PD-L2 mRNA levels were determined by qRT-PCR in BT549 cells expressing a stably transduced, DOX-inducible miR-200c vector were treated with DOX to induce expression of miR-200c, or vehicle control. 24 hours after DOX treatment began, cells were treated with interferon γ (IFNγ, 10 ng/mL) or vehicle. Cells were harvested 72 hours after the commencement of DOX treatment. ****P<0.0001, as determined by one-way ANOVA. **(C)** PD-L1 expression was measured by flow cytometry. BT549 cells expressing a stably transduced, DOX-inducible miR-200c vector were treated with DOX to induce expression of miR-200c, or vehicle control. 24 hours after DOX treatment began, cells were treated with interferon γ (IFNγ, 10 ng/mL) or vehicle. Cells were harvested 72 hours after the commencement of DOX treatment and stained for PD-L1. n=3 samples, data shown is representative of two independent experiments. *** p<0.001, **** p<0.0001, as determined by unpaired t-test. **(~~C~~D)** Model of the potential effects of restoration of miR-200c on factors that can regulate T cell function.

Supplemental Figure 1. Comparison of Gene Signatures following miR-200c Restoration in TNBC Cells. (A) Clustering of the EMT-signatures showed that the miR-200c induced TNBC

cells have the “epithelial-like” gene expressions, whereas the untreated cells have the “mesenchymal-like” gene expressions. Red and green colors in the heatmap represent high and low gene expressions**. (B)** List of commonly altered genes similar in the TNBC cells after miR-200c as compared to the GSE62230.

Supplemental Figure 2. Expanded GSEA results following miR-200c restoration in TNBC cells. (A) List of enriched pathways following miR-200c restoration in BT549-200c cells. **(B)** GSEA enrichment plots for gene signatures involved in immune modulation.

Supplemental Figure 3. Extended Figure 3. (A) Relative miR-200c miRNA levels in BT549-200c cells after 72 hours of no treatment, DOX alone, NFkB activation alone, or the combination of DOX and NFkB activation. Relative miR-200c levels were normalized to U6 snRNA. **(B)** Relative HMOX-1 mRNA levels were determined by qRT-PCR in multiple TNBC cell lines following transient transfection with either a negative control mimic or miR-200c mimic after 48 hours.. ***P<0.001, **P<0.01, *P<0.05 as determined by unpaired t-test.

Supplemental Figure 4. LAT1 expression in breast cancer clinical samples. (A) Relative mRNA expression of LAT1 in two TNBC cell lines (BT549 and MDA-231) after culture in forced-suspension conditions for 24 hours. β-actin was used as an endogenous control. Statistics were performed using a unpaired t-test. **(B-E)** Using the Curtis Breast Cohort, LAT1 expression was compared between **(B)** normal breast versus invasive ductal carcinoma, **(C)** ER+ and ER- breast tumor samples, **(D)** breast tumor samples based on grade, and **(E)** overall survival of patients split into LAT1-high or –low groups based on median LAT1 gene expression. **(F-G)** Using the KM Plotter tool, **(F)** overall and **(G)** distant metastasis-free survival were determined based on median LAT1 gene expression.

References (49/50)

1. Liedtke, C., et al., *Response to neoadjuvant therapy and long-term survival in patients with triple-negative breast cancer.* J Clin Oncol, 2008. **26**(8): p. 1275-81.
2. Dent, R., et al., *Triple-negative breast cancer: clinical features and patterns of recurrence.* Clin Cancer Res, 2007. **13**(15 Pt 1): p. 4429-34.
3. Lin, N.U., et al., *Clinicopathologic features, patterns of recurrence, and survival among women with triple-negative breast cancer in the National Comprehensive Cancer Network.* Cancer, 2012. **118**(22): p. 5463-72.
4. Neelakantan, D., et al., *EMT cells increase breast cancer metastasis via paracrine GLI activation in neighbouring tumour cells.* Nat Commun, 2017. **8**: p. 15773.
5. Yu, M., et al., *Circulating breast tumor cells exhibit dynamic changes in epithelial and mesenchymal composition.* Science, 2013. **339**(6119): p. 580-4.
6. Frisch, S.M. and H. Francis, *Disruption of epithelial cell-matrix interactions induces apoptosis.* J Cell Biol, 1994. **124**(4): p. 619-26.
7. Howe, E.N., et al., *miR-200c targets a NF-kappaB up-regulated TrkB/NTF3 autocrine signaling loop to enhance anoikis sensitivity in triple negative breast cancer.* PLoS One, 2012. **7**(11): p. e49987.
8. Barton, V.N., et al., *Androgen receptor supports an anchorage-independent, cancer stem cell-like population in triple-negative breast cancer.* Cancer Res, 2017.
9. Schafer, Z.T., et al., *Antioxidant and oncogene rescue of metabolic defects caused by loss of matrix attachment.* Nature, 2009. **461**(7260): p. 109-13.
10. D'Amato, N.C., et al., *A TDO2-AhR Signaling Axis Facilitates Anoikis Resistance and Metastasis in Triple-Negative Breast Cancer.* Cancer Res, 2015. **75**(21): p. 4651-64.

11. Opitz, C.A., et al., *An endogenous tumour-promoting ligand of the human aryl hydrocarbon receptor.* Nature, 2011. **478**(7368): p. 197-203.
12. Novikov, O., et al., *An Aryl Hydrocarbon Receptor-Mediated Amplification Loop That Enforces Cell Migration in ER-/PR-/Her2- Human Breast Cancer Cells.* Mol Pharmacol, 2016. **90**(5): p. 674-688.
13. Mezrich, J.D., et al., *An interaction between kynurenine and the aryl hydrocarbon receptor can generate regulatory T cells.* J Immunol, 2010. **185**(6): p. 3190-8.
14. Fallarino, F., et al., *T cell apoptosis by tryptophan catabolism.* Cell Death Differ, 2002. **9**(10): p. 1069-77.
15. Bockmeyer, C.L., et al., *MicroRNA profiles of healthy basal and luminal mammary epithelial cells are distinct and reflected in different breast cancer subtypes.* Breast Cancer Res Treat, 2011. **130**(3): p. 735-45.
16. Castilla, M.A., et al., *MicroRNA-200 family modulation in distinct breast cancer phenotypes.* PLoS One, 2012. **7**(10): p. e47709.
17. Gregory, P.A., et al., *The miR-200 family and miR-205 regulate epithelial to mesenchymal transition by targeting ZEB1 and SIP1.* Nat Cell Biol, 2008. **10**(5): p. 593-601.
18. Park, S.M., et al., *The miR-200 family determines the epithelial phenotype of cancer cells by targeting the E-cadherin repressors ZEB1 and ZEB2.* Genes Dev, 2008. **22**(7): p. 894-907.
19. Howe, E.N., D.R. Cochrane, and J.K. Richer, *The miR-200 and miR-221/222 microRNA families: opposing effects on epithelial identity.* J Mammary Gland Biol Neoplasia, 2012. **17**(1): p. 65-77.
20. Humphries, B. and C. Yang, *The microRNA-200 family: small molecules with novel roles in cancer development, progression and therapy.* Oncotarget, 2015. **6**(9): p. 6472-98.
21. Knezevic, J., et al., *Expression of miR-200c in claudin-low breast cancer alters stem cell functionality, enhances chemosensitivity and reduces metastatic potential.* Oncogene, 2015. **34**(49): p. 5997-6006.
22. Dongre, A., et al., *Epithelial-to-Mesenchymal Transition Contributes to Immunosuppression in Breast Carcinomas.* Cancer Res, 2017. **77**(15): p. 3982-3989.
23. Mak, M.P., et al., *A Patient-Derived, Pan-Cancer EMT Signature Identifies Global Molecular Alterations and Immune Target Enrichment Following Epithelial-to-Mesenchymal Transition.* Clin Cancer Res, 2016. **22**(3): p. 609-20.
24. Solano, M.E., et al., *Progesterone and HMOX-1 promote fetal growth by CD8+ T cell modulation.* J Clin Invest, 2015. **125**(4): p. 1726-38.
25. Jones, A.C., et al., *Prostate field cancerization: deregulated expression of macrophage inhibitory cytokine 1 (MIC-1) and platelet derived growth factor A (PDGF-A) in tumor adjacent tissue.* PLoS One, 2015. **10**(3): p. e0119314.
26. Chen, L., et al., *Metastasis is regulated via microRNA-200/ZEB1 axis control of tumour cell PD-L1 expression and intratumoral immunosuppression.* Nat Commun, 2014. **5**: p. 5241.
27. Noman, M.Z., et al., *The immune checkpoint ligand PD-L1 is upregulated in EMT-activated human breast cancer cells by a mechanism involving ZEB-1 and miR-200.* Oncoimmunology, 2017. **6**(1): p. e1263412.
28. Iliopoulos, D., et al., *Loss of miR-200 inhibition of Suz12 leads to polycomb-mediated repression required for the formation and maintenance of cancer stem cells.* Mol Cell, 2010. **39**(5): p. 761-72.
29. Vrba, L., et al., *Role for DNA methylation in the regulation of miR-200c and miR-141 expression in normal and cancer cells.* PLoS One, 2010. **5**(1): p. e8697.
30. Hu, X., et al., *A miR-200 microRNA cluster as prognostic marker in advanced ovarian cancer.* Gynecol Oncol, 2009. **114**(3): p. 457-64.

31. Pilotte, L., et al., *Reversal of tumoral immune resistance by inhibition of tryptophan 2,3-dioxygenase.* Proc Natl Acad Sci U S A, 2012. **109**(7): p. 2497-502.
32. Cochrane, D.R., et al., *MicroRNAs link estrogen receptor alpha status and Dicer levels in breast cancer.* Horm Cancer, 2010. **1**(6): p. 306-19.
33. Suzuki, S., et al., *Expression of indoleamine 2,3-dioxygenase and tryptophan 2,3-dioxygenase in early concepti.* Biochem J, 2001. **355**(Pt 2): p. 425-9.
34. Liu, X., et al., *Selective inhibition of IDO1 effectively regulates mediators of antitumor immunity.* Blood, 2010. **115**(17): p. 3520-30.
35. Piechowski, J., *Trophoblastic-like transdifferentiation: A key to oncogenesis.* Crit Rev Oncol Hematol, 2016. **101**: p. 1-11.
36. Mellor, A.L., et al., *Prevention of T cell-driven complement activation and inflammation by tryptophan catabolism during pregnancy.* Nat Immunol, 2001. **2**(1): p. 64-8.
37. Fallarino, F., et al., *The combined effects of tryptophan starvation and tryptophan catabolites down-regulate T cell receptor zeta-chain and induce a regulatory phenotype in naive T cells.* J Immunol, 2006. **176**(11): p. 6752-61.
38. Li, D.D., et al., *Differential expression and regulation of Tdo2 during mouse decidualization.* J Endocrinol, 2014. **220**(1): p. 73-83.
39. Halldorsson, S., et al., *Metabolic re-wiring of isogenic breast epithelial cell lines following epithelial to mesenchymal transition.* Cancer Lett, 2017. **396**: p. 117-129.
40. Latchman, Y., et al., *PD-L2 is a second ligand for PD-1 and inhibits T cell activation.* Nat Immunol, 2001. **2**(3): p. 261-8.
41. Yearley, J.H., et al., *PD-L2 Expression in Human Tumors: Relevance to Anti-PD-1 Therapy in Cancer.* Clin Cancer Res, 2017. **23**(12): p. 3158-3167.
42. Schumacher, A., et al., *Blockage of heme oxygenase-1 abrogates the protective effect of regulatory T cells on murine pregnancy and promotes the maturation of dendritic cells.* PLoS One, 2012. **7**(8): p. e42301.
43. Noh, S.J., et al., *Expression of nerve growth factor and heme oxygenase-1 predict poor survival of breast carcinoma patients.* BMC Cancer, 2013. **13**: p. 516.
44. Gao, C., F.H. Peng, and L.K. Peng, *MiR-200c sensitizes clear-cell renal cell carcinoma cells to sorafenib and imatinib by targeting heme oxygenase-1.* Neoplasma, 2014. **61**(6): p. 680-9.
45. Segerer, S.E., et al., *MIC-1 (a multifunctional modulator of dendritic cell phenotype and function) is produced by decidual stromal cells and trophoblasts.* Hum Reprod, 2012. **27**(1): p. 200-9.
46. Roth, P., et al., *GDF-15 contributes to proliferation and immune escape of malignant gliomas.* Clin Cancer Res, 2010. **16**(15): p. 3851-9.
47. Lambert, J.R., et al., *Reduced expression of GDF-15 is associated with atrophic inflammatory lesions of the prostate.* Prostate, 2015. **75**(3): p. 255-65.
48. Paralkar, V.M., et al., *Cloning and characterization of a novel member of the transforming growth factor-beta/bone morphogenetic protein family.* J Biol Chem, 1998. **273**(22): p. 13760-7.
49. Zingg, D., et al., *The Histone Methyltransferase Ezh2 Controls Mechanisms of Adaptive Resistance to Tumor Immunotherapy.* Cell Rep, 2017. **20**(4): p. 854-867.

Figure 1

A

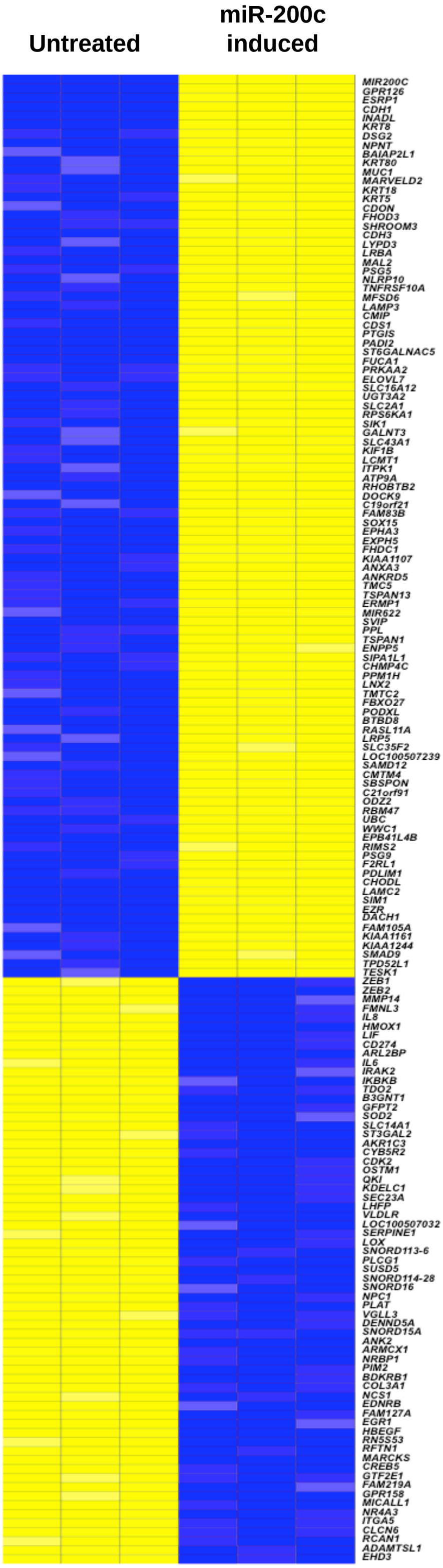

B

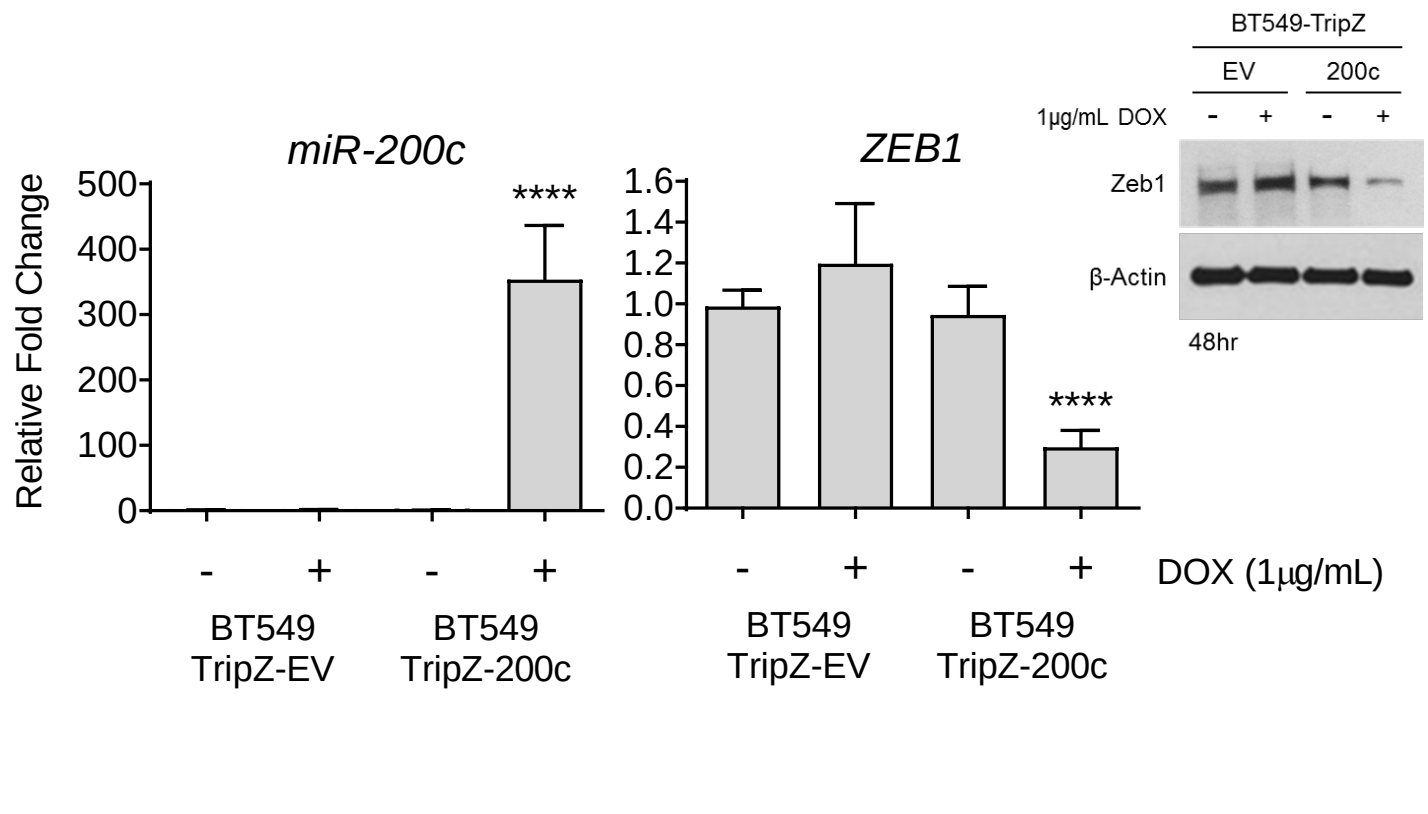

C

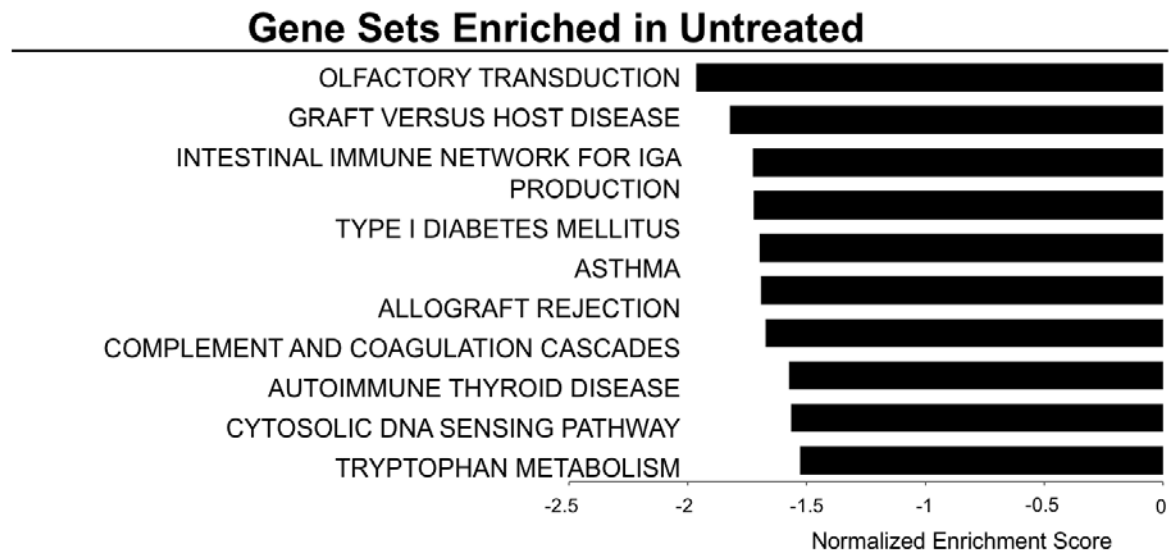

D

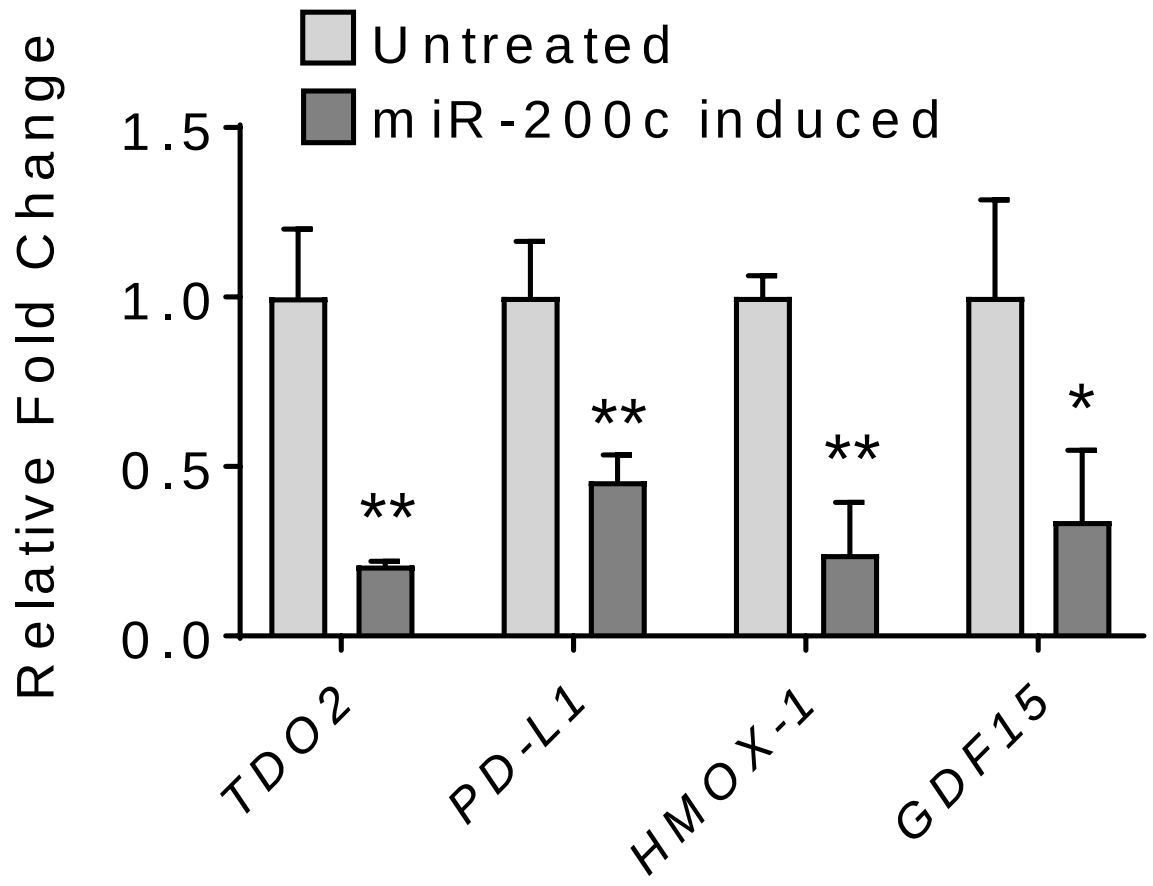

Figure 2

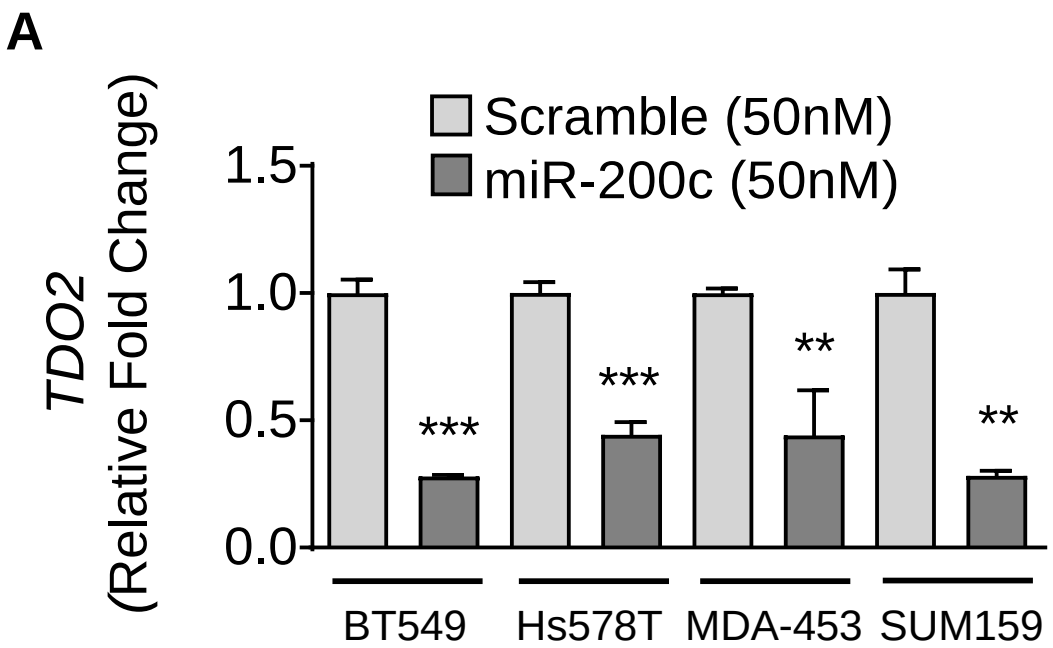
A
TDO2 (Relative Fold Change)
Scramble (50nM)
miR-200c (50nM)
1.5
1.0
0.5
0.0
***
***
**
**
BT549
Hs578T
MDA-453
SUM159

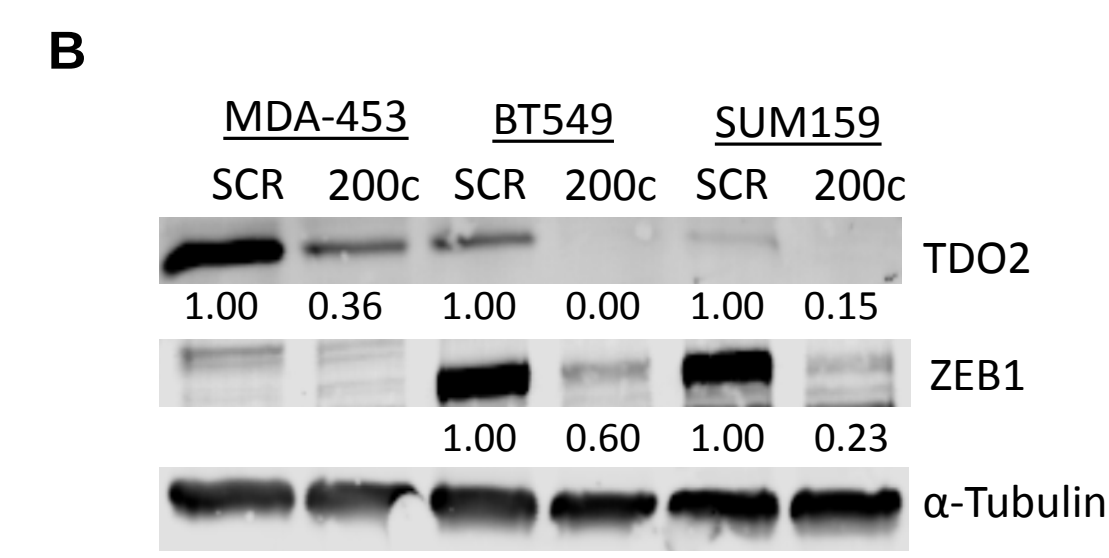
B
MDA-453
BT549
SUM159
SCR
200c
SCR
200c
SCR
200c
TDO2
1.00
0.36
1.00
0.00
1.00
0.15
ZEB1
1.00
0.60
1.00
0.23
α-Tubulin

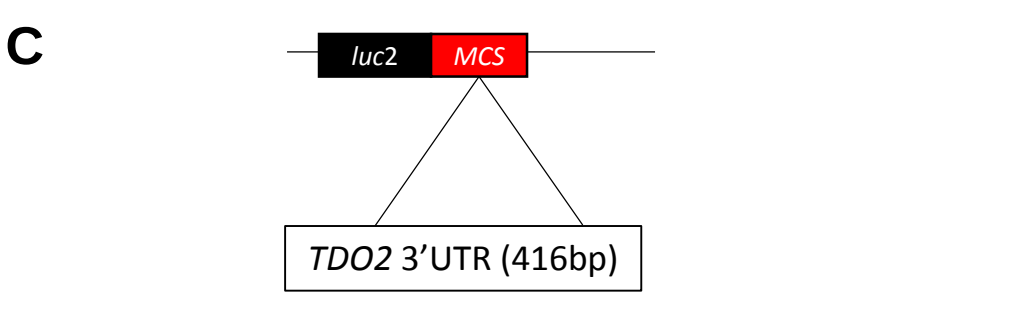
C
luc2
MCS
TDO2 3'UTR (416bp)
Position 395-400
5' ...UUUUUAAAAUAAUAAAGUAUUAA... WT 3'UTR TDO2
3' AGGUAGUAAUGGGCCGUCAUAAU 5' miR-200c-3p
5' ...UUUUUAAAAUAAUAACAGUCGAA MUT 3'UTR TDO2
******

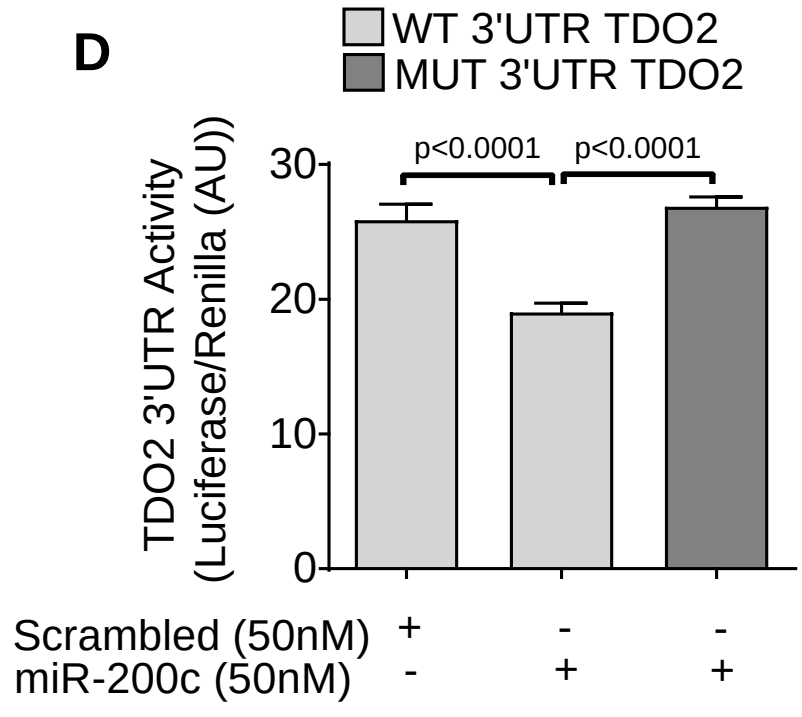
D
WT 3'UTR TDO2
MUT 3'UTR TDO2
TDO2 3'UTR Activity (Luciferase/Renilla (AU))
p<0.0001
p<0.0001
30
20
10
0
Scrambled (50nM) + - -
miR-200c (50nM) - + +

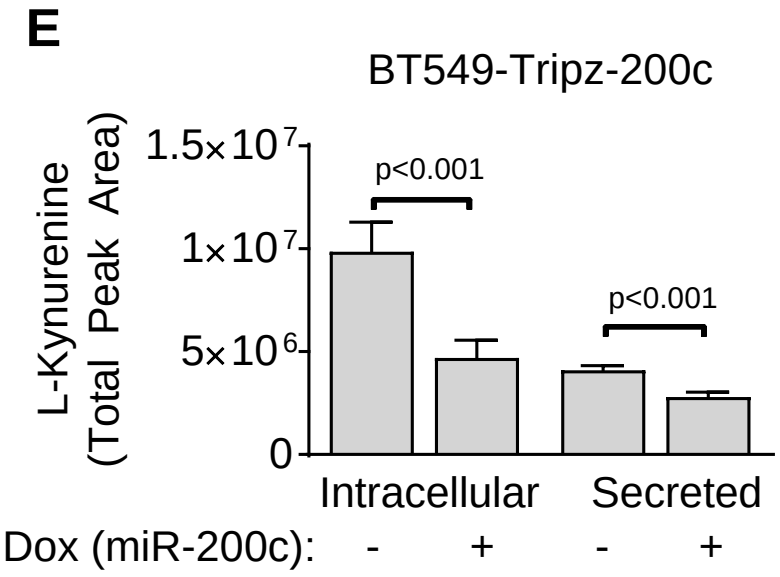
E
BT549-Tripz-200c
L-Kynurenine (Total Peak Area)
1.5×10^7
1×10^7
5×10^6
0
p<0.001
p<0.001
Intracellular
Secreted
Dox (miR-200c): - + - +

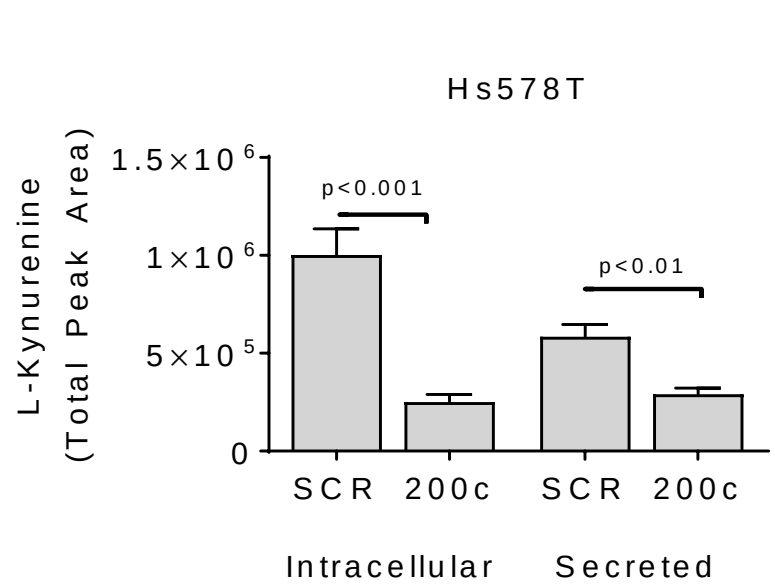
Hs578T
L-Kynurenine (Total Peak Area)
1.5×10^6
1×10^6
5×10^5
0
p<0.001
p<0.01
SCR
200c
SCR
200c
Intracellular
Secreted

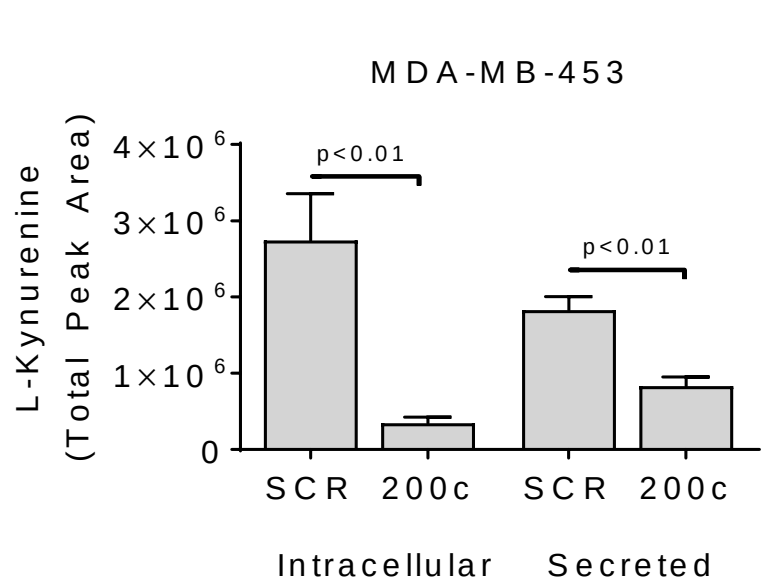
MDA-MB-453
L-Kynurenine (Total Peak Area)
4×10^6
3×10^6
2×10^6
1×10^6
0
p<0.01
p<0.01
SCR
200c
SCR
200c
Intracellular
Secreted

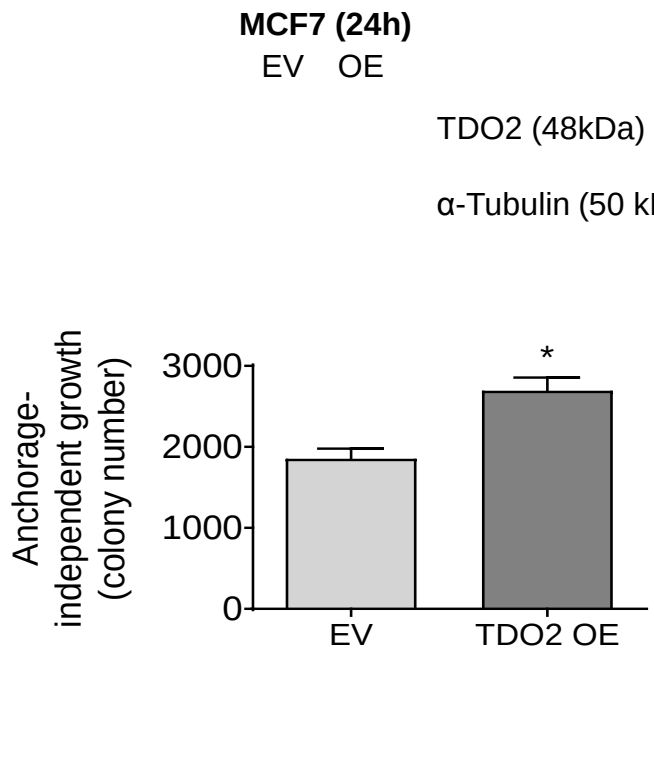
F
MCF7 (24h)
EV OE
TDO2 (48kDa)
α-Tubulin (50 kDa)
Anchorage-independent growth (colony number)
3000
2000
1000
0
*
EV
TDO2 OE

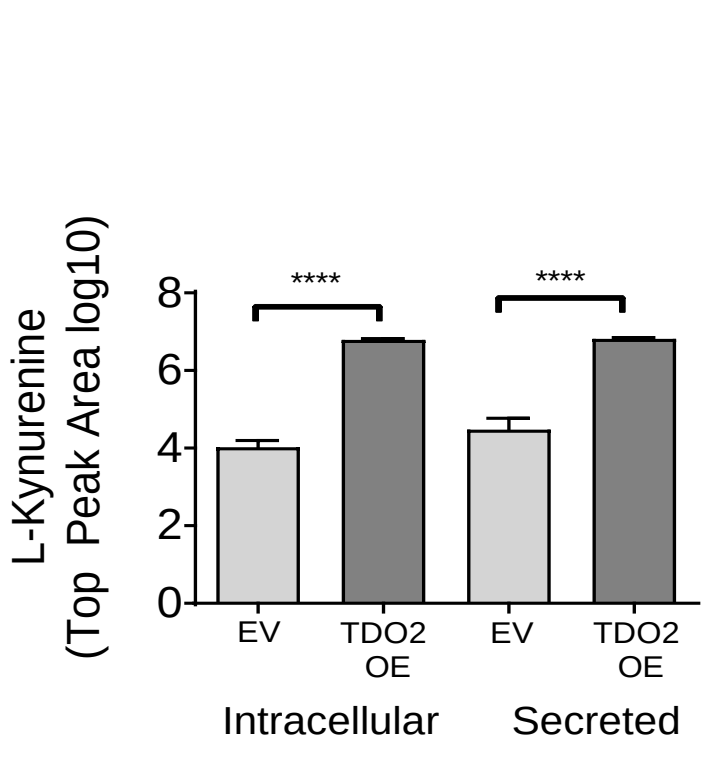
G
L-Kynurenine (Top Peak Area log10)
8
6
4
2
0
****
****
EV
TDO2 OE
EV
TDO2 OE
Intracellular
Secreted

Figure 3

A

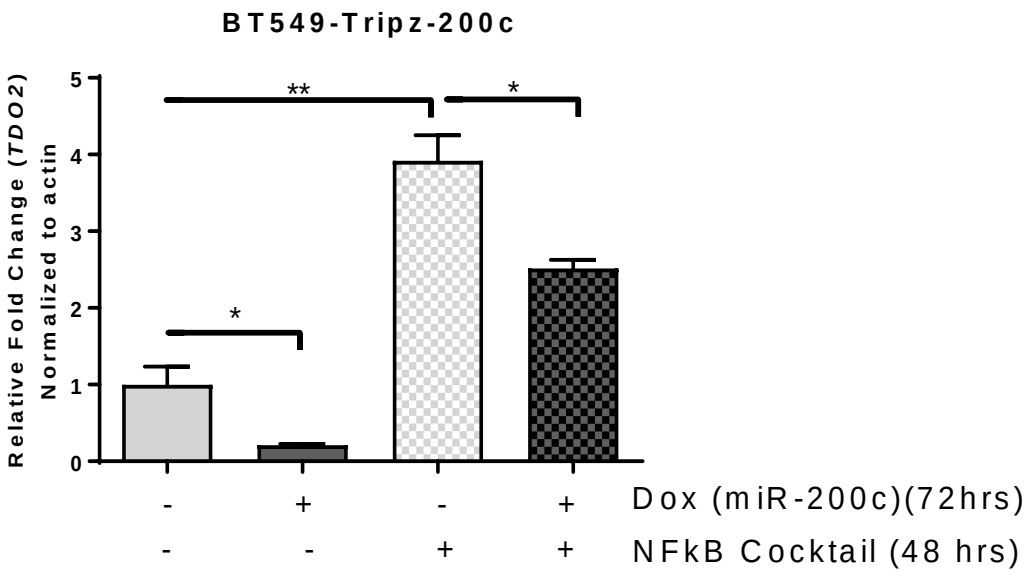

B

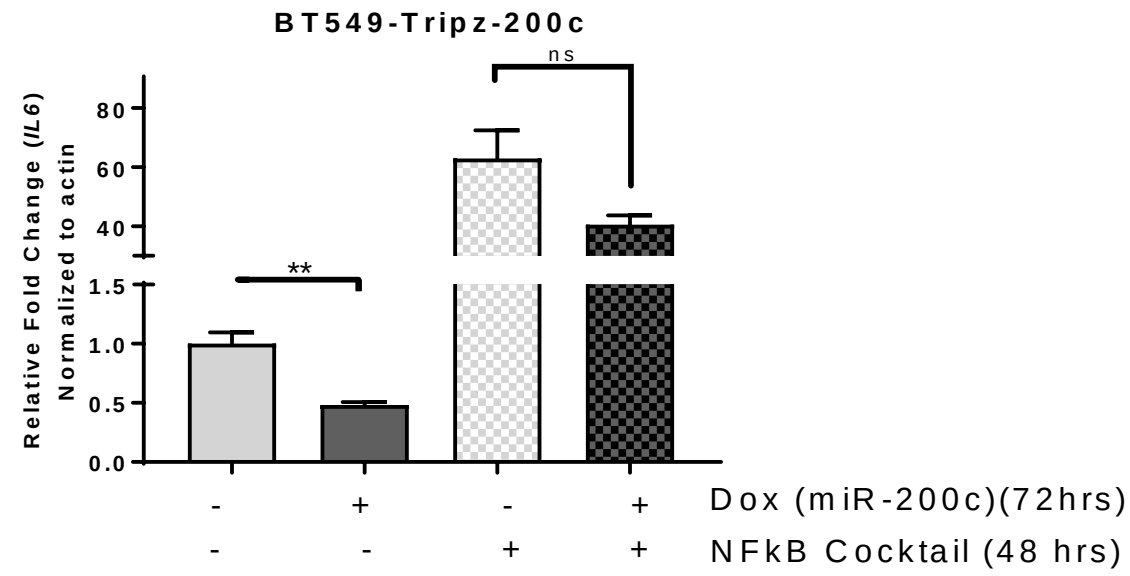

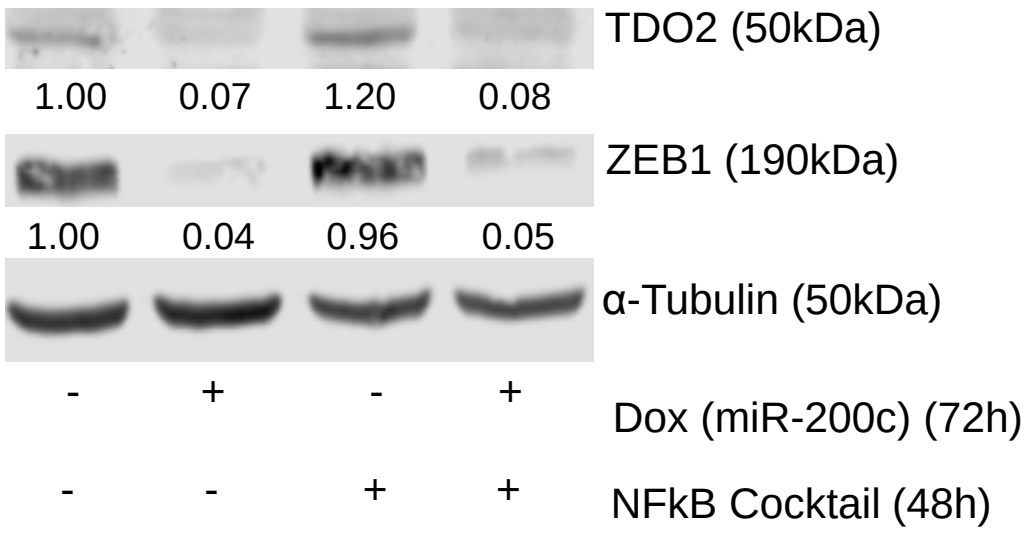

C

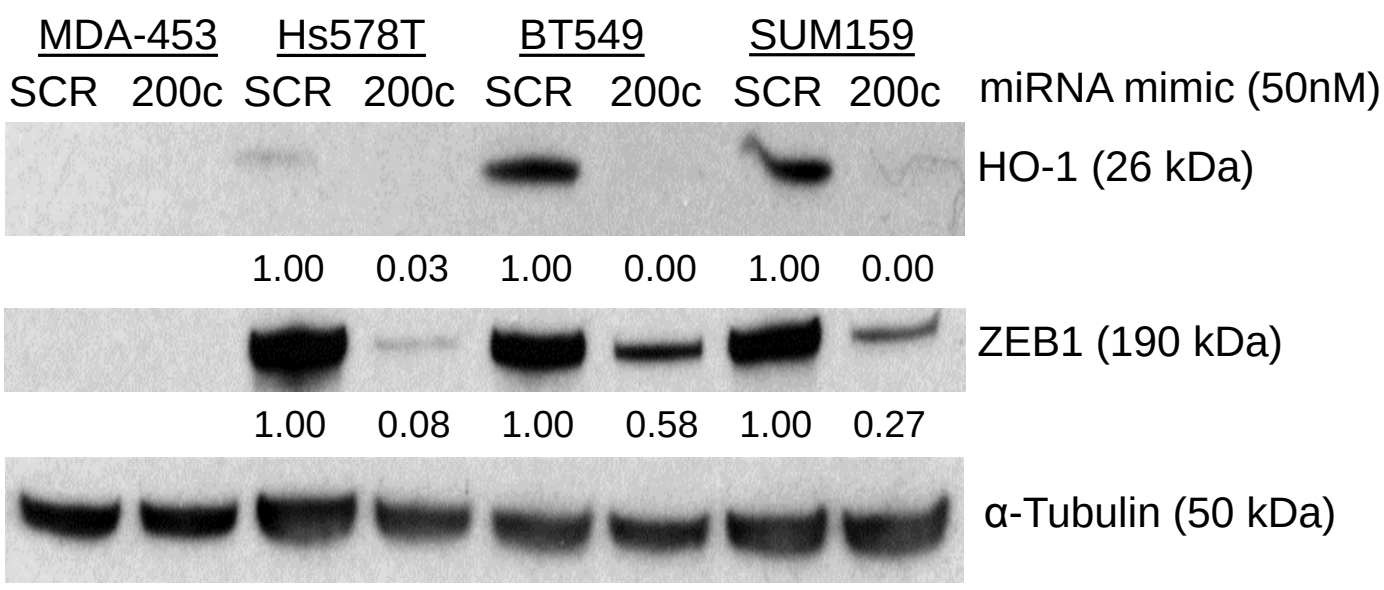

D

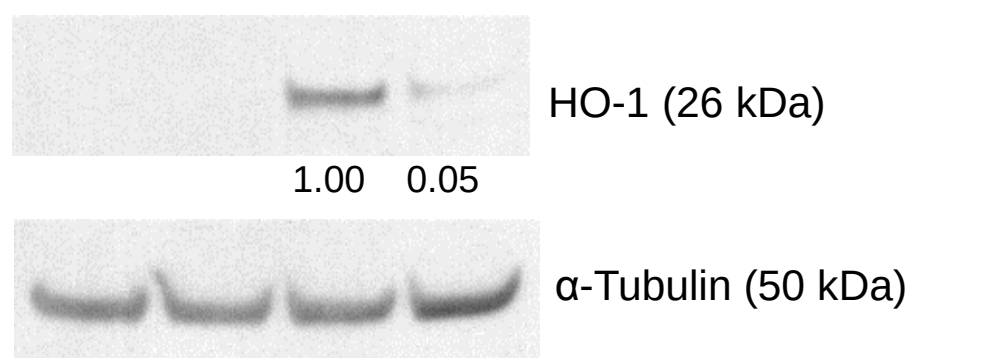

E

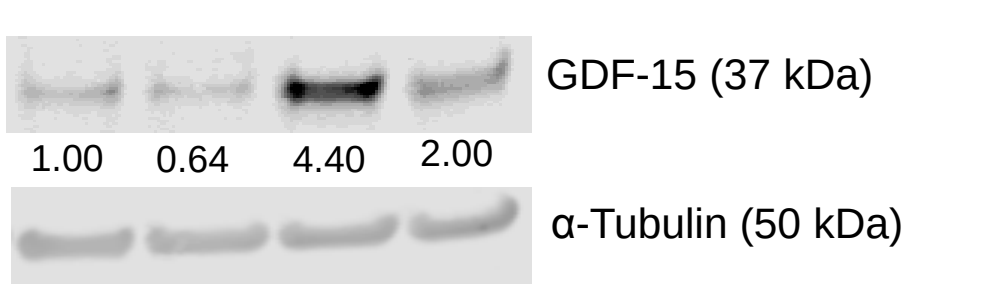

F

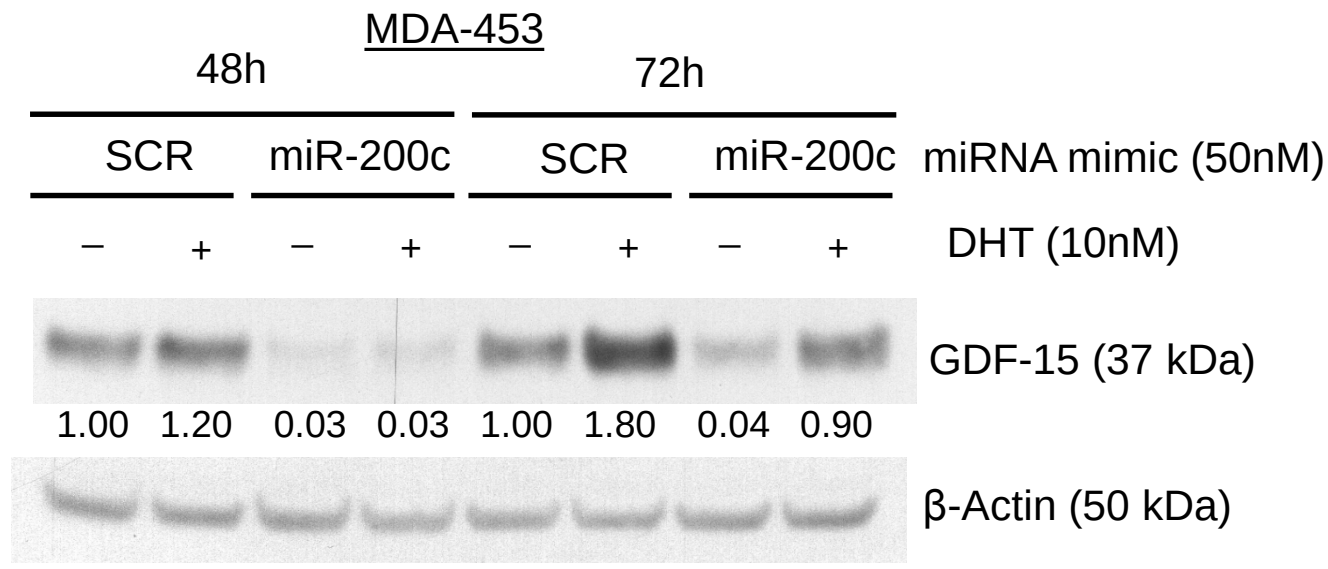

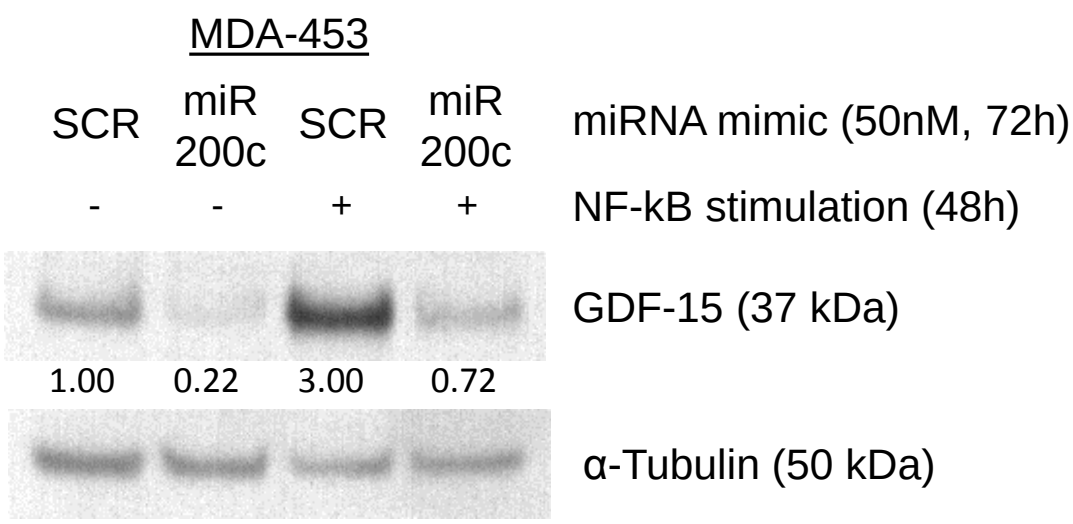

Figure 4

A

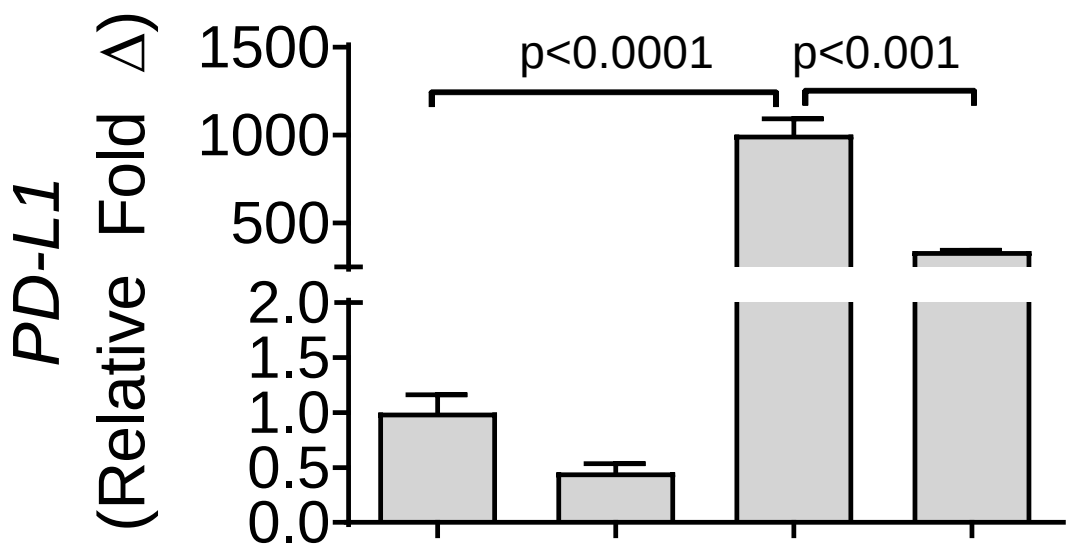

B

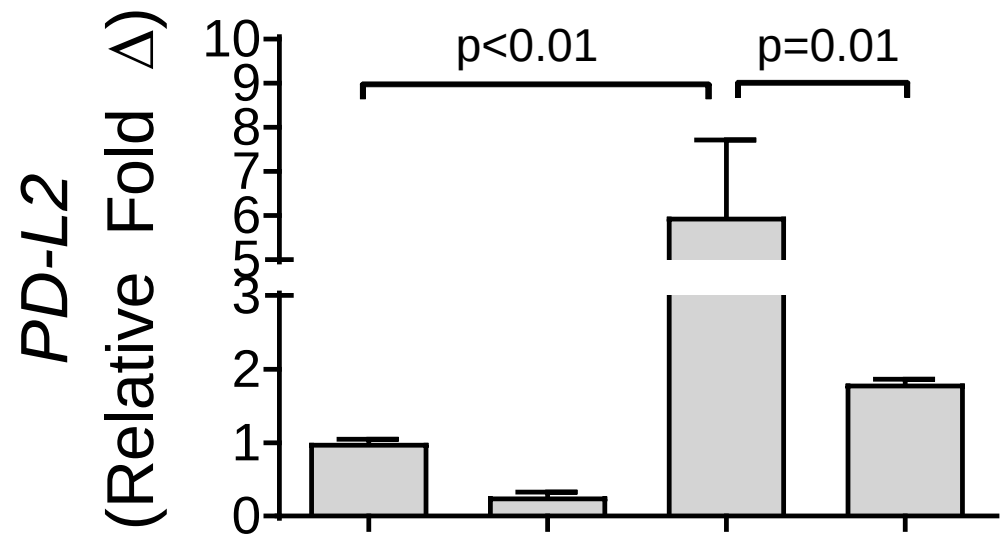

-	+	-	+	Dox (miR-200c)(72h)	-	+	-	+
-	-	+	+	IFN stimulation (48h)	-	-	+	+

C

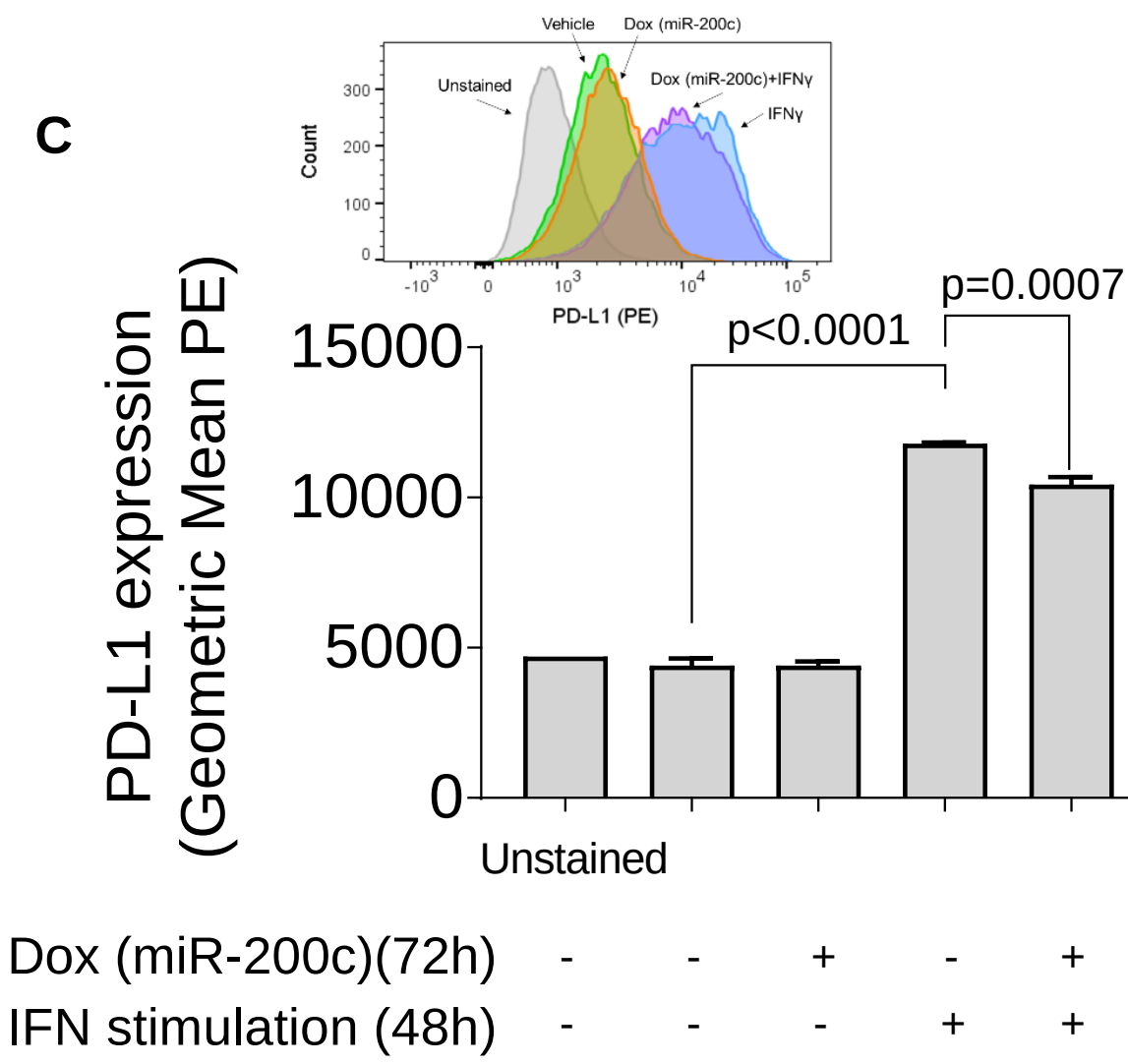

Dox (miR-200c)(72h)	-	-	+	-	+
IFN stimulation (48h)	-	-	-	+	+

D

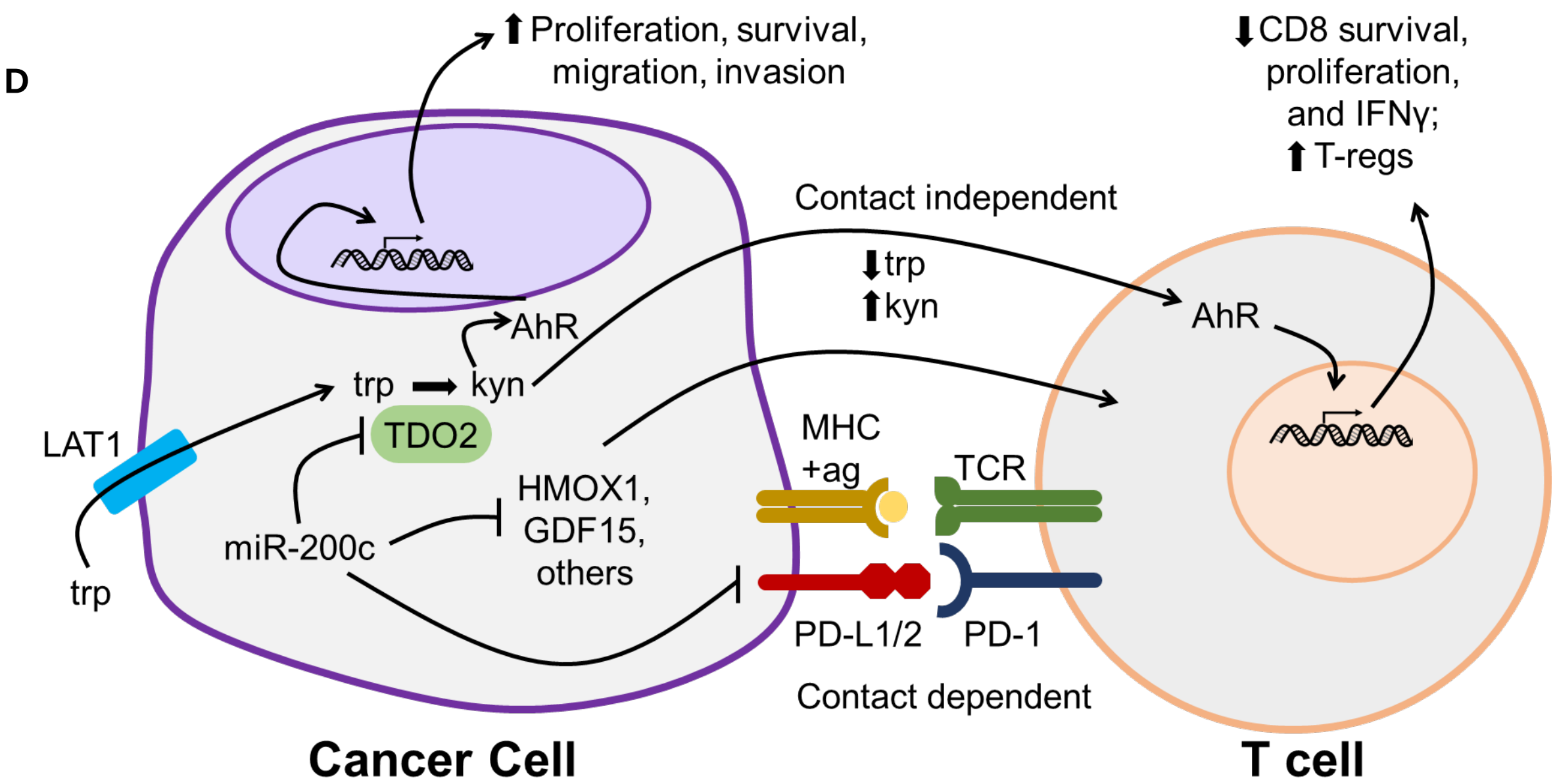

Supplemental Figure S1

A

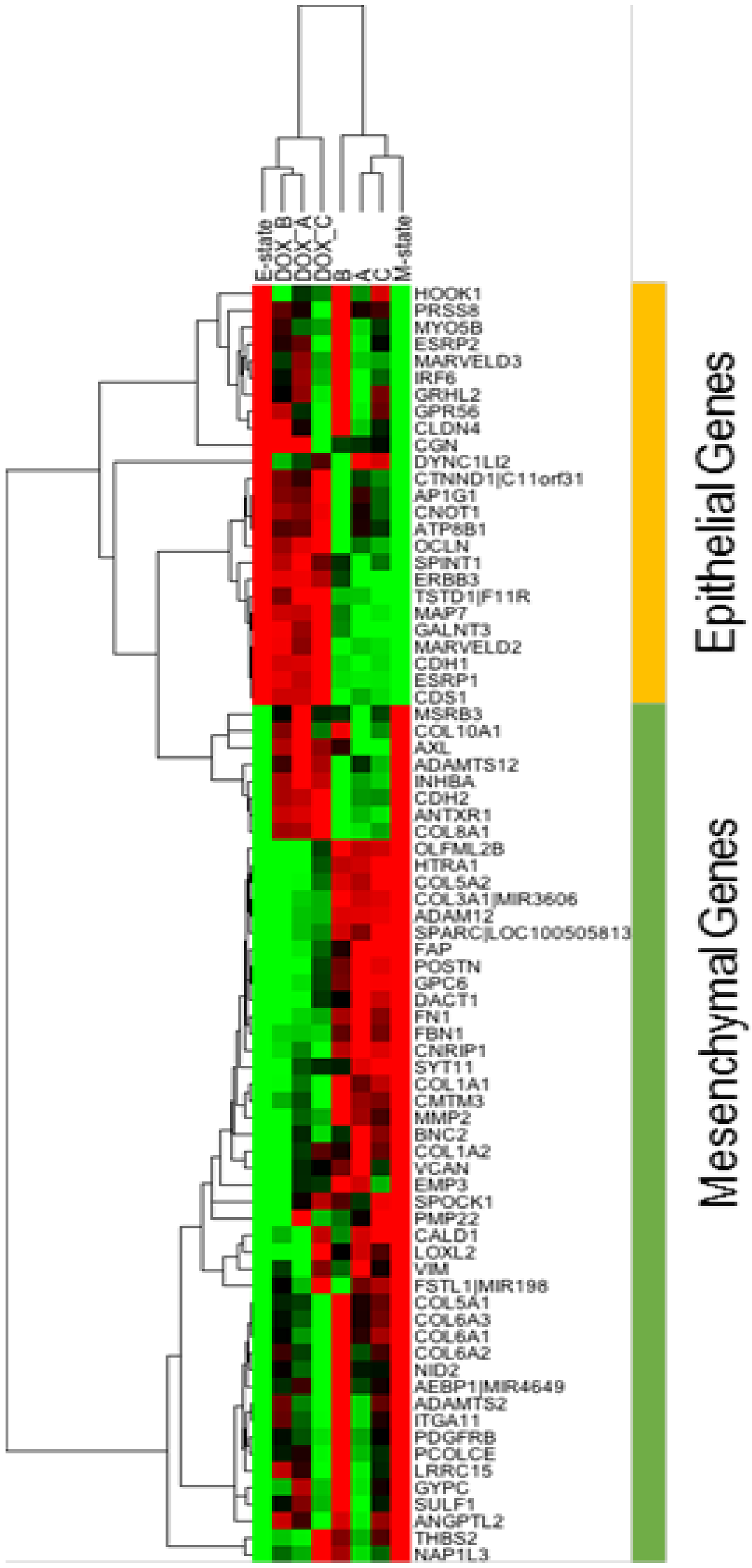

B

COMMONLY ALTERED GENES FOLLOWING MIR-200C RESTORATION (COMPARED TO GSE62230)	
UPREGULATED FOLLOWING MIR-200C RESTORATION	DOWNREGULATED FOLLOWING MIR-200C RESTORATION
ELOVL7	ADAMTSL1
LAMC2	CD274
GALNT3	PIM2
KRT18	HBEGF
KRT8	RCAN1
F2RL1	EHD3
LRBA	OSTM1
NPNT	ITGA5
RBM47	CREB5
FHDC1	GFPT2
LNX2	BDKRB1
MARVELD2	LOX
TPD52L1	EDNRB
CMTM4	MICALL1
EZR	IKBKB
TSPAN1	ARL2BP
PPL	ZEB1
KRT80	PLCG1
SAMD12	VGLL3
CDH1	EGR1
WWC1	HMOX1
SLC2A1	NRBP1
KIAA1161	FMNL3
FHOD3	CDK2
LRP5	GPR158
DOCK9	TDO2
MUC1	
RPS6KA1	
FUCA1	
UBC	
PODXL	
CDS1	
TESK1	
SOX15	
BAIAP2L1	
RIMS2	
CDON	
LYPD3	
FBXO27	
LAMP3	
TNFRSF10A	
SIPA1L1	
KRT5	
PPM1H	
ITPK1	
DSG2	
EPHA3	
MAL2	
CDH3	
ENPP5	
NLRP10	
PTGIS	
ATP9A	
UGT3A2	
CHODL	
KIF1B	
KIAA1107	
RHOBTB2	
TSPAN13	
EXPH5	
TMC5	
SMAD9	
SIM1	
SLC43A1	
PRKAA2	
SHROOM3	
ST6GALNAC5	
PDLIM1	

Supplemental Figure S2

A

Rank	Gene Set Name	Gene Set Size	Normalized Enrichment Score	Nominal *p*-value
1	Olfactory transduction	368	-1.96	0.0000
2	Graft versus host disease	37	-1.82	0.0000
3	Intestinal immune network for IgA production	47	-1.73	0.0048
4	Type I diabetes mellitus	42	-1.72	0.0000
5	Asthma	30	-1.70	0.0034
6	Allograft rejection	37	-1.69	0.0111
7	Complement and coagulation cascades	66	-1.67	0.0032
8	Autoimmune thyroid disease	52	-1.57	0.0050
9	Cytosolic DNA sensing pathway	53	-1.57	0.0189
10	**Tryptophan Metabolism**	40	-1.53	0.0185
11	Antigen processing and presentation	78	-1.52	0.0080
12	Toll-like receptor signaling pathway	97	-1.52	0.0139
13	Nodd-like receptor signaling pathway	59	-1.49	0.0258
14	Leishmania infection	69	-1.47	0.0235
15	Hematopoietic cell lineage	83	-1.43	0.0228
16	Glycosaminoglycan biosynthesis keratan sulfate	15	-1.27	0.1838
17	Viral myocarditis	67	-1.21	0.1615
18	Neuroactive ligand receptor interaction	265	-1.20	0.0837
19	Cytokine-cytokine receptor interaction	250	-1.20	0.1059
20	ECM receptor interaction	79	-1.17	0.1993
21	Rig-I-like receptor signaling pathway	70	-1.17	0.2000
22	Prion diseases	35	-1.14	0.2648
23	Glycosaminoglycan degradation	20	-1.11	0.3292
24	Apoptosis	83	-1.09	0.3105
25	Epithelial cell signaling in helicobacter pylori infection	66	-1.05	0.3914

B

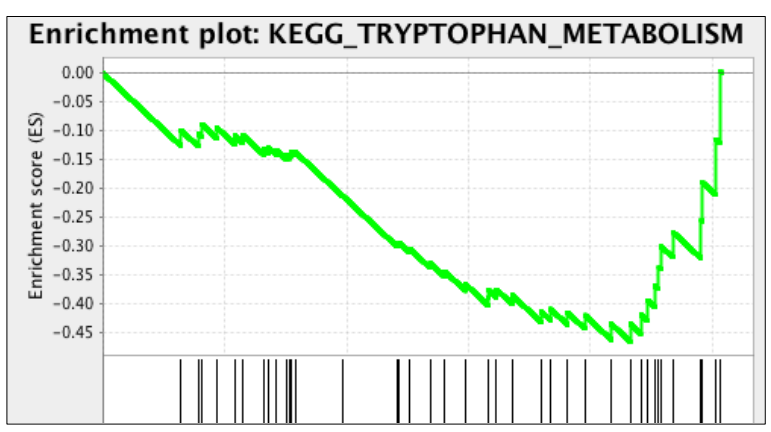

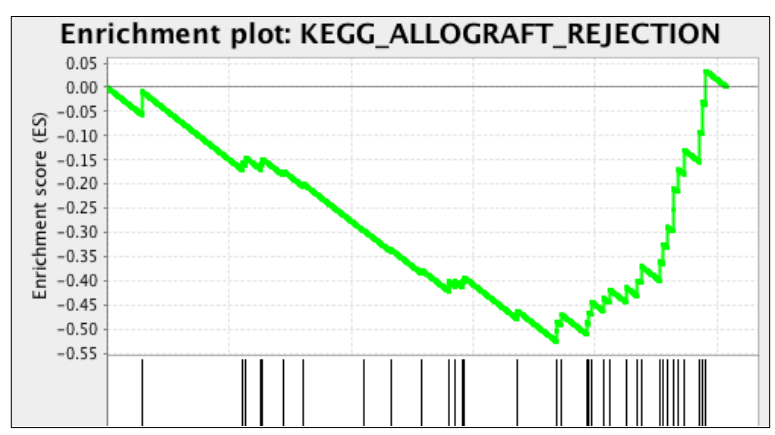

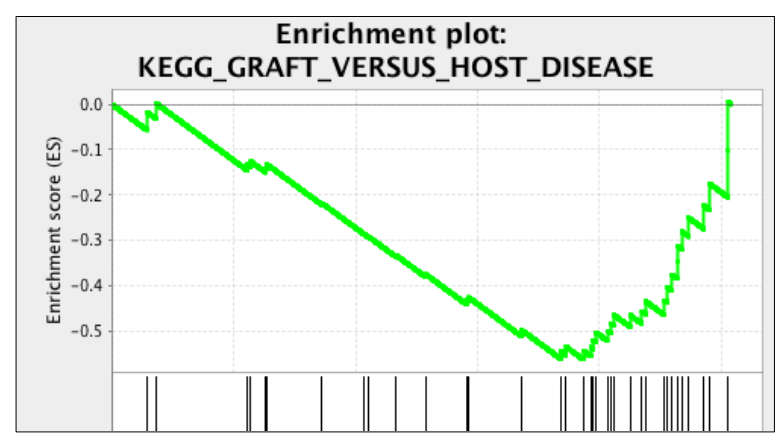

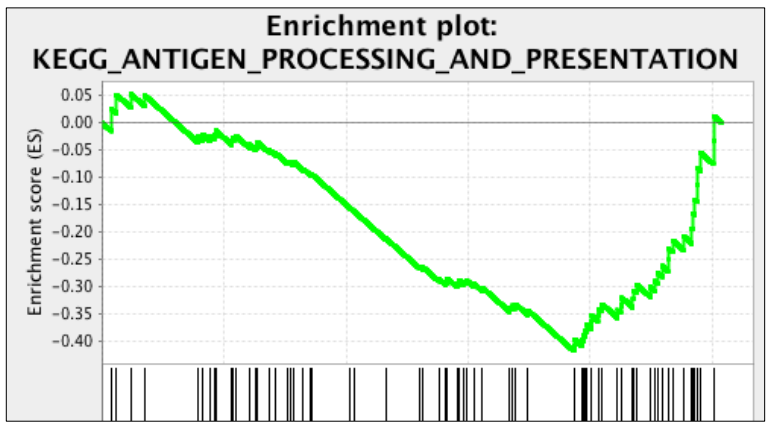

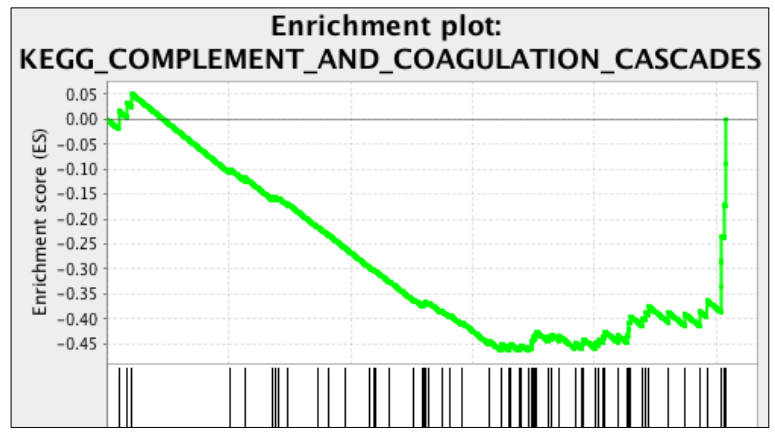

Supplemental Figure S3

A

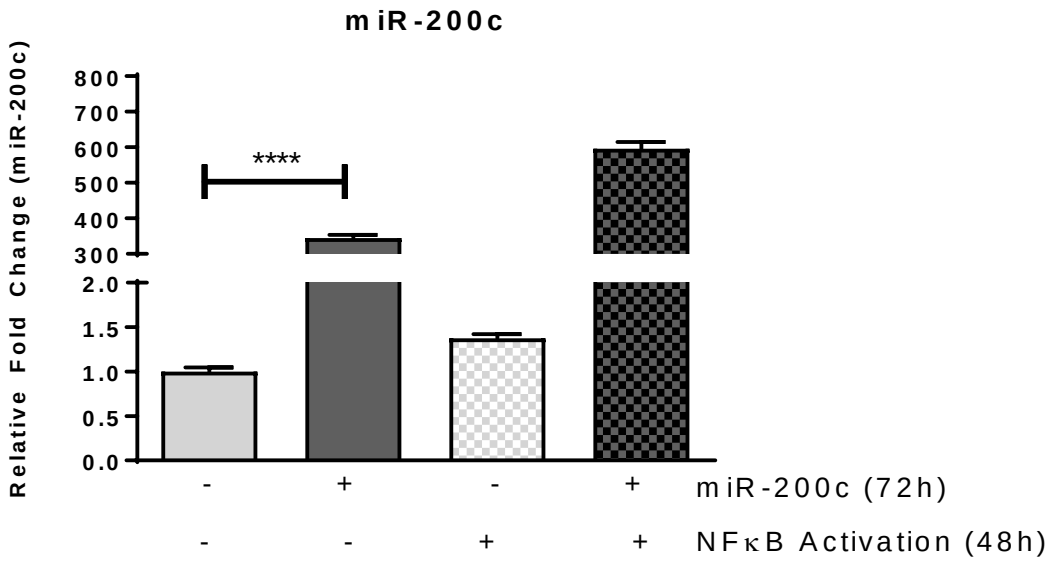

B

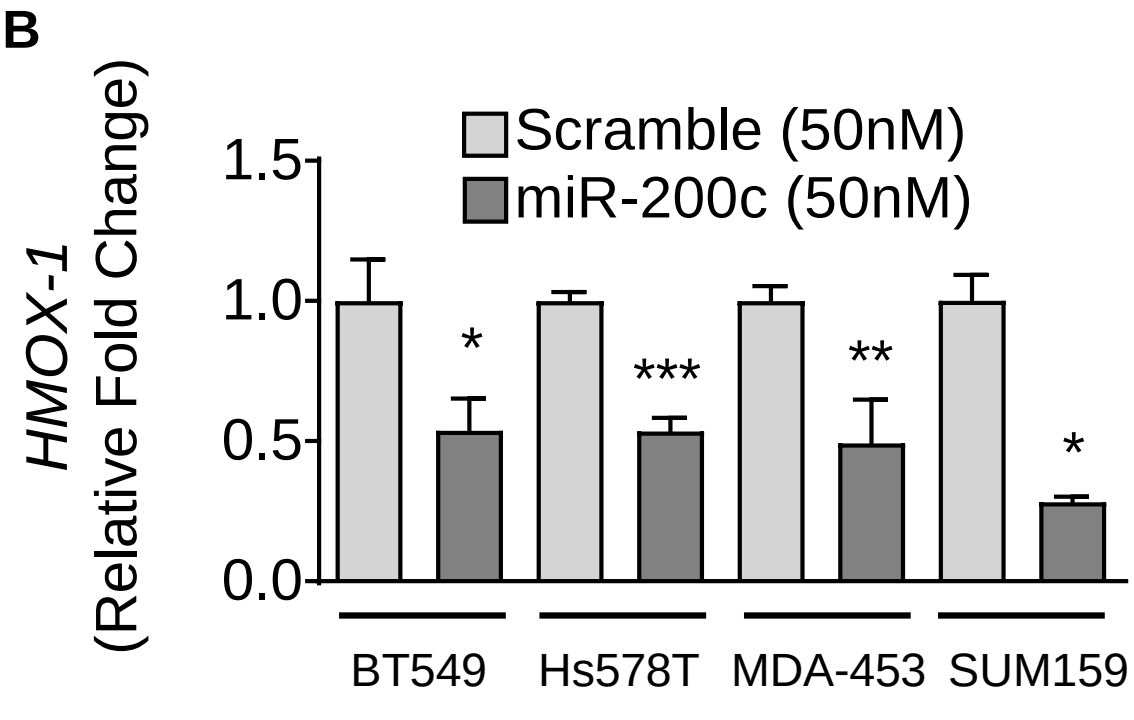

Supplemental Figure S4

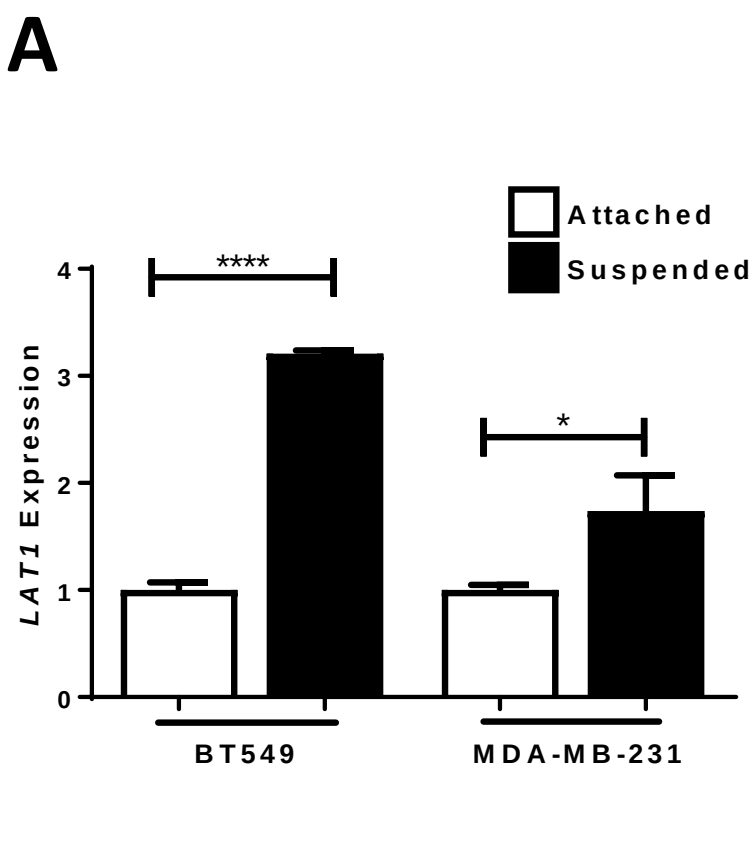

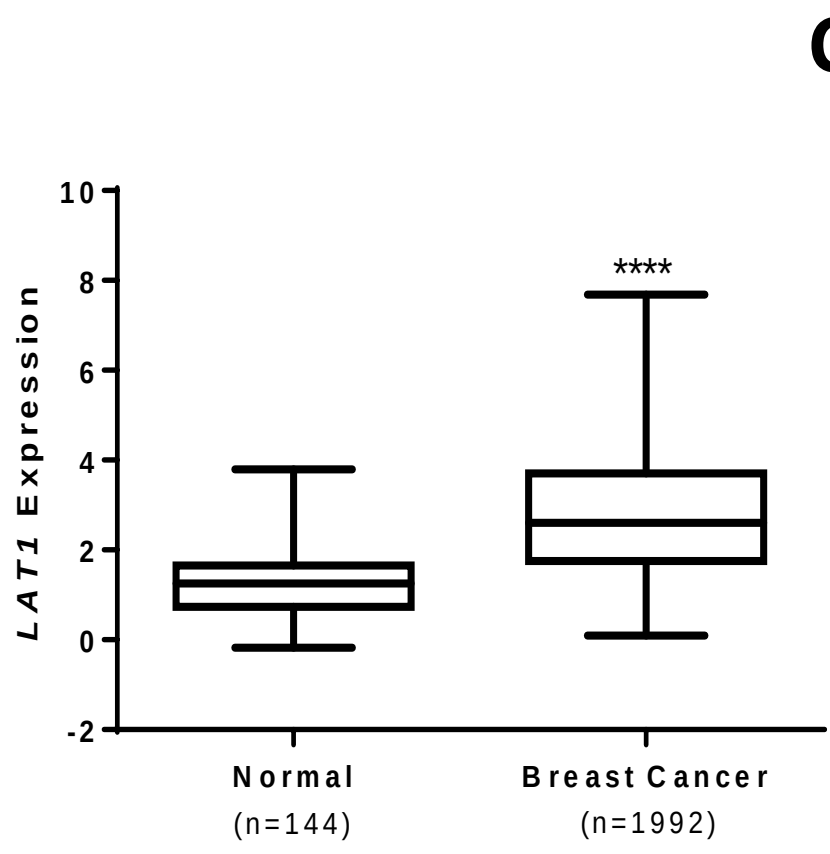

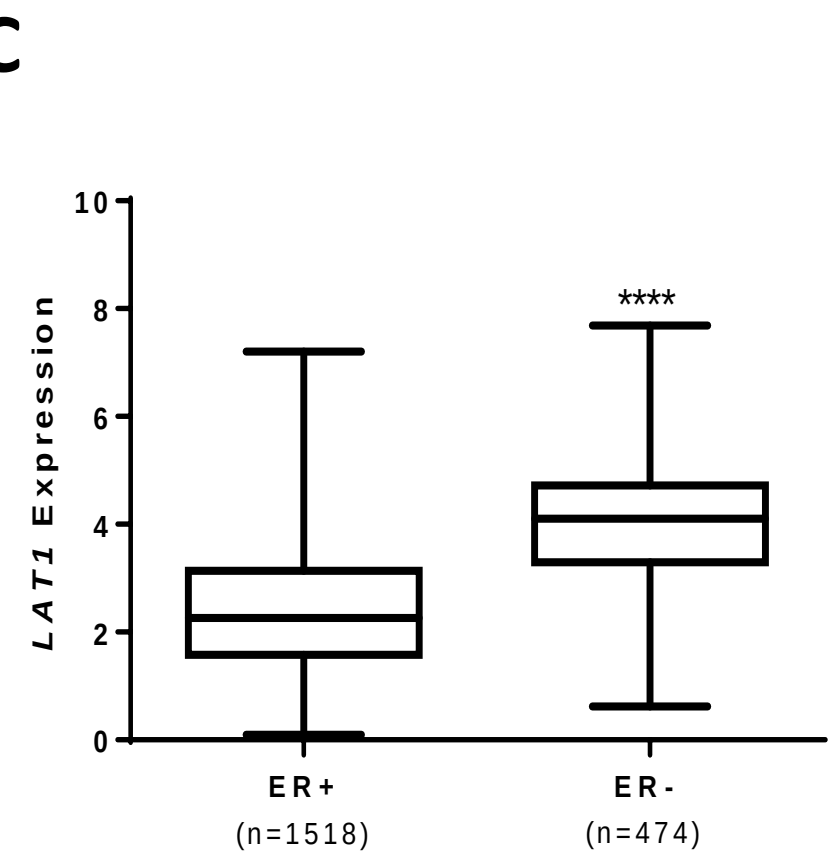

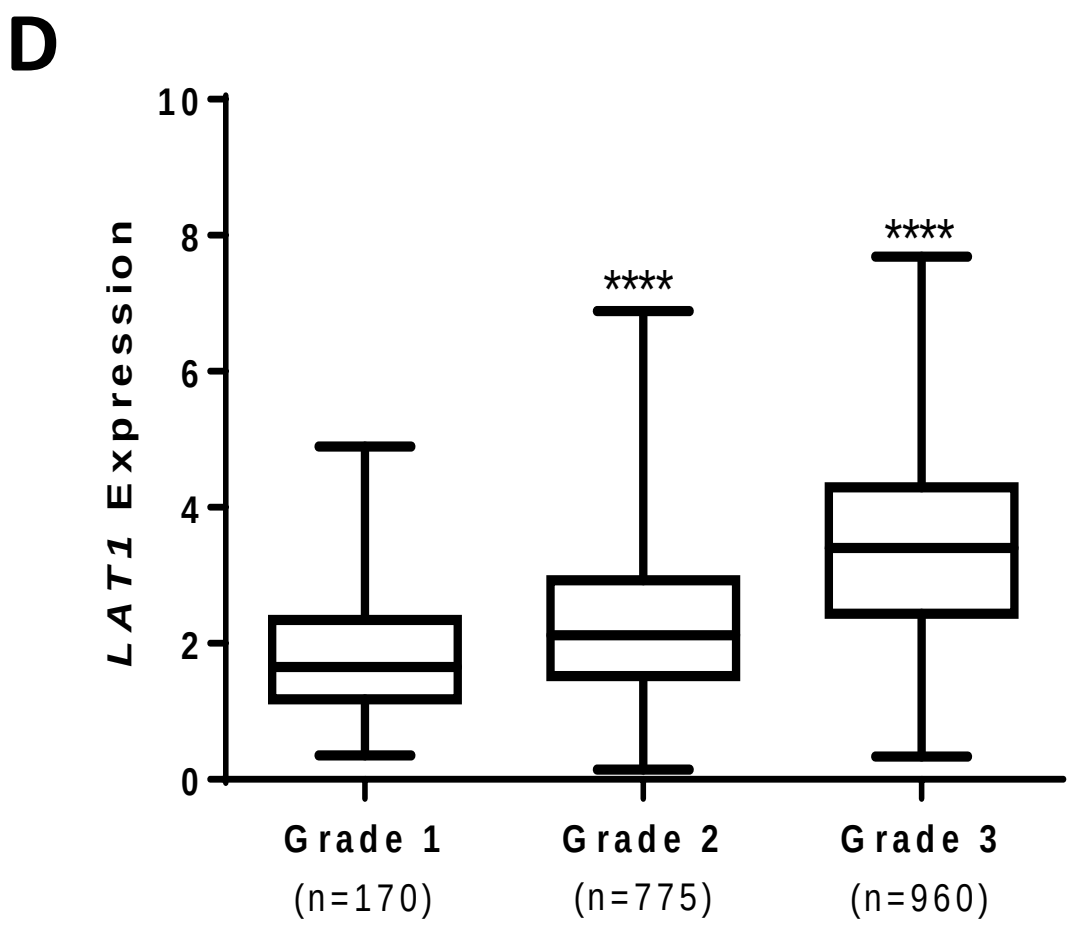

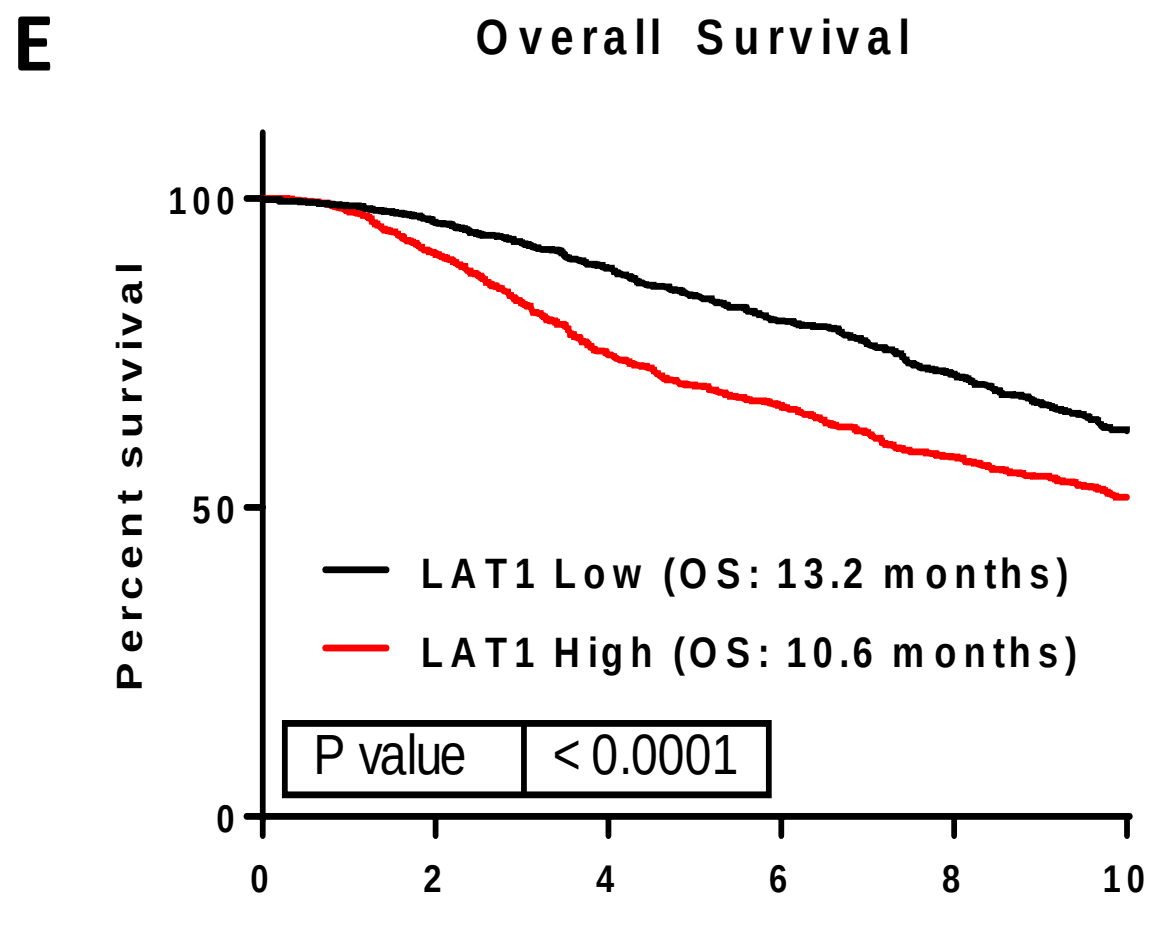

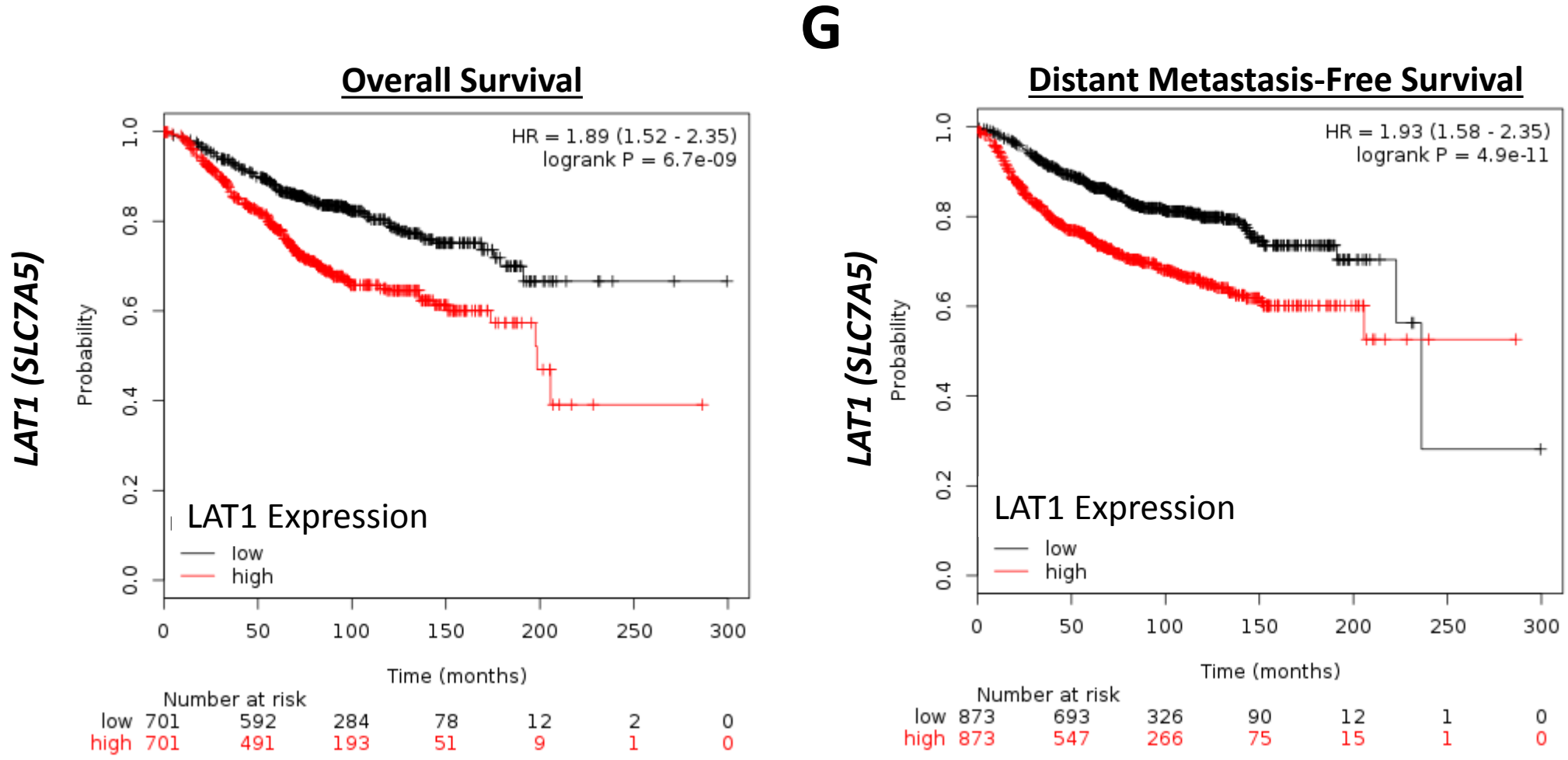

A role for tryptophan 2,3-dioxygenase in CD8 T cell suppression and evidence of tryptophan catabolism in breast cancer patient plasma

Authors and Affiliations

Lisa I Greene[1], Tullia C. Bruno[2], Jessica L. Christenson[1], Angelo D'Alessandro[3], Rachel Culp-Hill[3], Kathleen Torkko[1], Virginia F. Borges[4], Jill E. Slansky[5], Jennifer K. Richer[1*]

[1] Department of Pathology, University of Colorado Anschutz Medical Campus, 12800 E. 19th Ave. Aurora, CO 80045
[2] Department of Immunology, University of Pittsburgh, 5117 Centre Ave, Pittsburgh, PA 15213
[3] Department of Biochemistry and Molecular Genetics, University of Colorado Anschutz Medical Campus, 12800 E. 19th Ave. Aurora, CO 80045
[4] Department of Medicine, Division of Medical Oncology, University of Colorado Anschutz Medical Campus, 12800 E. 19th Ave. Aurora, CO 80045
[5] Department of Immunology and Microbiology, University of Colorado Anschutz Medical Campus, 12800 E. 19th Ave. Aurora, CO 80045

Running Title

TDO2 and tryptophan catabolism in breast cancer

Keywords

TDO2, breast cancer, kynurenine, T cell, immunotherapy

Financial Support

DOD BCRP Award Number W81XWH-15-1-0039 to JKR and NRSA F31 Award Number CA203486-01A1 to LIG.

Conflict of Interest Disclosure Statement

The authors declare no conflicts of interest.

Manuscript Notes

Abstract: 231
Body of Text: 3111
Figures: 5
Supplementary Figures: 3
Supplementary Tables: 1

***Corresponding author**
Jennifer K. Richer, Ph.D.
Department of Pathology
University of Colorado, Anschutz Medical Campus
12800 E 19th Ave Aurora, CO 80045, USA
Phone: (303) 724-3735
Fax: (303) 724-3712
Email: jennifer.richer@ucdenver.edu

Abstract

Tryptophan catabolism is an attractive target for reducing tumor progression and improving antitumor immunity in multiple cancers. In triple-negative breast cancer (TNBC), tumor infiltration by CD8 T cells correlates with improved prognosis, and a significant effort is underway to improve CD8 T cell antitumor activity. In this study, primary human immune cells were used to demonstrate that the tryptophan catabolite kynurenine induces CD8 T cell death, and that anchorage-independent TNBC utilizes the tryptophan catabolizing enzyme tryptophan 2,3-dioxygenase (TDO) to inhibit CD8 T cell viability. Publicly available data revealed that high *TDO2,* the gene encoding TDO, correlates with poor breast cancer outcomes, while expression of the gene encoding the more commonly studied tryptophan catabolizing enzyme *IDO1* did not. Quantitative detection of tryptophan and its catabolites – including kynurenine – in the plasma from 77 pre-surgical breast cancer patients and 40 cancer-free donors indicated a strong correlation between substrate and catabolite in both groups. Interestingly, both tryptophan and kynurenine were lower in the plasma from breast cancer patients compared to controls, particularly in women with estrogen receptor-negative and stage 3 and 4 disease. Together, these data underscore the importance of breast cancer tryptophan catabolism, particularly in aggressive disease, and suggest that future pharmacological efforts should focus on developing drugs that target both TDO and IDO1.

Introduction

Triple-negative breast cancer (TNBC) is an aggressive disease that lacks FDA-approved targeted therapies for the majority of patients (1). Importantly, TNBCs with high levels of immune infiltrate have more favorable prognoses (2, 3). Specifically, a high ratio of tumor-infiltrating cytotoxic CD8 T cells to immunosuppressive FoxP3+ T regulatory cells correlates with improved breast cancer-specific survival in chemoresistant TNBC (4). Indeed, TNBC has high expression of programmed cell death 1-ligand 1 (PD-L1) compared to other breast cancer subtypes, suggestive of evasion from immune attack (5-7). Active clinical trials are investigating the efficacy of targeting the PD-1/PD-L1 axis and other immune-directed interventions as treatments for TNBC; however, results in TNBC patients treated with the anti-PD-1 agent pembrolizumab indicate promising but limited efficacy (8, 9).

We previously discovered that aberrant expression and activity of the hepatic tryptophan-catabolizing enzyme tryptophan-2,3-dioxygenase (TDO) in TNBC cell lines supports anchorage-independent cell growth and late-stage metastasis through an autocrine mechanism, whereby the tryptophan catabolite kynurenine activates the aryl-hydrocarbon receptor (AhR) in the breast cancer cells (10). However, it is clear that kynurenine also has suppressive paracrine effects on immune cells (11, 12). Most studies have focused on the tryptophan catabolizing enzyme indoleamine-2,3-dioxygenase (IDO) in cancer, and current inhibitors of this pathway in clinical trials only target IDO activity. *TDO2* (the gene encoding TDO), however, is significantly higher in estrogen receptor (ER) negative (-) compared to ER+ breast tumors, and *TDO2* correlates with overall survival in breast cancer patients, suggesting a potential failure of current tryptophan catabolizing agents in effectively targeting tumor cell enzymatic activity (10).

Alterations in blood tryptophan and kynurenine levels have been examined in multiple human cancers (13-15). Lower serum tryptophan correlates with poor prognosis in melanoma, consistent with an increase in tryptophan catabolism (15). A small-scale study showed that plasma from post-surgical (lumpectomy or mastectomy) breast cancer patients has reduced tryptophan and elevated kynurenine compared to cancer-free controls, as measured by ultra-high pressure liquid

chromatography (UHPLC), but importantly this study may not have been able to measure any potential effects of the primary tumor on systemic levels of these molecules (13). Another breast cancer study found relatively higher intratumoral kynurenine in ER- versus ER+ tumors (14). The issue of whether decreased tryptophan or increased kynurenine levels reflect the activity of tumor tryptophan catabolizing enzymes remains unresolved in breast cancer patient plasma.

Here, we demonstrate that kynurenine increased primary human CD8 T cell death, and that conditioned media from anchorage-independent TNBC cells suppressed primary human CD8 T cell function through a TDO-dependent mechanism, demonstrating a mechanism of enhanced immune evasion during metastasis. Furthermore, we quantified tryptophan and kynurenine – as well as a series of tryptophan catabolites – in plasma from 77 pre-surgical breast cancer patients using UHPLC-MS and detected significant differences in plasma from women with breast cancer versus no breast cancer, ER+ versus negative tumors, and with increasing disease stage.

Materials and Methods

Cell Culture

BT549 cells, purchased from ATCC in 2008 and authenticated prior to use by Short Tandem Repeat DNA Profiling (Promega), were grown in RPMI Medium 1640 with 10% fetal bovine serum (FBS), penicillin/streptomycin (P/S) and insulin supplementation. Suspension culture was achieved using plates coated with 12 mg/mL poly(2-hydroxyethyl methacrylate) (Sigma-Aldrich) reconstituted in 95% ethanol. Ethanol evaporated overnight, and plates were washed with PBS prior to use.

Primary Human T Cell Isolation and Activation

Blood was collected by venipuncture into tubes with heparin (BD Biosciences Vacutainer Systems) from donors under a University of Colorado Anschutz Medical Campus Colorado Institutional Review Board (COMIRB)-approved protocol. Lymphocytes were isolated by adding 10 mL of Ficoll-Paque PLUS (GE Healthcare) per 20 mL of blood diluted in Hanks' Balanced Salt Solution, then centrifuging

at 2000 rpm for 25 minutes without deceleration. CD8 T cells were resuspended in PBS containing 0.5% BSA and 2 mM EDTA for selection using positive isolation kits (Dynabeads, Invitrogen). After isolation, cells were labeled with carboxyfluorescein succinimidyl ester (CFSE, Invitrogen) according to manufacturer's instructions, then resuspended in RPMI medium containing 10% FBS, P/S, non-essential amino acids, sodium pyruvate, and HEPES. T cells were activated in plates coated with 0.5 µg/mL of CD3 antibody (clone OKT3, eBioscience) and 1.0 µg/mL of soluble CD28 antibody (clone CD28.2, eBioscience) for 5 days. For intracellular staining, T cells were stimulated for 4 hours after the activation using phorbol-12-myristate-13-acetate (PMA) at 20 ng/mL, ionomycin at 1 µg/mL, and GolgiStop (BD Biosciences).

Cell Staining and Flow Cytometry

T cells were stained with antibodies for CD3 (clone HIT3a, Biolegend) and CD8 (clone RPA-T8, Biolegend) at a 1:100 dilution and an intracellular stain for interferon gamma (clone 4S.B3, eBioscience) at a 1:50 dilution. Intracellular staining was achieved using an intracellular fixation and permeabilization buffer set (eBioscience). Dead cells were detected by positivity for a viability dye according to manufacturer's instructions (Fixable Viability Dye BV421, eBioscience). Flow cytometry was conducted using an LSR II (BD Biosciences) and data were analyzed using FlowJo software (Tree Star, Inc).

TDO2 and AhR Inhibition

The TDO2 inhibitor 680C91 (Sigma-Aldrich) or the AhR antagonist CH-223191 (TOCRIS Bioscience) prepared in dimethyl sulfoxide (DMSO) were used.

Breast Cancer Patient Plasma

Blood and was acquired as described above from pre-surgical breast cancer patients under a COMIRB and HRPOapproved protocol (COMIRB 15-2225 and HRPO A-18613). The characteristics of the cohort are described in Supplementary Table 1.

UHPLC-MS Targeted Metabolomic Analysis of Tryptophan Catabolism

Tryptophan ($^{15}N_2$) and kynurenine (ring-D_4, 3,3-D_2) were purchased from Cambridge Isotope Laboratories, Incorporated. To ensure linearity over 5 orders of magnitude, lysis buffer (LB), a 5:3:2 ratio of MeOH:acetonitrile:H_2O, and 0.1% formic acid aliquots were each spiked with varying ranges of heavy-labeled tryptophan and kynurenine (50 µM, 5 µM, 500 nM, 50 nM, 5 nM, 500 pM) and analyzed by ultra-high pressure liquid chromatography coupled to mass spectrometry – UHPLC-MS. Plasma (20 µL) was extracted at 1:5 and 1:10 in LB containing 5 µM heavy labeled tryptophan and kynurenine as previously described, then diluted 1:5, 1:10 and 1:20 with H_2O and run on UHPLC-MS (16, 17). Sample extracts were analyzed via UHPLC-MS (Vanquish, Q Exactive – Thermo Fisher, Bremen, Germany) using C18 reverse-phase chromatography and positive electrospray ionization (ESI) (16, 18). A Kinetex C18 column, 2.1x x150 mm, 1.7 µm particle size (Phenomenex) was used and equipped with a C18 guard column (Phenomenex). The method is a variant of previously published methods (19). Samples were resolved at 45°C with a gradient elution over 4 minutes, flowing at 450 µL/min. Mobile phase A is 0.1% formic acid in water, mobile phase B is 0.1% formic acid in acetonitrile. 5% B and 95% A is held from 0.00–0.50 minutes. From 0.50–1.10 minutes, B increases to 95% B and 5% A. This condition is held from 1.10 – 2.75 minutes. From 2.75–3.00 minutes A decreases to the initial condition of 5% B and 95% A and is held from 3.00–4.00 minutes. The Q Exactive mass spectrometer was operated in positive ion mode using electrospray ionization, scanning in Full MS mode (1 µscan) from 100 to 1500 m/z at 70,000 resolution, with 4 kV spray voltage, 45 sheath gas,15 auxiliary gas. Calibration was performed prior to analysis using the Pierce Positive Ion Calibration Solution (Thermo Fisher Scientific). Metabolite assignments and heavy isotopologue detection for absolute quantitation against internal standards were determined against in

house standard libraries and KEGG database searches through Maven (20). Technical reproducibility was assessed by monitoring internal heavy labeled standard mixes as reported (16). Calculation of absolute quantification for measured metabolites was performed using the following formula: [light] = (abundance light) / (abundance heavy) * [heavy] (dilution factor) where dilution factor is 10 for an extraction of 10 µL plasma in 90 µL lysis buffer.

Statistical Analyses

Prism Graphpad Version 7.02 was used for all statistical analyses. All tests are two-sided with statistical significance set at $p<0.05$. Statistical tests and sample sizes are described in the figure legends. *$p<0.05$, **$p<0.01$, ***$p<0.001$, ****$p<0.0001$.

Results

Primary human CD8 T cell response to kynurenine and cancer cell conditioned media

Infiltration into breast tumors by cytotoxic CD8 T cells correlates with improved prognosis in ER- breast cancer (4, 21-23). To test the effect of kynurenine on primary human peripheral blood cytotoxic T cells, CD8+ cells isolated from peripheral blood of healthy human donors (Figure 1A) were treated with increasing doses of kynurenine over a 5-day T cell receptor (TCR) activation protocol. At 50 and 100 µM kynurenine, CD8 T cell death increased as measured by a fixable viability dye (Figure 1B), while CFSE analysis indicated no change in proliferation (Figure 1C), demonstrating a direct impact of kynurenine specifically on human CD8 T cell viability. To test whether kynurenine acts through AhR to affect CD8 T cell viability, CD8 T cells were treated with increasing doses of kynurenine with or without the AhR antagonist CH-223191 (24). Treatment with CH-223191 significantly reduced the cytotoxic effect of 50 µM kynurenine (Figure 1D-E), indicating that kynurenine acts in part on CD8 T cells through AhR.

We previously reported that TNBC cells surviving under anchorage-independent culture conditions increased expression and activity of TDO, resulting in increased intracellular and secreted

kynurenine (10). In the present study, we asked whether such anchorage-independent cells have enhanced immune evasion. BT549 TNBC cells were cultured in attached (ATT) or suspended (SUS) conditions for 24 or 48 hours. Primary human CD8 T cells were cultured in these conditioned media (CM) with CD3 and CD28 antibodies for 5 days. CD8 T cells cultured in SUS CM were less viable than those cultured in ATT CM (Figure 2A). Since kynurenine decreased interferon-gamma (IFNγ) mRNA in murine cytotoxic T cells (25), we tested whether CM from attached versus suspended TNBC cells would affect primary human CD8 T cell production of IFNγ. Indeed, the SUS CM significantly reduced IFNγ production compared to ATT CM (Figure 2B and 2C). To determine if the effects of SUS CM were due to increased TDO activity, TNBC cells were plated in ATT or SUS conditions with or without TDO-specific inhibitor 680C91 for 48 hours. While SUS CM again increased CD8 T cell death, this effect was significantly abrogated when SUS cells were treated with TDO inhibitor 680C91 (Figure 2D), suggesting that TDO activity is at least partially responsible for the CM effect. However, treating the CD8 T cells with the AhR antagonist CH-223191 did not rescue the effect of SUS CM, suggesting additional effects of TNBC TDO2 activity on the CD8 T cells (Figure 2E).

TDO2 RNA expression correlates with breast cancer outcomes, and tryptophan catabolism is altered in breast cancer

We previously reported that *TDO2* is significantly higher in breast cancer versus normal breast tissue and in ER-negative versus ER-positive disease, and that above-median *TDO2* correlated with poor overall survival in the Curtis et al dataset (10). In the current study, we used the KM Plotter tool to investigate breast cancer outcomes associated with both *TDO2* and *IDO1* expression (26). High *TDO2* in primary breast cancer correlated with worse overall survival and reduced distant metastasis-free survival (Figure 3A), while *IDO1* did not (Figure 3B).

To further understand how tryptophan catabolism is altered in breast cancer subtypes, we measured plasma concentrations of tryptophan and its main catabolites, including kynurenine using

UHPLC-MS (Supplementary Table 1). In the plasma from cancer-free “normal” women, the concentration of tryptophan ranged from 69.50-294.49 μM, while in women with breast cancer the range was 38.04-260.77 μM. Meanwhile, the plasma concentration of kynurenine in normal women ranged from 3.46-13.61 μM, and from 2.19-19.83 μM in women with breast cancer. Strikingly, there was a significant positive correlation between tryptophan and kynurenine both in plasma from normal women (Figure 4A) and women with breast cancer (Figure 4B). A comparison of the plasma concentrations of tryptophan and kynurenine in women with breast cancer versus normal controls demonstrated that women with breast cancer had significantly reduced tryptophan (mean = 141.39 μM) compared to normal (mean = 173.32 μM) (Figure 4C). Interestingly and surprisingly, the concentration of kynurenine was also significantly lower in the plasma of women with breast cancer (mean = 7.12 μM) compared to normal controls (mean = 9.02 μM) (Figure 4D).

Given previous reports that *TDO2* is significantly higher in ER- versus ER+ disease, the plasma tryptophan and kynurenine concentrations in women with ER- and ER+ breast cancer were next compared (10). There was no significant difference in either plasma tryptophan or kynurenine in women with ER+ and ER- disease (Figure 4C-D), though lower levels of tryptophan and anthranilate were observed in plasma from women with ER-HER2- disease (Supplemental Figure 1). However, ER- breast cancer patients had significantly reduced plasma tryptophan compared to normal controls, while ER+ breast cancer patients did not (Figure 4C). Plasma kynurenine from both ER- and ER+ breast cancer subsets was significantly lower than that from normal controls (Figure 4D). Of note, these decreases were more marked in women with non-pregnancy-associated breast cancer (PABC) in comparison to PABC patients (where PABC is defined as a diagnosis with 5 years of pregnancy), with the highest relative levels of tryptophan (and its catabolites hydroxytryptophan, kynurenine and kynurenic acid) detected in normal women who did not give birth within the past 5 years. Interestingly, normal women who had given birth within the past five years had intermediate levels of tryptophan and its catabolites in between normal women who had given birth within the past five years and PABC/non-PABC patients (Supplementary Figure 2). To examine whether either plasma tryptophan

or kynurenine correlated with breast cancer aggressiveness, breast cancer stage at diagnosis was used. Both tryptophan (Figure 4E) and kynurenine (Figure 4F) were significantly lower in stage 3/4 breast cancer patient plasma than in plasma from normal controls, while there was no difference in either tryptophan or kynurenine when comparing stage 0/1 patients versus normal (Figure 4E-F). Interestingly, there was also a decrease in the kynurenine catabolite kynurenic acid in stage 3/4 breast cancer patients compared to patients with stage 1/2 disease (Supplementary Figure 3).

To examine whether tryptophan catabolism correlated with breast cancer outcomes in this data set, we divided the patient data into tryptophan-low and tryptophan-high groups based on the median concentration of plasma tryptophan, and compared the progression-free survival of these groups, where progression was defined as local, regional, or distant recurrence, or patient death. While there was no significant difference in progression-free survival between these groups in either ER+ (Figure 5A) or ER- (Figure 5B) breast cancer patients, there was a notable trend towards patients with lower than median plasma tryptophan having poorer outcomes (Figure 5B), consistent with a negative impact of reduced tryptophan in ER- disease.

Discussion

While tryptophan catabolism is known to mediate tumor immune evasion, the impact of IDO or TDO activity on CD8 T cells was thought to occur through indirect suppression via regulatory T cell activation. We demonstrate here that the direct impact of kynurenine on primary human CD8 T cells is to reduce viability in the setting of activation through the T cell receptor. We previously reported that TDO activity increased in TNBC cells under anchorage-independent conditions, resulting in increased intracellular and secreted kynurenine (10). Critically, we show here that conditioned media from TNBC cells cultured under anchorage-independent conditions limits the viability and IFNγ production of primary human CD8 T cells, and that this cell death is abrogated by the specific TDO inhibitor 680C91, suggesting that anchorage-independent TNBC cells are highly immunosuppressive through TDO-mediated activity. A high ratio of cytotoxic CD8 T cells to Treg cells correlates with

improved clinical outcomes in TNBC (27, 28). Thus, the power of TDO-positive metastatic TNBC cells to suppress CD8 T cells both directly and indirectly via the induction of Tregs (12) could be a critical mechanism of disease progression.

Although inhibition of TDO activity in suspended TNBC cells reversed the effects of conditioned media on the viability and function of CD8 cells, inhibition of the receptor for kynurenine, AhR, in the CD8 cells was not sufficient to mitigate this effect. One possible explanation for the differential effects of TDO as compared to AhR inhibition is that the effect of TDO activity on CD8 T cells is due to the combined effects of both tryptophan depletion and kynurenine secretion. Kynurenines combined with tryptophan depletion downregulate the TCR zeta-chain and decreases cytokine production in murine CD8 T cells (25), and IDO-mediated tryptophan depletion inhibits mTOR and PKC-θ activation to induce murine T cell anergy and autophagy (29). AhR antagonism would interfere with kynurenine-mediated AhR activation, but would not abrogate tryptophan depletion.

To our knowledge, the present study includes the largest metabolomic analysis of tryptophan and kynurenine in plasma from pre-surgery breast cancer patients, allowing assessment of the impact of an existing breast tumor on systemic tryptophan and kynurenine levels. Given that others have reported higher kynurenine and lower tryptophan levels in breast cancer patients compared to healthy donors (13), our finding of a strong maintenance of balanced levels of substrate to catabolite in plasma from both breast cancer patients and cancer-free donors was unexpected. This may be attributable to the strong ability of the kidneys to handle increased kynurenine and it is documented that increased TDO/IDO activity does not necessarily result in increased plasma kynurenine (30, 31). Interestingly, we found that compared to healthy donors, tryptophan was only significantly lower in the plasma of patients with ER-negative tumors. This finding suggests a particularly important role of elevated tumor tryptophan catabolism in ER-negative disease. An expanded follow-up metabolomic study that includes more patients with ER- and stage 3/4 disease is imperative to determine if plasma tryptophan and kynurenine associate with tumoral enzymatic activity and outcomes. It is likely that

measurement of TDO/IDO protein levels or activity in primary tumor and/or circulating tumor cells would be more informative than plasma levels of tryptophan and kynurenine, and the levels of the enzymes in tumors should be correlated with tumor-infiltrating lymphocyte composition in future studies. Additionally, it is possible that further flux through the kynurenine pathway in tumor cells could account for the comparatively low kynurenine concentration in plasma from women with breast cancer. Metabolomic tracing of tumor tryptophan could help elucidate the ultimate fate of this amino acid in tumors. Given that the development of specific antibodies against TDO and IDO has historically been difficult, this will be a significant hurdle to overcome in the development of biomarkers for patients who may benefit from tryptophan catabolism-targeted therapies.

Acknowledgements

The authors wish to thank the University of Colorado School of Medicine Biological Mass Spectrometry Core Facility for their contributions to this manuscript. We also acknowledge the shared resources of the University of Colorado Cancer Center NCI Support Grant (P30CA046934), particularly the Tissue Culture Core. We thank Emily Rozzo and Michelle Borakove for assistance in patient sample collection and analysis guidance. Finally, we thank the blood donors that made these studies possible.

References

1. Liedtke C, Mazouni C, Hess KR, Andre F, Tordai A, Mejia JA, et al. Response to neoadjuvant therapy and long-term survival in patients with triple-negative breast cancer. Journal of clinical oncology : official journal of the American Society of Clinical Oncology. 2008;26(8):1275-81.

2. Aaltomaa S, Lipponen P, Eskelinen M, Kosma VM, Marin S, Alhava E, et al. Lymphocyte infiltrates as a prognostic variable in female breast cancer. Eur J Cancer. 1992;28A(4-5):859-64.

3. Denkert C, von Minckwitz G, Brase JC, Sinn BV, Gade S, Kronenwett R, et al. Tumor-infiltrating lymphocytes and response to neoadjuvant chemotherapy with or without carboplatin in human epidermal growth factor receptor 2-positive and triple-negative primary breast cancers. J Clin Oncol. 2015;33(9):983-91.

4. Miyashita M, Sasano H, Tamaki K, Hirakawa H, Takahashi Y, Nakagawa S, et al. Prognostic significance of tumor-infiltrating CD8+ and FOXP3+ lymphocytes in residual tumors and alterations in these parameters after neoadjuvant chemotherapy in triple-negative breast cancer: a retrospective multicenter study. Breast cancer research : BCR. 2015;17:124.

5. Ali HR, Glont SE, Blows FM, Provenzano E, Dawson SJ, Liu B, et al. PD-L1 protein expression in breast cancer is rare, enriched in basal-like tumours and associated with infiltrating lymphocytes. Ann Oncol. 2015;26(7):1488-93.

6. Mittendorf EA, Philips AV, Meric-Bernstam F, Qiao N, Wu Y, Harrington S, et al. PD-L1 expression in triple-negative breast cancer. Cancer Immunol Res. 2014;2(4):361-70.

7. Sabatier R, Finetti P, Mamessier E, Adelaide J, Chaffanet M, Ali HR, et al. Prognostic and predictive value of PDL1 expression in breast cancer. Oncotarget. 2015;6(7):5449-64.

8. Nanda R, Chow LQ, Dees EC, Berger R, Gupta S, Geva R, et al. Pembrolizumab in Patients With Advanced Triple-Negative Breast Cancer: Phase Ib KEYNOTE-012 Study. J Clin Oncol. 2016;34(21):2460-7.

9. Kwa MJ, Adams S. Checkpoint inhibitors in triple-negative breast cancer (TNBC): Where to go from here. Cancer. 2018.

10. D'Amato NC, Rogers TJ, Gordon MA, Greene LI, Cochrane DR, Spoelstra NS, et al. A TDO2-AhR signaling axis facilitates anoikis resistance and metastasis in triple-negative breast cancer. Cancer Res. 2015;75(21):4651-64.

11. Opitz CA, Litzenburger UM, Sahm F, Ott M, Tritschler I, Trump S, et al. An endogenous tumour-promoting ligand of the human aryl hydrocarbon receptor. Nature. 2011;478(7368):197-203.

12. Mezrich JD, Fechner JH, Zhang X, Johnson BP, Burlingham WJ, Bradfield CA. An interaction between kynurenine and the aryl hydrocarbon receptor can generate regulatory T cells. J Immunol. 2010;185(6):3190-8.

13. Lyon DE, Walter JM, Starkweather AR, Schubert CM, McCain NL. Tryptophan degradation in women with breast cancer: a pilot study. BMC Res Notes. 2011;4:156.

14. Tang X, Lin CC, Spasojevic I, Iversen ES, Chi JT, Marks JR. A joint analysis of metabolomics and genetics of breast cancer. Breast cancer research : BCR. 2014;16(4):415.

15. Weinlich G, Murr C, Richardsen L, Winkler C, Fuchs D. Decreased serum tryptophan concentration predicts poor prognosis in malignant melanoma patients. Dermatology. 2007;214(1):8-14.

16. D'Alessandro A, Nemkov T, Yoshida T, Bordbar A, Palsson BO, Hansen KC. Citrate metabolism in red blood cells stored in additive solution-3. Transfusion. 2017;57(2):325-36.

17. Nemkov T, Hansen KC, D'Alessandro A. A three-minute method for high-throughput quantitative metabolomics and quantitative tracing experiments of central carbon and nitrogen pathways. Rapid Commun Mass Spectrom. 2017;31(8):663-73.

18. Clasquin MF, Melamud E, Rabinowitz JD. LC-MS data processing with MAVEN: a metabolomic analysis and visualization engine. Curr Protoc Bioinformatics. 2012;Chapter 14:Unit14 1.

19. D'Alessandro A, Nemkov T, Hansen KC, Szczepiorkowski ZM, Dumont LJ. Red blood cell storage in additive solution-7 preserves energy and redox metabolism: a metabolomics approach. Transfusion. 2015;55(12):2955-66.

20. Gray N, Lewis MR, Plumb RS, Wilson ID, Nicholson JK. High-Throughput Microbore UPLC-MS Metabolic Phenotyping of Urine for Large-Scale Epidemiology Studies. J Proteome Res. 2015;14(6):2714-21.

21. Mahmoud SM, Paish EC, Powe DG, Macmillan RD, Grainge MJ, Lee AH, et al. Tumor-infiltrating CD8+ lymphocytes predict clinical outcome in breast cancer. Journal of clinical oncology : official journal of the American Society of Clinical Oncology. 2011;29(15):1949-55.

22. Ali HR, Provenzano E, Dawson SJ, Blows FM, Liu B, Shah M, et al. Association between CD8+ T-cell infiltration and breast cancer survival in 12,439 patients. Ann Oncol. 2014;25(8):1536-43.

23. Liu F, Lang R, Zhao J, Zhang X, Pringle GA, Fan Y, et al. CD8(+) cytotoxic T cell and FOXP3(+) regulatory T cell infiltration in relation to breast cancer survival and molecular subtypes. Breast Cancer Res Treat. 2011;130(2):645-55.

24. Kim SH, Henry EC, Kim DK, Kim YH, Shin KJ, Han MS, et al. Novel compound 2-methyl-2H-pyrazole-3-carboxylic acid (2-methyl-4-o-tolylazo-phenyl)-amide (CH-223191) prevents 2,3,7,8-TCDD-induced toxicity by antagonizing the aryl hydrocarbon receptor. Mol Pharmacol. 2006;69(6):1871-8.

25. Fallarino F, Grohmann U, You S, McGrath BC, Cavener DR, Vacca C, et al. The combined effects of tryptophan starvation and tryptophan catabolites down-regulate T cell receptor zeta-chain and induce a regulatory phenotype in naive T cells. J Immunol. 2006;176(11):6752-61.

26. Szasz AM, Lanczky A, Nagy A, Forster S, Hark K, Green JE, et al. Cross-validation of survival associated biomarkers in gastric cancer using transcriptomic data of 1,065 patients. Oncotarget. 2016;7(31):49322-33.

27. Asano Y, Kashiwagi S, Goto W, Kurata K, Noda S, Takashima T, et al. Tumour-infiltrating CD8 to FOXP3 lymphocyte ratio in predicting treatment responses to neoadjuvant chemotherapy of aggressive breast cancer. Br J Surg. 2016;103(7):845-54.

28. Miyashita M, Sasano H, Tamaki K, Chan M, Hirakawa H, Suzuki A, et al. Tumor-infiltrating CD8+ and FOXP3+ lymphocytes in triple-negative breast cancer: its correlation with pathological complete response to neoadjuvant chemotherapy. Breast Cancer Res Treat. 2014;148(3):525-34.

29. Metz R, Rust S, Duhadaway JB, Mautino MR, Munn DH, Vahanian NN, et al. IDO inhibits a tryptophan sufficiency signal that stimulates mTOR: A novel IDO effector pathway targeted by D-1-methyl-tryptophan. Oncoimmunology. 2012;1(9):1460-8.

30. Kolodziej LR, Paleolog EM, Williams RO. Kynurenine metabolism in health and disease. Amino Acids. 2011;41(5):1173-83.

31. Takikawa O, Yoshida R, Kido R, Hayaishi O. Tryptophan degradation in mice initiated by indoleamine 2,3-dioxygenase. J Biol Chem. 1986;261(8):3648-53.

Figure Legends

Figure 1: Increased kynurenine leads to primary human CD8 T cell death, which is reversed by an AhR antagonist. (A) Representative example of gating strategy for flow cytometric analysis: CD8 T cells were gated based on double positivity for CD8 (PE-Cy7) and CD3 (PerCP-Cy5.5). Cell death was determined by positive staining for the fixable viability stain BV421. Proliferation was measured by CFSE dilution. **(B)** Cells were activated with CD3 and CD28 antibodies for 5 days in the indicated concentration of kynurenine and CD8 T cell death was determined. Each dot represents cells from one human donor. N=9 donors, mean with standard deviation, one-way ANOVA. **(C)** Cells were treated with kynurenine as described in (B) and assayed for CD8 T cell proliferation. N=9 donors, one-way ANOVA. **(D)** Representative images (10x magnification) of CD8 T cells on activation Day 5 that were treated with indicated concentrations of kynurenine and either 10 μM of the AhR antagonist CH-223191 (AhRa) or DMSO. **(E)** CD8 T cells were activated, treated with 10 μM AhRa or vehicle control (DMSO), and assayed for cell death. N=6, mean with standard deviation, paired t-tests.

Figure 2: The effect of conditioned media from suspended TNBC cells on primary human CD8 T cells is similar to that of purified kynurenine, and is reversed by TDO2 inhibitor 680C91. (A) Conditioned media was collected from BT549 TNBC cells grown in attached (ATT) or suspended (SUS) culture conditions for either 24 or 48 hours as indicated. CD8 T cells were isolated from the blood of normal donors and activated for 5 days with CD3 and CD28 antibodies in the conditioned media. Each line represents the response of CD8 T cells from one donor. Cell death was measured as described in Figures 1A and B. N=9, paired t-tests. **(B)** Representative flow cytometric analysis of CD8 T cells for IFNγ production is shown. **(C)** IFNγ production by CD8 T cells cultured in conditioned media for 48 hours. N=7, paired t-tests. **(D)** CD8 T cells were activated in conditioned media and either 0.1 μM 680C91 (to inhibit TDO activity) or vehicle control (DMSO). Each line represents the response of CD8 T cells from one human volunteer donor. N=5, paired t-tests. **(E)** CD8 T cells were

activated in conditioned media and treated with either 10 μM CH-223191 (to inhibit AhR activation) or vehicle control (DMSO). N=5, paired t-tests.

Figure 3: *TDO2* expression correlates with breast cancer outcomes, while expression of the more commonly studied *IDO1* does not. (A) Patients were split into *TDO2*-high (red, n=699) or *TDO2*–low (black, n=703) groups based on median *TDO2* gene expression. Overall survival (left) and distant metastasis-free survival (right) was plotted using KmPlot.com. **(B)** Patients were split into *IDO1*-high (red, n=701) or *IDO1*–low (black, n=701) groups based on median gene expression, and overall survival and distant-metastasis free survival was plotted. N=1402, hazard ratios are given with 95% confidence intervals, logrank test.

Figure 4: Tryptophan and kynurenine are reduced in breast cancer plasma. Ultra-high performance liquid chromatography/mass spectrometry was used to measure tryptophan and kynurenine concentrations in the plasma from normal women and women with breast cancer. The concentrations of tryptophan and kynurenine correlate significantly and positively in both normal **(A)** (n=40) and breast cancer patient **(B)** (n=77) plasma by Pearson and Spearman tests. Comparison of tryptophan **(C)** and kynurenine **(D)** concentrations in plasma from normal women, all breast cancer patients in the cohort, and ER+ versus ER- breast cancer patients. Mean with standard deviation, $p<0.05$ one-way ANOVA and Tukey's multiple comparisons test. Comparison of tryptophan **(E)** and kynurenine **(F)** concentrations plotted by breast cancer stage is shown. Mean with standard deviation, one-way ANOVA and Tukey's multiple comparisons test.

Figure 5: Breast cancer patient plasma tryptophan and progression-free survival. Ultra-high performance liquid chromatography/mass spectrometry was used to measure tryptophan concentrations in the plasma from women with breast cancer. Kaplan-Meyer curves plotting progression-free survival of breast cancer patients with ER+ disease (n=49) **(A)** or ER- disease

(n=28) **(B)** are shown, where progression was defined by local, regional, or distant recurrence, or patient death in the years after surgery. Logrank test.

Supplemental Figure 1: Alterations in tryptophan catabolites in breast cancer subtypes. Ultra-high performance liquid chromatography/mass spectrometry was used to measure the concentrations of tryptophan and its catabolites in the plasma from women with breast cancer. Subtypes are defined by ER and HER2 positivity. Two-tailed t-test, *p<0.05.

Supplemental Figure 2: Alterations in tryptophan catabolites in breast cancer and pregnancy-associated breast cancer. Ultra-high performance liquid chromatography/mass spectrometry was used to measure the concentrations of tryptophan and its catabolites in the plasma from women with or without breast cancer, where pregnancy status was known. Two-tailed t-test, *p<0.05, **p<0.01, ***p<0.001, ****p<0.0001.

Supplemental Figure 3: Alterations in tryptophan catabolites by breast cancer stage. Ultra-high performance liquid chromatography/mass spectrometry was used to measure the concentrations of tryptophan and its catabolites in the plasma from women with breast cancer, and data was divided by breast cancer stage at diagnosis. Two-tailed t-test, **p<0.01.

Supplementary Table 1. Summary of patient data.

	Breast Cancer	Normal
n	77	40
Age, years (mean and range)	39 (25-76)	35 (23-61)
BMI (mean and range)	25.3 (18.5-43.6)	25.1 (18.5-37.0)
Type		
Ductal	67 (87.0%)	
Ductal+Lobular	5 (6.5%)	
Lobular	0	
Inflammatory	3 (3.9%)	
Type		
DCIS	1 (1.3%)	
Luminal A	8 (10.4%)	
Luminal B	40 (51.9%)	
HER2 Positive	9 (11.7%)	
Triple Negative	18 (23.4%)	
Stage		
0	1 (1.3%)	
1	22 (28.6%)	
2	35 (45.5%)	
3	13 (16.9%)	
4	4 (5.2%)	
Recurrence	10 (13.0%)	

BMI: body mass index

DCIS: ductal carcinoma in situ

Figure 1

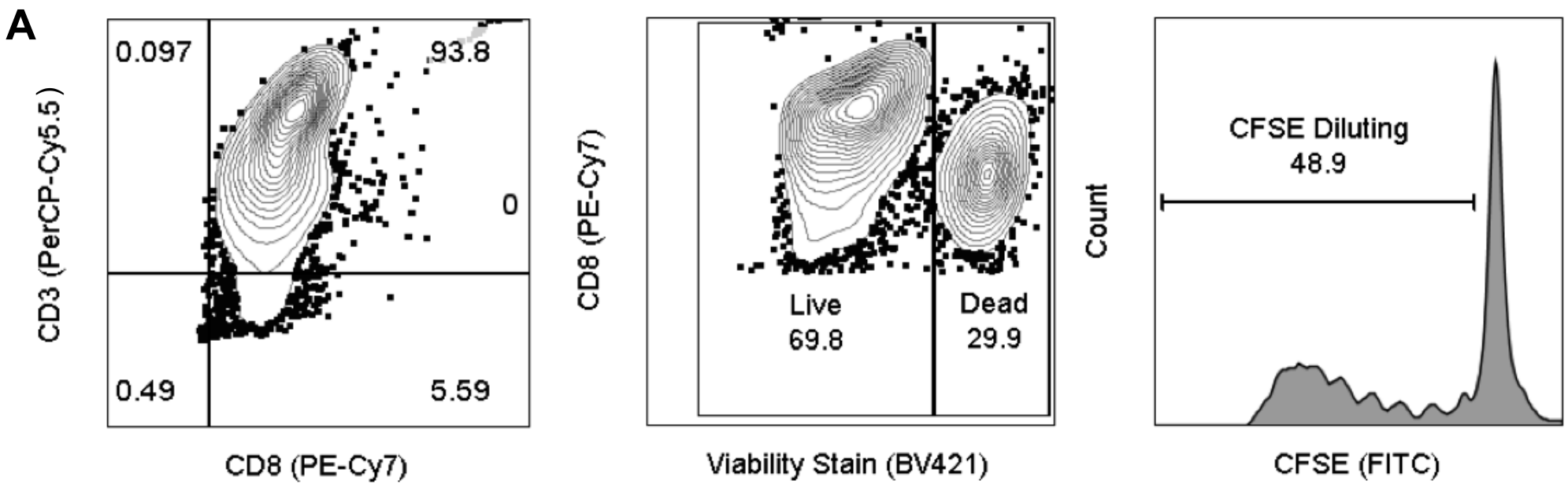
A
0.097
93.8
0
0.49
5.59
CD3 (PerCP-Cy5.5)
CD8 (PE-Cy7)
CD8 (PE-Cy7)
Live
69.8
Dead
29.9
Viability Stain (BV421)
Count
CFSE Diluting
48.9
CFSE (FITC)

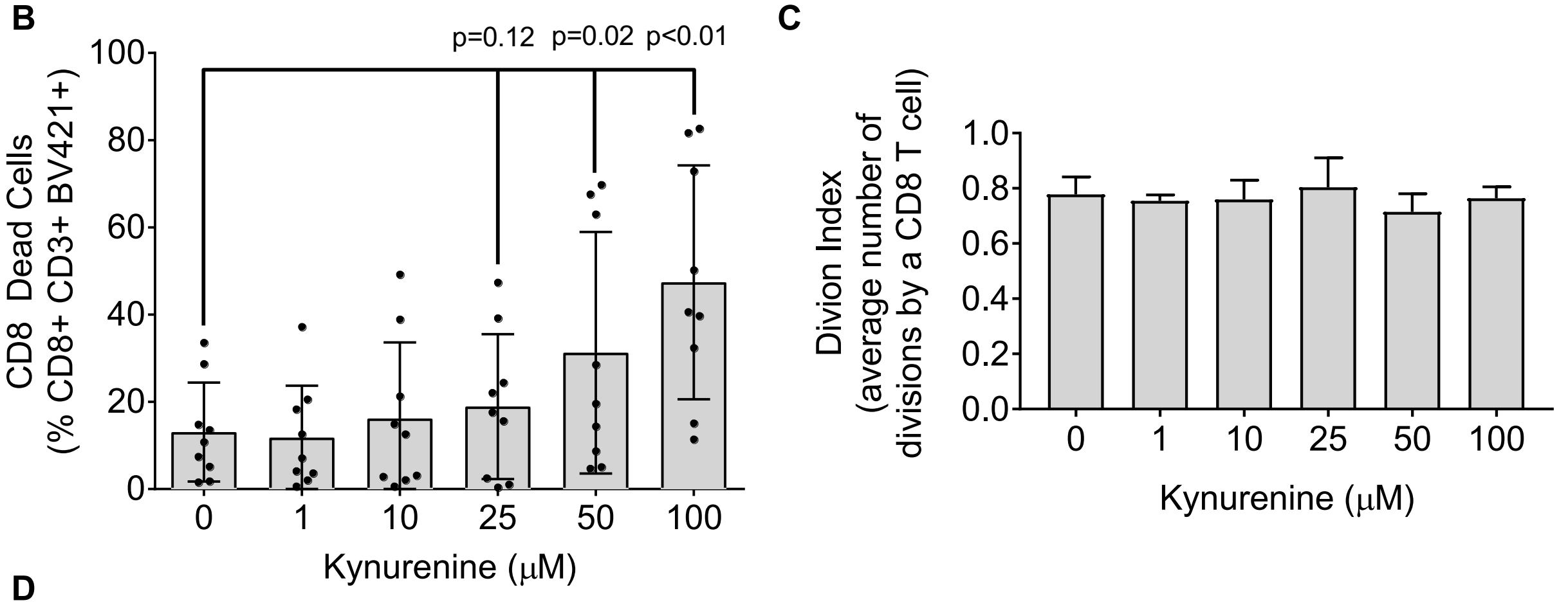
B
p=0.12 p=0.02 p<0.01
CD8 Dead Cells
(% CD8+ CD3+ BV421+)
Kynurenine (μM)
C
Dision Index
(average number of
divisions by a CD8 T cell)
Kynurenine (μM)
D
Vehicle
(DMSO)
10 μM
AhRa
μM Kynurenine
E
ns
p=0.02
p=0.02
CD8 Dead Cells
(% CD8+ CD3+ BV421+)
50 μM kyn:
AhRa:

Figure 2

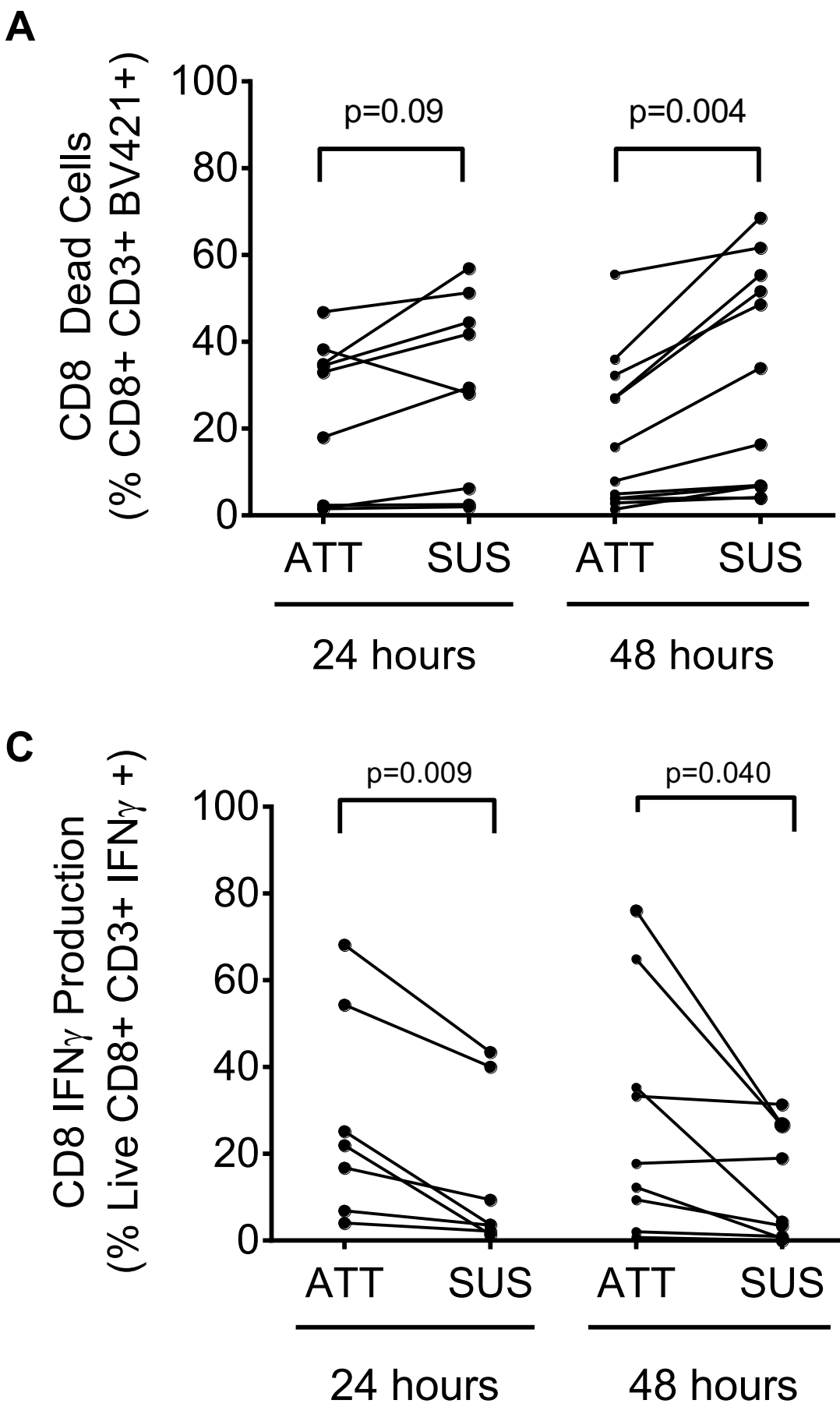
A
CD8 Dead Cells
(% CD8+ CD3+ BV421+)
100
80
60
40
20
0
p=0.09
p=0.004
ATT
SUS
ATT
SUS
24 hours
48 hours

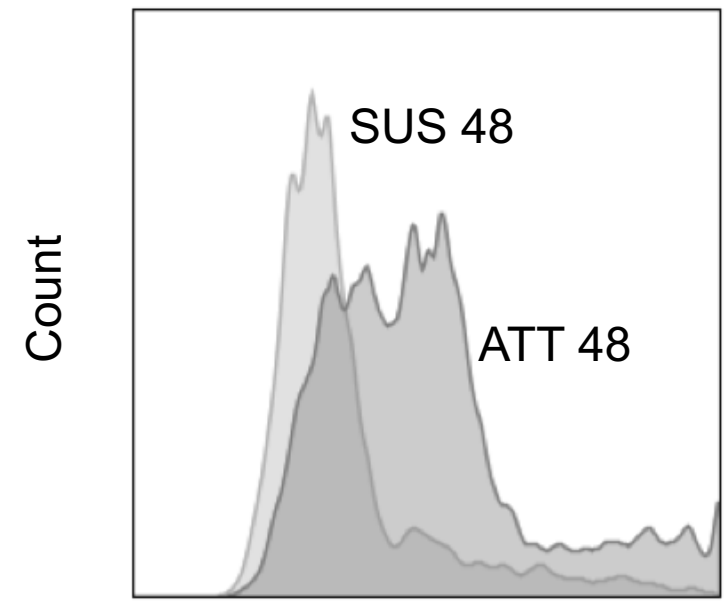
B
Count
SUS 48
ATT 48
IFNγ (APC)

C
CD8 IFNγ Production
(% Live CD8+ CD3+ IFNγ +)
100
80
60
40
20
0
p=0.009
p=0.040
ATT
SUS
ATT
SUS
24 hours
48 hours

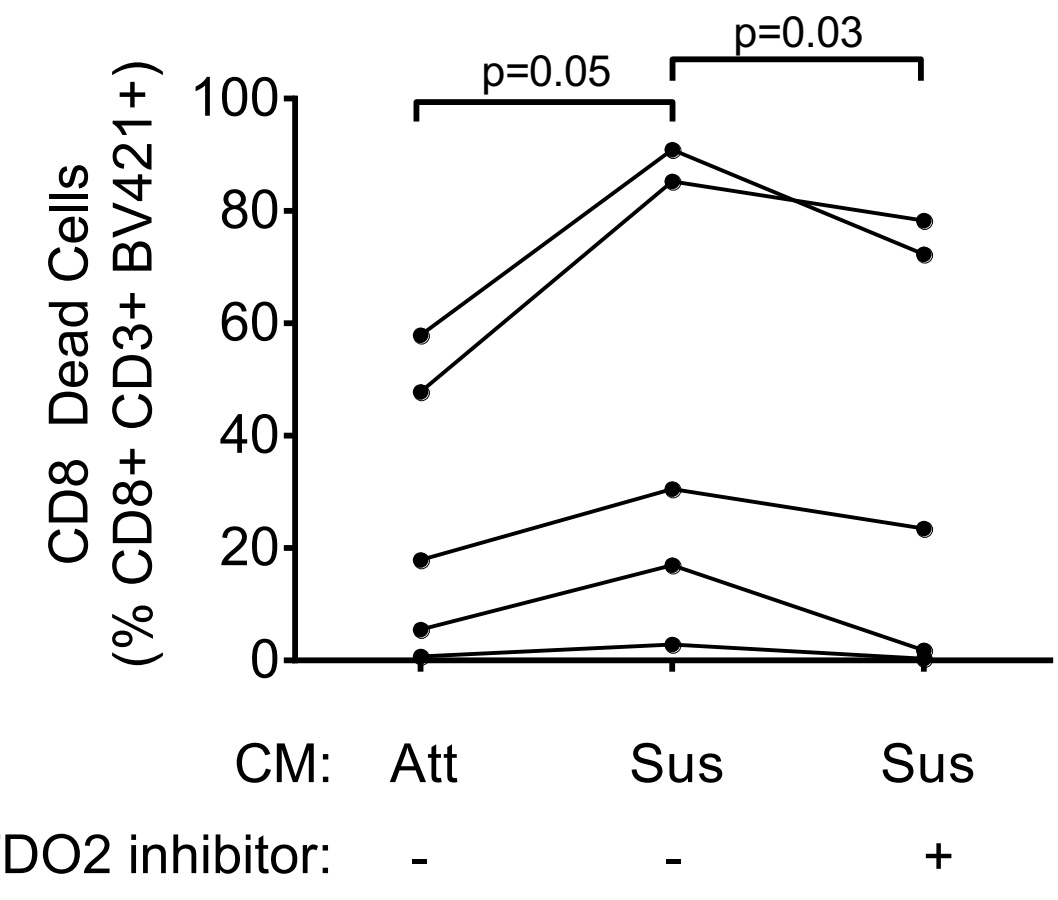
D
CD8 Dead Cells
(% CD8+ CD3+ BV421+)
100
80
60
40
20
0
p=0.05
p=0.03
CM: Att Sus Sus
TDO2 inhibitor: - - +

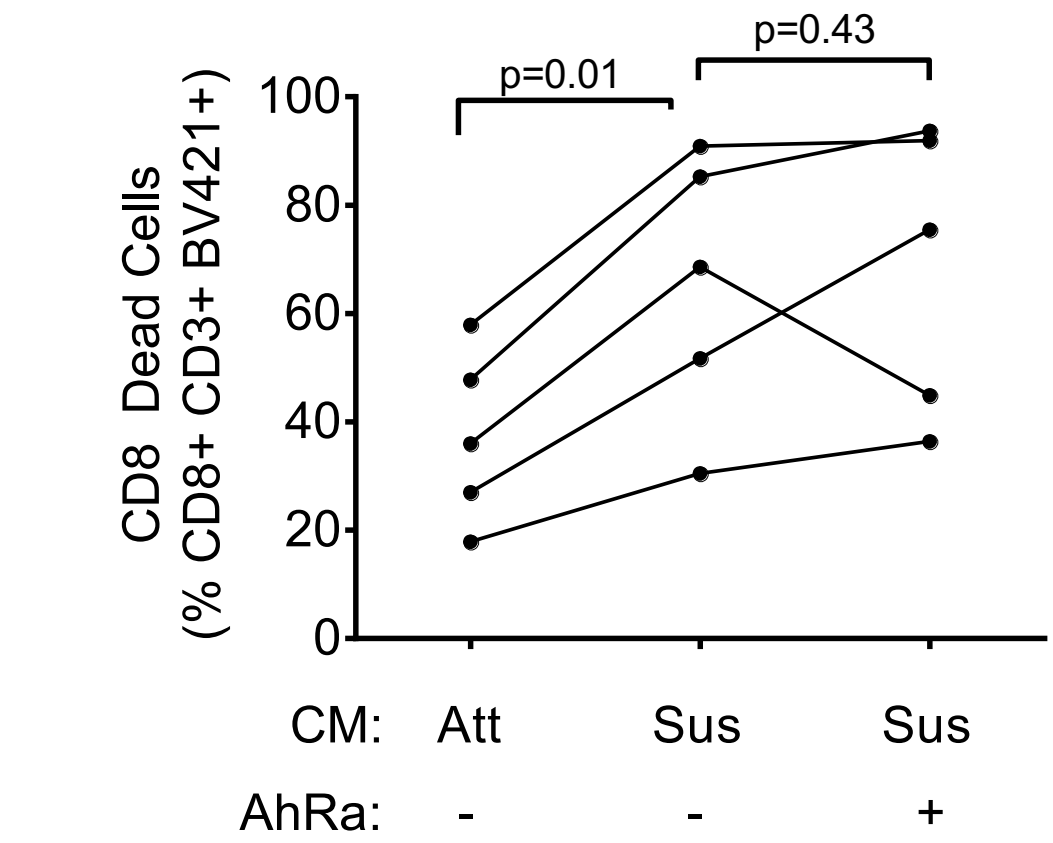
E
CD8 Dead Cells
(% CD8+ CD3+ BV421+)
100
80
60
40
20
0
p=0.01
p=0.43
CM: Att Sus Sus
AhRa: - - +

Figure 3

A

TDO2

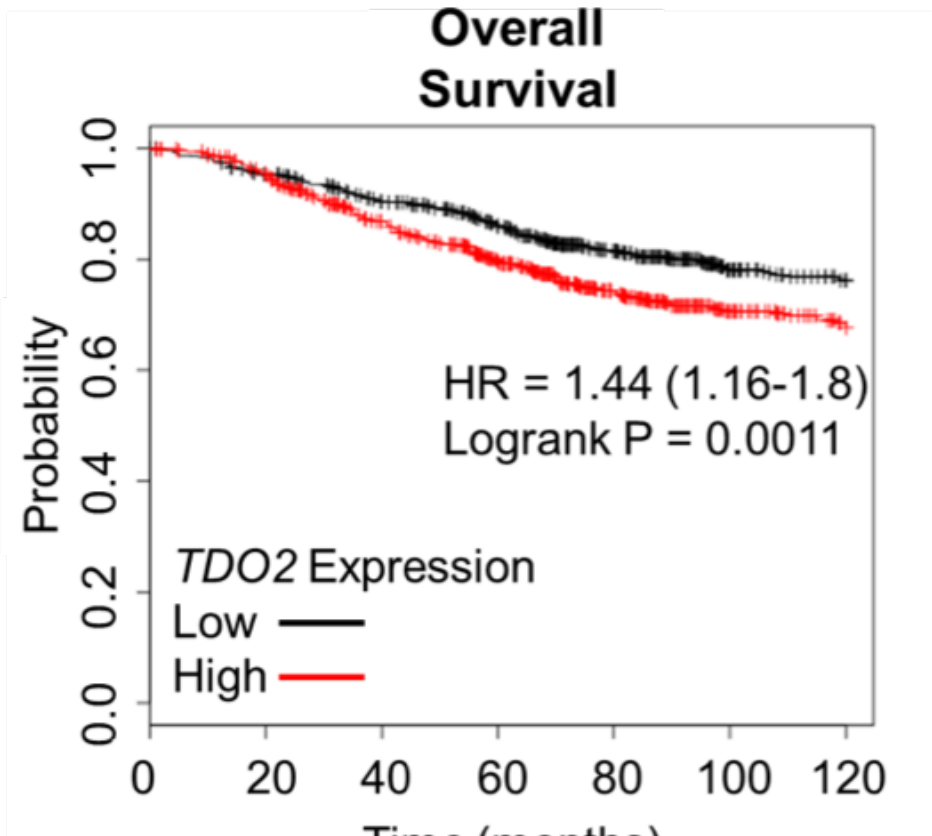

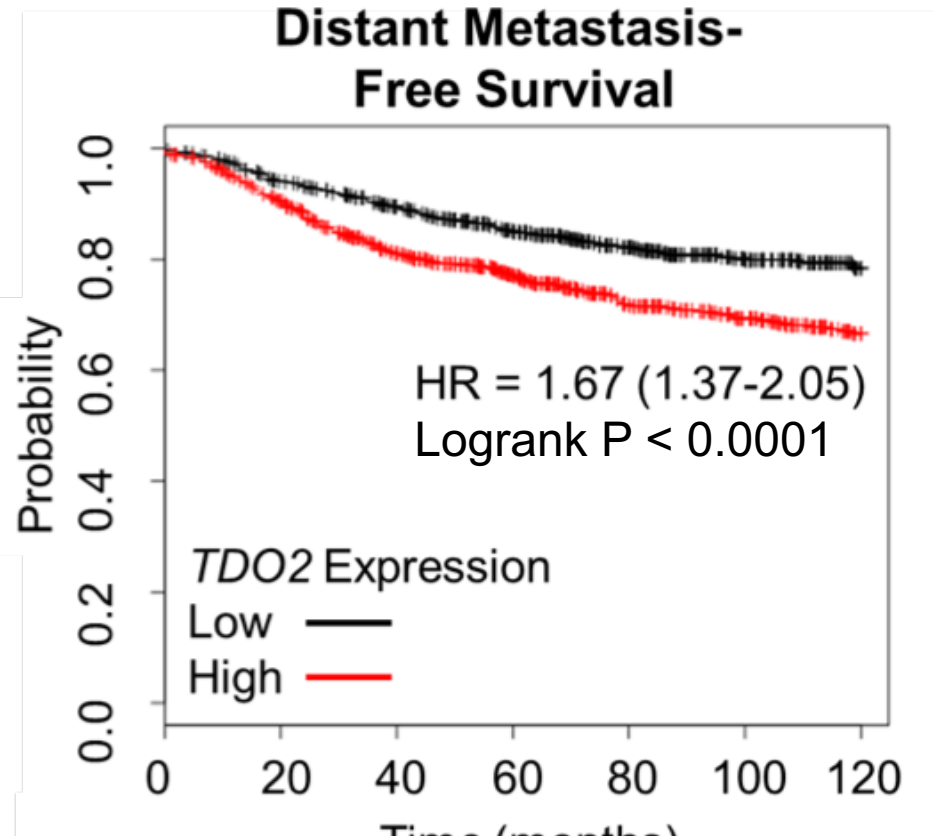

B

IDO1

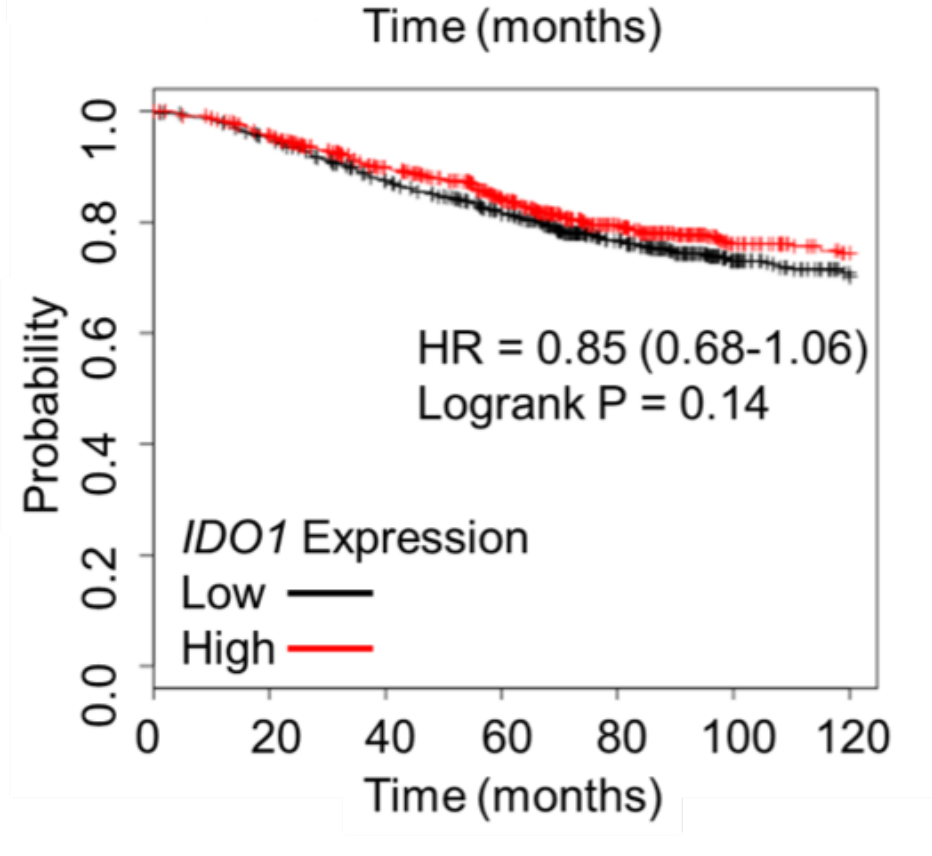

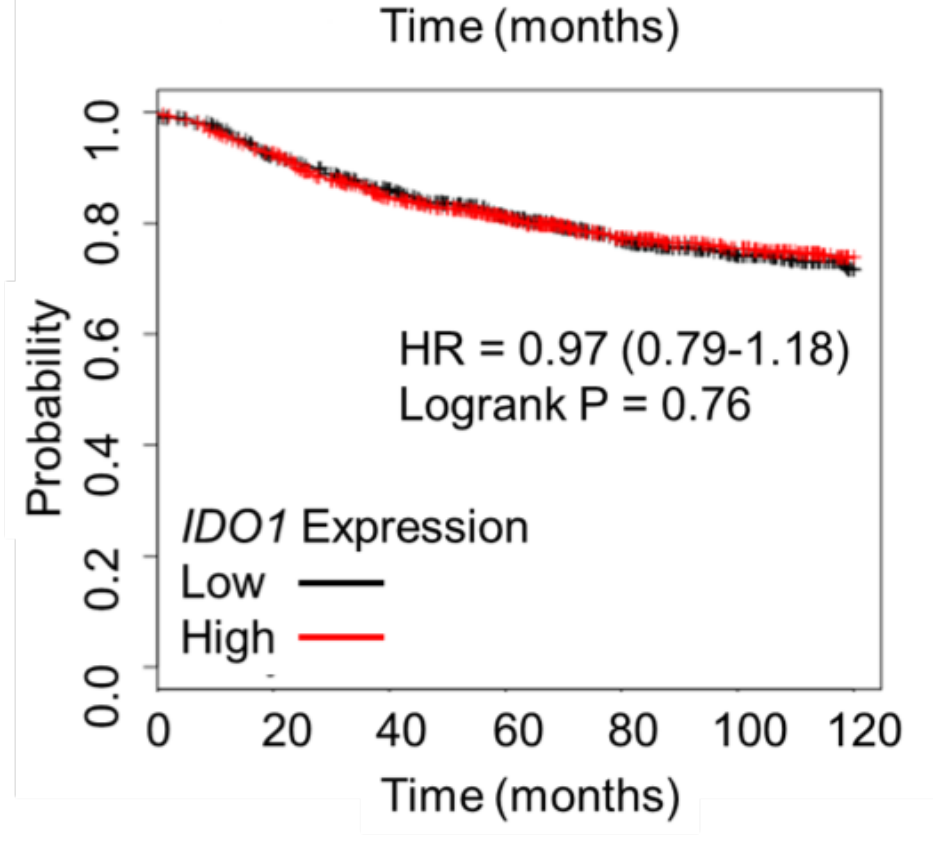

Figure 4

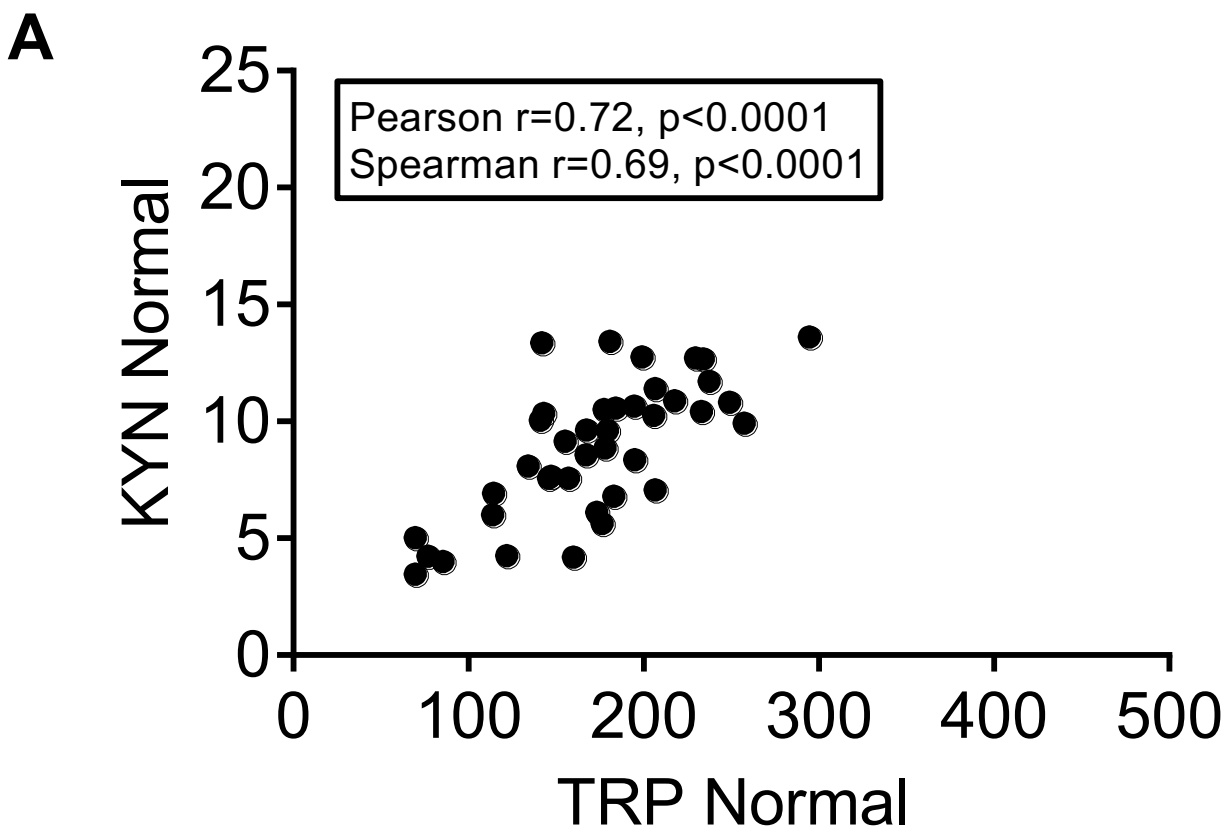
A
KYN Normal
Pearson r=0.72, p<0.0001
Spearman r=0.69, p<0.0001
0
5
10
15
20
25
0
100
200
300
400
500
TRP Normal

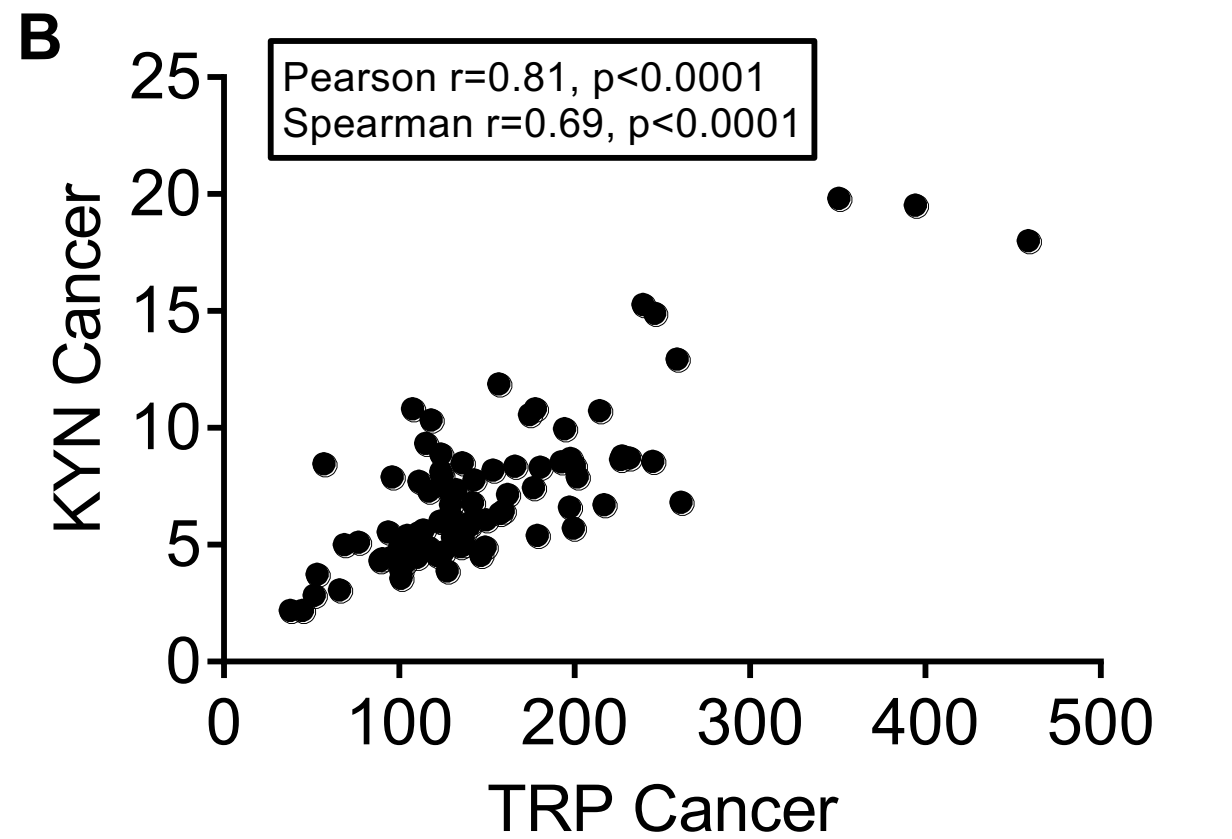
B
KYN Cancer
Pearson r=0.81, p<0.0001
Spearman r=0.69, p<0.0001
0
5
10
15
20
25
0
100
200
300
400
500
TRP Cancer

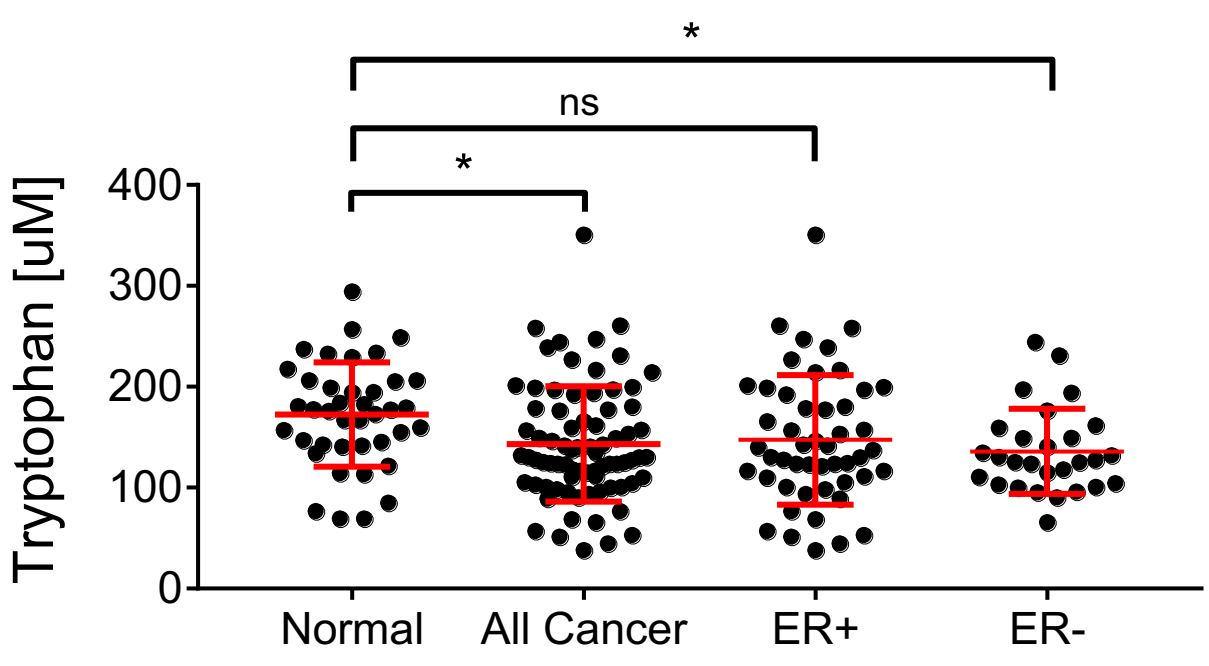
C
Tryptophan [uM]
*
ns
*
0
100
200
300
400
Normal
All Cancer
ER+
ER-

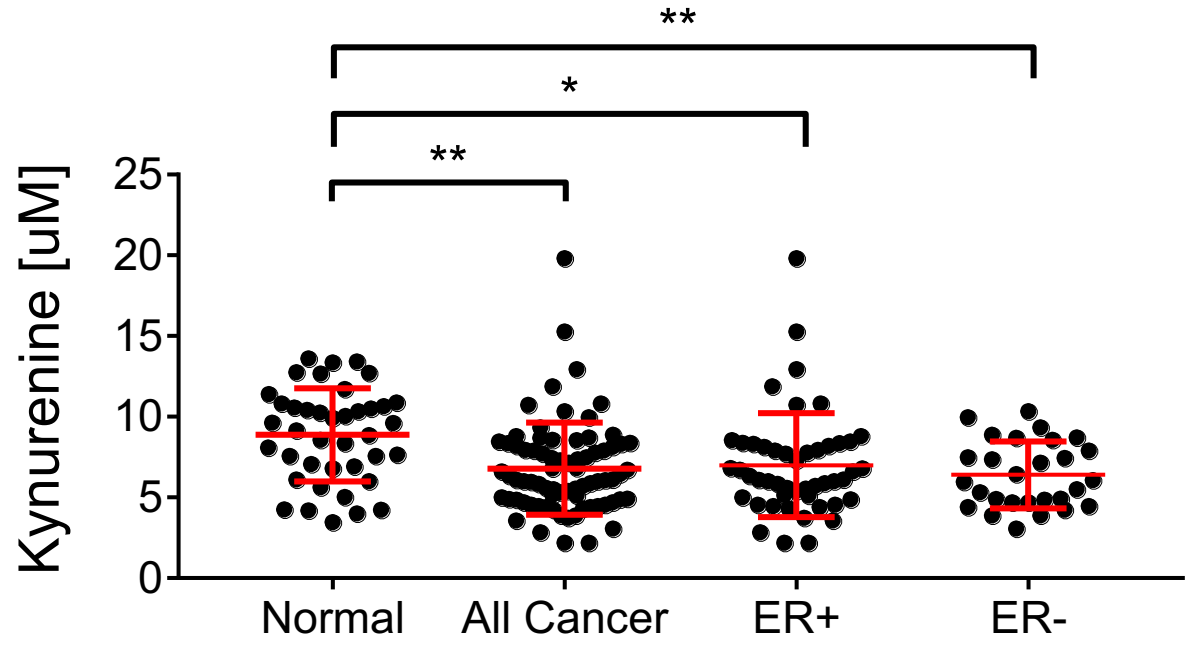
D
Kynurenine [uM]
**
*
**
0
5
10
15
20
25
Normal
All Cancer
ER+
ER-

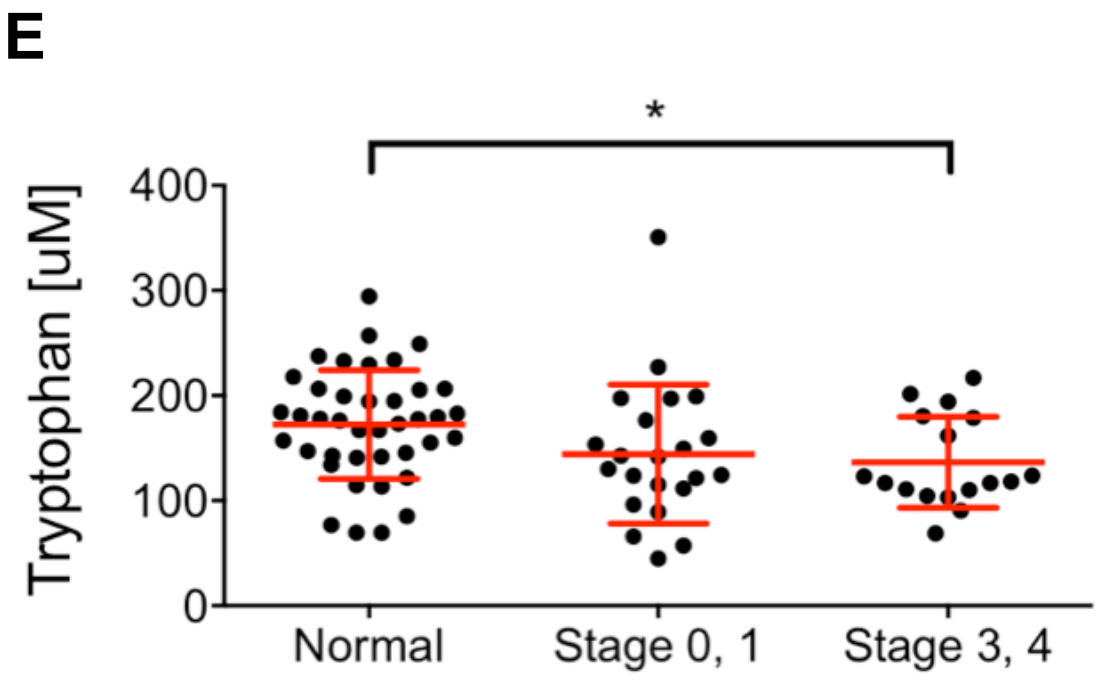
E
Tryptophan [uM]
*
0
100
200
300
400
Normal
Stage 0, 1
Stage 3, 4

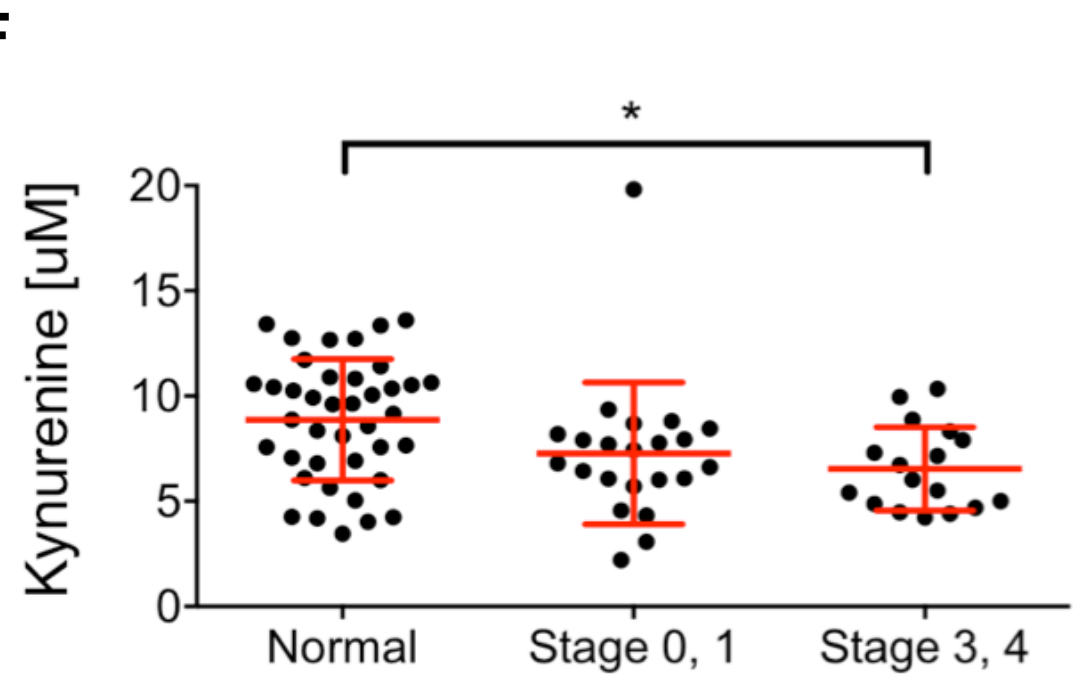
F
Kynurenine [uM]
*
0
5
10
15
20
Normal
Stage 0, 1
Stage 3, 4

Figure 5

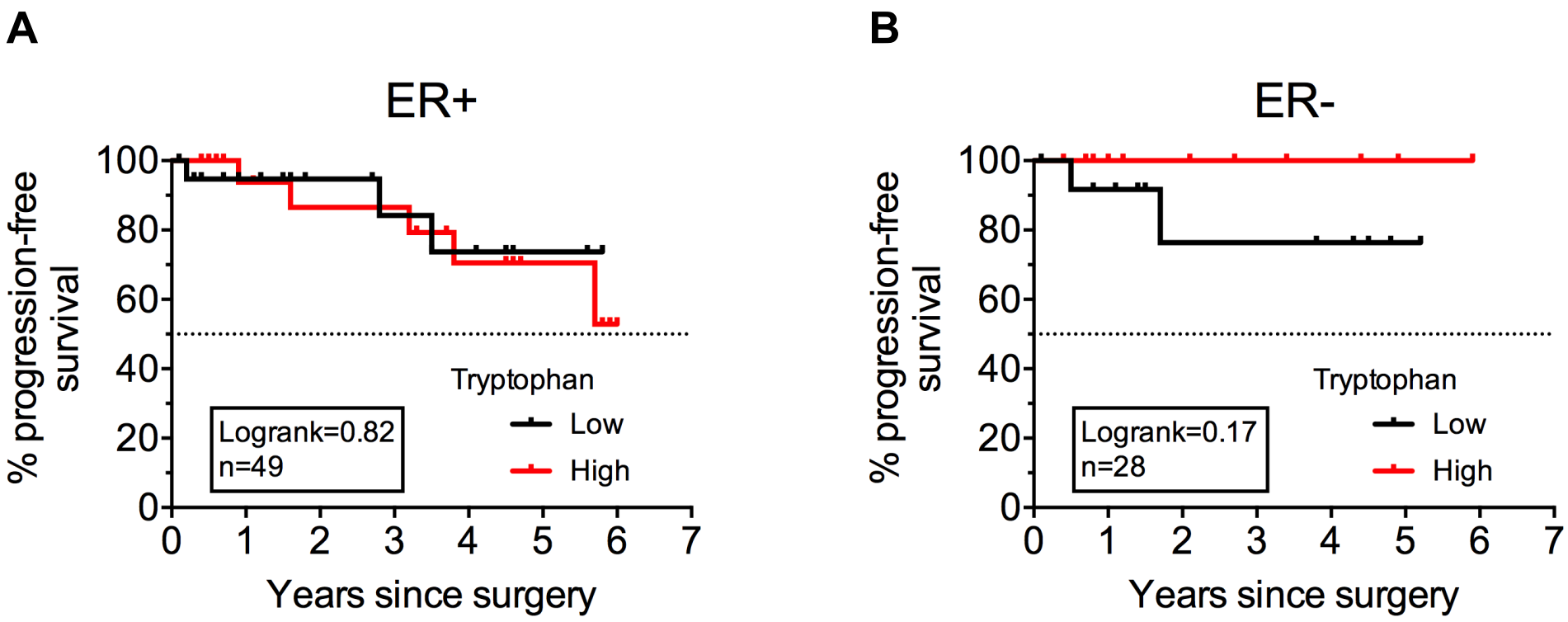
A
ER+
% progression-free survival
100
80
60
40
20
0
Logrank=0.82
n=49
Tryptophan
Low
High
0 1 2 3 4 5 6 7
Years since surgery
B
ER-
% progression-free survival
100
80
60
40
20
0
Logrank=0.17
n=28
Tryptophan
Low
High
0 1 2 3 4 5 6 7
Years since surgery

Supplemental Figures

Supplemental Figure 1

ER+ HER2-

ER+ HER2+

ER- HER2+

ER- HER2-

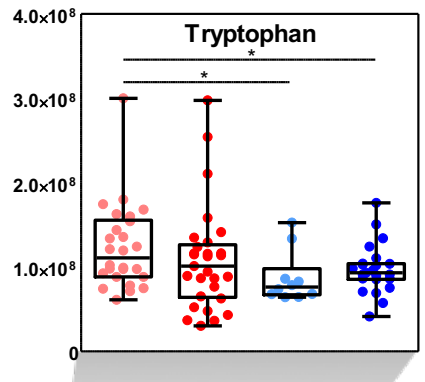

Serotonin ← L-Tryptophan → Hydroxy-Tryptophan

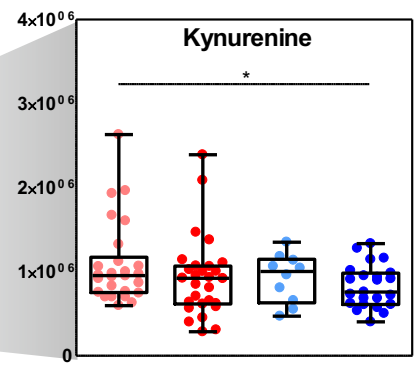

Kynureninic acid ← Kynurenine

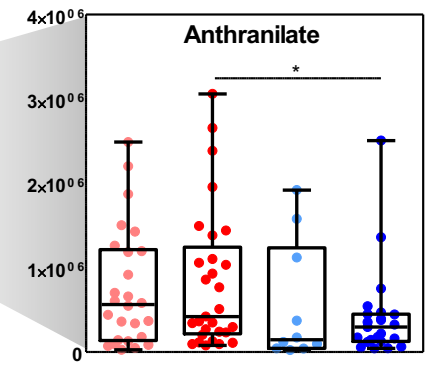

Xanthurenic acid ← Hydroxy-Kynurenine → Anthranilate

Picolinic acid ← Hydroxy-Anthranilate → Quinolinic acid

Nicotinamide

Supplemental Figure 2

Non-PABC

PABC

Normal, no birth last 5 yrs.

Normal, yes birth last 5 yrs.

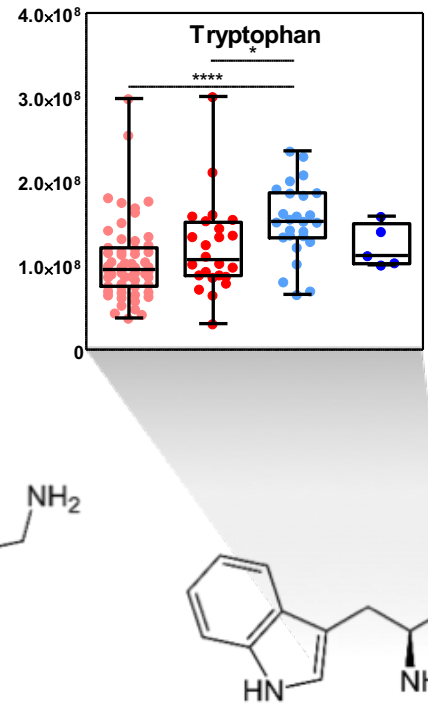

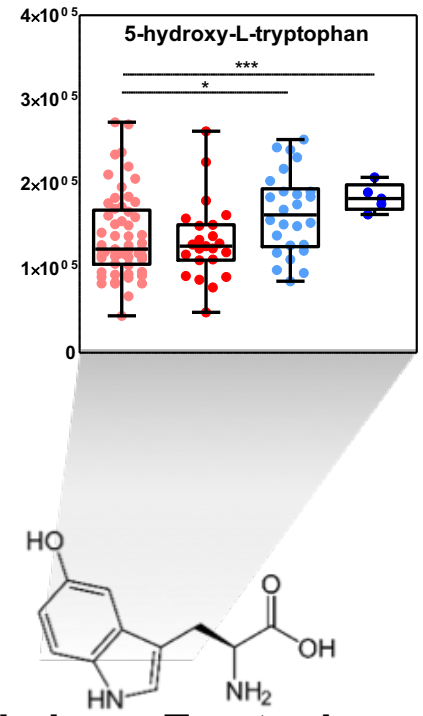

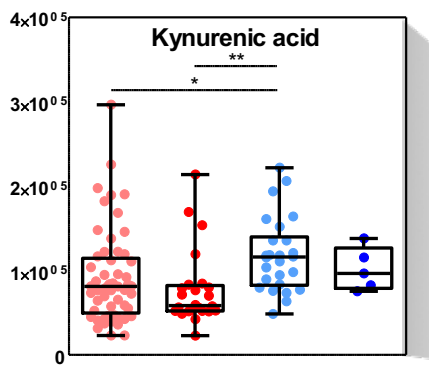

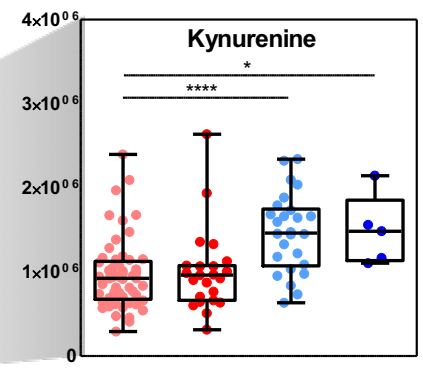

Serotonin ← L-Tryptophan → Hydroxy-Tryptophan

Kynureninic acid ← Kynurenine

Xanthurenic acid ← Hydroxy-Kynurenine

Anthranilate

Picolinic acid ← Hydroxy-Anthranilate → Quinolinic acid

Nicotinamide

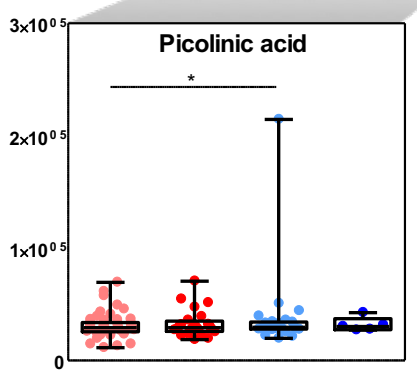

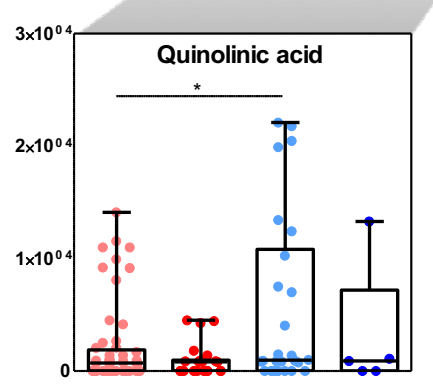

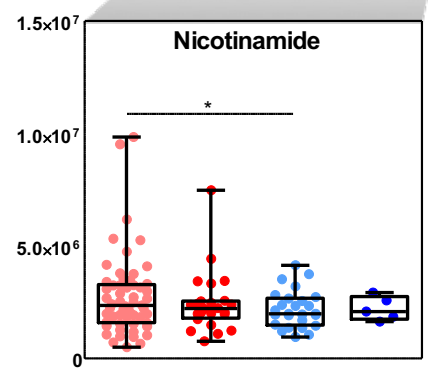

Stage I/II Breast Cancer

Stage III/IV Breast Cancer

Serotonin

L-Tryptophan

Hydroxy-Tryptophan

Kynureninic acid

Kynurenine

Xanthurenic acid

Hydroxy-Kynurenine

Anthranilate

Picolinic acid

Hydroxy-Anthranilate

Quinolinic acid

Nicotinamide